



THE HONG KONG
POLYTECHNIC UNIVERSITY

香港理工大學

Pao Yue-kong Library

包玉剛圖書館

Copyright Undertaking

This thesis is protected by copyright, with all rights reserved.

By reading and using the thesis, the reader understands and agrees to the following terms:

1. The reader will abide by the rules and legal ordinances governing copyright regarding the use of the thesis.
2. The reader will use the thesis for the purpose of research or private study only and not for distribution or further reproduction or any other purpose.
3. The reader agrees to indemnify and hold the University harmless from and against any loss, damage, cost, liability or expenses arising from copyright infringement or unauthorized usage.

If you have reasons to believe that any materials in this thesis are deemed not suitable to be distributed in this form, or a copyright owner having difficulty with the material being included in our database, please contact lbsys@polyu.edu.hk providing details. The Library will look into your claim and consider taking remedial action upon receipt of the written requests.

The Hong Kong Polytechnic University
The Department of Electrical Engineering

**Optimization of Power Flow With
Transient Stability Constraints
Using Semi-Infinite Programming**

Submitted by

Xia Yan

A thesis submitted in partial fulfilment of the
requirements for the Degree of Doctor of Philosophy

September 2006



Pao Yue-kong Library
PolyU • Hong Kong

CERTIFICATE OF ORIGINALITY

I hereby declare that this thesis is my own work and that, to the best of my knowledge and belief, it reproduces no material previously or neither written nor material which has been accepted for the award of any other degree or diploma, except where due acknowledgement has been made in the text.

Signed

XIA Yan

ABSTRACT OF THE THESIS ENTITLED

**Optimization of Power Flow With
Transient Stability Constraints
Using Semi-Infinite Programming**

submitted by

XIA Yan

for the degree of Doctor of Philosophy

at The Hong Kong Polytechnic University in September 2006

Increased economical pressure and intensified transactions, especially in competitive environment, have forced modern electric power systems to operate much closer to their security limits than ever before. Nowadays, dynamic instability has become a major threat for system operation. Dynamic stability requires that when any of a specified set of disturbances (e.g. outages of generators or transmission lines) occurs, a feasible operation point should be able to withstand the fault and ensure that the power system moves to a new stable equilibrium after the clearance of the fault without violating equality and inequality constraints even during transient period of the dynamics. Due to the huge loss and expensive control cost associated with transient instability, dynamic security assessment must be considered in planning and operation analysis together with economic objectives. Mathematically,

dynamic security assessment can be considered as an extended optimal power flow (OPF) problem, in which transient stability, for example, is regarded as one of the security constraints for the system operation, with the optimal objective to be obtained under a given set of system parameters by adjusting available controlling schemes. This research aims to develop a practical framework based on existing OPF techniques for integrated economy and dynamic security optimization such that the final system could be operated in an optimal state with lowest generation cost, for instance, and guaranteed dynamic security.

By introducing transient stability indices to conventional OPF, OPF with transient stability constraints is generalized as a semi-infinite programming (SIP) problem with a finite number of state and control variables for the operation state and an infinite number of constraints for transient stability in the functional space of time domain. In this thesis, "infinite" constraints for transient stability mean that the stability has to be satisfied in the infinitely many continuous time points in the transients. Two transient stability indices based on rotor angle limit and potential energy boundary surface (PEBS) concept are employed. The features and performance of the two indices are compared theoretically and numerically.

General scheme of the solution of SIP is extended to solve transient stability constrained OPF problem. Numerical methods for SIP are developed to locally reduce transient stability constraints to be finite-dimensional constraints based on L_1 and L_∞ norm. L_1 and L_∞ norm are defined as the norm integration and maximal norm of the violation of the semi-infinite constraints in their functional spaces, respectively. This transformation transcribes transient stability constrained OPF to conventional OPF with a finite number of constraints, which is solvable by using nonlinear programming theories and algorithms.

The locally reduced SIP problem of transient stability constrained OPF is solved by direct nonlinear primal-dual interior point method. The theoretical difficulties in forming the Jacobian and Hessian Matrices of the transient stability constraints are overcome by using implicit relationship between the transient stability constraints

and the differential-algebra-equations (DAEs) for the dynamic performance. The solution of the multi-local optimization in the buildup of L_∞ penalty functions is proposed based on intermediate value theorem. In addition, an improved BFGS (Broyden-Fletcher-Goldfarb-Shanno) method, which is a quasi-Newton method with superlinear convergence, is exploited to avoid the complicated derivation of Hessian matrix. By splitting the Hessian matrix into two parts - an 'easy' part for conventional OPF and a 'difficult' part for transient stability constraints, only the 'difficult part' is approximated according to BFGS updating while the 'easy' part is calculated accurately. Moreover, a new concept referred as "the most effective section" of transient stability constraints is proposed to alleviate the huge computational efforts and improve the convergence of the optimization calculation.

The calculation of dynamic available transfer capability (ATC) and dynamic security dispatch are formulated as transient stability constrained OPF problems and are solved by the proposed methodology. The proposed methodology is fully validated in both the WSCC 9-bus system and New England 39-bus system. The necessity of transient stability involvement in OPF is illustrated in the case studies. The good performance of the introduction of the most effective section of transient stability constraints is illustrated in the case study of ATC computation. The effectiveness of transient stability constraints based on rotor angle limits and PEBS are compared and discussed. The advantage of the use of improved BFGS method to avoid complex Hessian matrix derivation is demonstrated. In the study of dynamic security dispatch, multi-contingency cases are handled by the proposed methodology in solving cases with difficult multiple contingencies for the improvement of the overall security level.

ACKNOWLEDGEMENTS

First and foremost, I would like to express my sincerest gratitude to Dr. Kevin Ka Wing Chan, my chief-advisor, for his willingness to guide me through the challenging path towards a doctoral degree. He was always available and made me feel free in discussing my work. He always encouraged me to work on problems interested me while at the same time offering me insightful guidance. I would also like to thank Professor Tak Shing Chung, my co-advisor, for his constructive criticism and kindness of offering useful resources. The experience and knowledge I gained by working with them is invaluable and will influence both personal and professional development profoundly.

I am grateful to Professor Mingbo Liu in South China University of Technology. I learned a great deal and gained valuable experience through discussions with him on optimization algorithms.

The dedication in this thesis is a testimony to the premium my parents have always placed on education, and to the innumerable sacrifices they have made over the years on my account. They have always been supportive of my educational goals despite my long absences from home, especially at important family events. I am truly indebted to them.

My time in Hong Kong has been made so much more valuable by friends, new and old, at and beyond the Hong Kong Polytechnic University, who have encouraged me, gently bullied me, and occasionally provided much-needed distraction at various stages along the course of my postgraduate experience. I shall not attempt to mention each one by name; I hope they know who they are, and how grateful I am to them for making my time here so worthwhile.

Last but not the least, I would like to acknowledge the financial support of the Research Grants Council of the Hong Kong Special Administrative Region (RGC No: PolyU 5103/02E), the Hong Kong Polytechnic University, and the Department of Electrical Engineering.

LIST OF PUBLICATIONS

1. Xia Yan, Chan Ka Wing, "Preventive Control for Transient Stability Enhancement with Optimal Power Flow Approach," submitted to Electric Power Systems Research.
2. Xia Yan, Chan Ka Wing, "Dynamic Constrained Optimal Power Flow Using Semi-infinite Programming," IEEE Trans. Power Syst., Vol. 21, No. 3, pp.1455-1457, Aug. 2006.
3. Xia Yan, Chan Ka Wing, Liu Mingbo, "Infeasibility Detection and Solution for Optimal Power Flow," APSCOM 2006, CDROM, Hong Kong, 30 Oct – 2 Nov 2006.
4. Xia Yan, Chan Ka Wing, Ho Fai Ho, "A Semi-Infinite Programming Algorithm for Dynamic Security-Constrained Generation Rescheduling," APSCOM 2006, CDROM, Hong Kong, 30 Oct – 2 Nov 2006.
5. Xia Yan, Chan Ka Wing, and Liu Mingbo, "Calculation of Optimal Power Flow with Transient Stability Constraints," Regional Inter-University Postgraduate Electrical and Electronic Engineering Conference 2005, CDROM, Hong Kong, 14-15 July, 2005.
6. Xia Yan, Chan Ka Wing, and Liu Mingbo, "Improved BFGS Method for Optimal Power Flow Calculation with Transient Stability Constraints," IEEE Power Engineering Society General Meeting 2005, vol.1, pp.434-439, San Francisco, California, USA, 12-16 June, 2005.
7. Xia Yan, Chan Ka Wing, and Liu Mingbo, "Direct Nonlinear Primal-Dual Interior-Point Method for Transient Stability Constrained Optimal Power Flow," IEE Proceedings-Generation, Transmission and Distribution, Vol 152, Issue 1, pp. 11 – 16, Jan. 2005.

8. Xia Yan, Chan Ka Wing, and Tak Shing Chung, "A TEF Approach For Solving Transient Stability Constrained OPF," PowerCon 2004, vol.2, pp.1485-1489, Singapore, 22-24 November, 2004.
9. Xia Yan, Chan Ka Wing, Liu Mingbo, and Wu Jie, "Calculation of Available Transfer Capability with Transient Stability Constraints," DRPT 2004, vol.1, pp.128-132, Hong Kong, 5-8 April 2004.

TABLE OF CONTENTS

Abstract	i
Acknowledgements	iv
List of Publications	v
Table of Contents	vii
List of Figures	xi
List of Tables	xiii
Chapter I Introduction	1
I.1 Background and Motivation.....	1
I.2 Current State of The Art.....	4
I.2.1 Transient Stability Analysis	4
I.2.2 Optimal Power Flow with Transient Stability Constraints	7
I.2.3 Semi-infinite Programming.....	10
I.3 Primary Contributions.....	12
I.4 Organization of This Thesis	13
Chapter II Transient Stability Constrained OPF	16
II.1 Formulation of Conventional OPF Problem	16
II.2 Transient Stability Assessment	18
II.2.1 Power System Model	18
II.2.2 Transient Stability Index Based on Rotor Angle Limit	20
II.2.3 Transient Stability Index Based on PEBS.....	21
II.2.4 Remarks on The Two Indices of Transient Stability	23
II.3 Transient Stability Constrained OPF.....	25

II.4 Summary	26
Chapter III Semi-infinite Programming and Transformation for Transient Stability Constraints	28
III.1 Preliminaries	29
III.2 Optimality Conditions.....	32
III.2.1 Optimality Conditions for Nonlinear Optimization	32
III.2.2 Optimality Conditions for SIP	34
III.3 SIP Solution Methods	35
III.3.1 Discretization Methods	36
III.3.2 Local Reduction Methods	39
III.3.3 Remarks on Numerical Methods.....	43
III.4 Algorithms for Solving SIP.....	44
III.4.1 Exact Penalty Functions for SIP	45
III.4.1.1 L_1 Penalty Functions.....	46
III.4.1.2 L_∞ Penalty Functions.....	47
III.4.2 Multi-local Optimization Subproblem	48
III.4.3 Algorithm and The Implementation.....	49
III.5 Transformation of Transient Stability Constraints.....	51
III.5.1 L_1 Norm Local Reduction for Transient Stability Constraints	52
III.5.2 L_∞ Norm Local Reduction for Transient Stability Constraints	53
III.5.3 Reformulated Transient Stability Constrained OPF	55
III.6 Summary	56
Chapter IV Implementation of Transient Stability Constrained OPF.....	57

IV.1	Introduction.....	57
IV.2	Direct Nonlinear Primal-Dual Interior Point Method.....	58
IV.3	Jacobian and Hessian Matrices.....	61
IV.3.1	Local Reduction Based on L_1 Norm.....	61
IV.3.2	Local Reduction Based on L_∞ Norm.....	63
IV.4	Overall Implementation of The Algorithm.....	66
IV.5	Improved BFGS Method.....	69
IV.6	Measures to Improve Computation Efficiency.....	70
IV.7	Summary.....	72
Chapter V	Calculation of Available Transfer Capability.....	74
V.1	Introduction.....	74
V.2	Modelling of ATC.....	76
V.3	Case Study and Discussions.....	79
V.3.1	WSCC 9-Bus System.....	79
V.3.1.1	Validation Test.....	80
V.3.1.2	Numerical Analysis.....	82
V.3.1.3	Numerical Comparison Between Rotor Angle Limit and PEBS.....	85
V.3.2	New England 39-Bus System.....	89
V.4	Summary.....	93
Chapter VI	Dynamic Security Dispatch.....	94
VI.1	Introduction.....	94
VI.2	Modeling of Dynamic Security Dispatch.....	96

VI.3 Case Study and Discussions.....	97
VI.3.1 Base Loading Conditions	97
VI.3.2 Heavy Loading Conditions	104
VI.3.3 Generation Rescheduling	106
VI.3.4 Computation Analysis.....	109
VI.4 Multi-contingency Constraints.....	110
VI.5 Summary	114
Chapter VII Conclusion and Future Work	115
VII.1 Conclusion	115
VII.2 Future Work	117
Reference.....	118
Appendix A WSCC 9-Bus System [135]	135
Appendix B New England 39-Bus System [55].....	137
Appendix C Numerical Solution to Ordinary Differential Equation.....	141
C1 Forth-order Runge-Kutta Method.....	141
C2 Implicit Integration Methods.....	142

LIST OF FIGURES

Figure II.1 Intuitionistic explanation for infinite-dimensional constraints	26
Figure III.1 Feasibility illustration under a standard semi-infinite constraint	30
Figure III.2 The unit disc as intersection of infinitely many halfplanes	31
Figure III.3 General scheme to solve SIP problem	36
Figure III.4 Intuitionistic explanation for L_1 norm local reduction.....	52
Figure III.5 Intuitionistic explanation for L_∞ norm local reduction.....	54
Figure IV.1 Intuitionistic explanation for local maximizer detection.....	65
Figure IV.2 Optimal solutions obtained from different starting points	68
Figure IV.3 Intuitionistic explanation of transient stability constraints.....	71
Figure V.1 Interconnected systems and their respective transmission interfaces.....	77
Figure V.2 One line diagram of the WSCC 9-bus system	80
Figure V.3 Comparison between swing curves of generator 2	81
Figure V.4 Change of maximum power flow mismatch, complementary gap and instability instant in the calculation by Method 2	82
Figure V.5 Change of maximum power flow mismatch, complementary gap and instability instant in the calculation by Method 3	83
Figure V.6 Computation related to transient stability by Method 3	84
Figure V.7 Optimization results with different rotor angle limits	86
Figure V.8 Simulation based on different rotor angle limits	86
Figure V.9 Dot product variation curve	88
Figure V.10 Swing curve based on the results by PEBS	88

Figure V.11 One line diagram of New England 39-bus system	89
Figure V.12 Dot product variation curve for Method 1	91
Figure V.13 Dot product variation curve for Method 2.....	91
Figure V.14 Swing curves for Method 1.....	92
Figure V.15 Swing curves for Method 2.....	92
Figure VI.1 Swing curves with pre-rescheduling for Case A	99
Figure VI.2 Swing curves after rescheduling for Case A	100
Figure VI.3 Swing curves with pre-rescheduling for Case B	101
Figure VI.4 Swing curves after rescheduling for Case B.....	101
Figure VI.5 Swing curves with pre-rescheduling for Case C	103
Figure VI.6 Swing curves after rescheduling for Case C.....	103
Figure VI.7 Swing curves with pre-rescheduling for Case D	105
Figure VI.8 Swing curves after rescheduling for Case D	106
Figure VI.9 Generation rescheduling in Case A	107
Figure VI.10 Generation rescheduling in Case B	107
Figure VI.11 Generation rescheduling in Case C	108
Figure VI.12 Generation rescheduling in Case D	108
Figure VI.13 Change of maximum power flow mismatch, complementary gap and instability instant in the optimization for Case B	110
Figure A.0.1 9-Bus System One-Line Diagram	135
Figure B.0.1 39-Bus System One-Line Diagram	137
Figure C.0.1 Illustration of trapezoidal rule.....	142

LIST OF TABLES

Table V.1 Optimal results obtained with the WSCC 9-bus system	81
Table V.2 Optimization results obtained with New England 39-bus system.....	90
Table VI.1 Comparison between generation pre-rescheduling and rescheduling.....	98
Table VI.2 Comparison between generation pre-rescheduling and rescheduling....	104
Table VI.3 List of severe contingencies.....	112
Table VI.4 Results of single contingency involved dispatch.....	112
Table VI.5 Results of multi-contingency involved dispatch.....	113
Table A.1 9-Bus System Load	135
Table A.2 Line and transformer data	136
Table A.3 Generator data	136
Table B.1 39-Bus System Load.....	137
Table B.2 Line and transformer data.....	138
Table B.3 Generator data	140

Chapter I INTRODUCTION

I.1 BACKGROUND AND MOTIVATION

Economics and security are often the two major inconsistent requirements for the normal operation of power systems, and it is inappropriate to treat them separately [1]. The overall aim of economy-security control is to operate the system at the lowest cost or in the most economic state, with guaranteed avoidance or survival of emergency conditions. This of necessity means operating the system within but as close as possible to its security limits.

The security constrained optimization of an electric power system is an extremely difficult task. This difficulty tends to increase with the advent of open market environment and competition in the industry [2,3]. Economical pressure and intensified transactions has forced modern electric power systems to be operated much closer to their security limits than ever before. In addition, the complexity of power systems is continually rising because of the increasing system size and stressing loads, larger power transfer over longer distance, greater interdependence among interconnected systems, more complicate coordination and interaction among various control systems, and the adoption of more advanced technologies, etc. The security of system operation is becoming more significant than ever before.

From the latest definition given by the IEEE/CIGRE Joint Task Force in [4], security of a power system refers to the degree of risk in its ability to survive imminent disturbances (contingencies) without interruption of customer service. It depends on the system operating conditions and the contingent probability of disturbances. In [2,4], security analysis is composed of both static and dynamic security analysis. However, most previous outcomes exist in the study of static security and optimal operation. The study to integrate dynamic security and economy in the same framework is still few despite the recognition of its importance.

Dynamic security requires that when any of a specified set of disturbances (e.g., outages of generators or transmission lines) occurs, a feasible operation point should be able to withstand the contingencies by surviving the subsequent transient events to arrive at an acceptable steady state operating condition after the clearance of the fault without violating equality and inequality constraints even during the transient period of the dynamics. Dynamic security must be included in the planning and operation of systems; otherwise, the system may not survive in credible contingencies, which causes huge losses, expensive control cost and even blackout throughout the system. The recently happened blackouts around the world, such as in North America and Europe in 2003 which affected a large number of customers, are good evidences that dynamic stability under large disturbances is still the most serious threat for the development of modern power systems [5-7].

Among various power system analyses, transient instability analysis is one of the essential components of dynamic security assessment. In most systems, it has been the dominant stability problem and hence more attention needs to be paid by the industry and engineers concerning system stability. When potential instability consequent to a sufficiently credible contingency is detected, preventive action has to be taken by system controllers [8].

As a result of the growing stress on today's power systems, great effort has been spent in the last decade to implement practical tools for dynamic security assessment [9]. In order to ensure the system security to survive in all possible abnormal conditions, advanced dynamic security assessment and control is in great need. There have been many technical challenging problems involving the analysis for both economics and dynamic security of power system operation within a single integrated framework, for example, preventive and emergency control [10-15], the calculation of dynamic available transfer capability in the interfaces of the interconnected grids [16-20], the dynamic security dispatch to improve the security level with less control cost [21-23], generation rescheduling [8,24-26], congestion management [27], etc. All of these efforts are attempting to formulate and solve their

corresponding problems with transient stability constraints by OPF or near OPF techniques.

Dynamic security assessment could be considered as an extended optimum power flow (OPF) problem, in which transient stability, for instance, is specifically regarded as one of the security constraints for the system operation, and the optimal objective is to be obtained under given set of system parameters by adjusting available controlling schemes. However, in practical operation, it is an extremely difficult task to reconcile the conflict between economics and security requirements in power systems operation. Early discussions on the feasibility of including stability constraints into standard OPF formulations can be found in [28,29]. Nevertheless, transient stability constrained OPF is a rather new advancement and its study is still in the experimental stage.

Conventionally, dynamic security assessment is mostly done by trial and error methods incorporating engineering experience and judgement. However, the trial process is not only time-consuming but also unsuitable for automated computation [16,30,31]. More importantly, it may sacrifice the optimality and even incur discriminations among market players in stressed power systems [32,33]. Thus, it has been one of the main challenges in OPF study to develop effective techniques for solving OPF problems with transient stability constraints efficiently [34].

Mathematically, transient stability constrained OPF is a semi-infinite programming (SIP) problem, which has finite dimension for optimal variables but infinite dimension for dynamic constraints in time domain. In this thesis, "infinite" dimension for dynamic constraints means that dynamic stability has to be satisfied in the infinitely many continuous time points in the time domain of transients. Even though the theoretical and practical manifestations of the SIP model have been established, its application for power engineering is still few [16,31,35,36] and more exploration is needed. This research aims to develop a general methodology for dynamic security constrained OPF based on SIP techniques. It provides a suitable preventive control scheme for economic system operation against dynamic security.

The framework is put forward based on the state-of-the-art transient stability analysis, OPF and SIP techniques.

I.2 CURRENT STATE OF THE ART

I.2.1 TRANSIENT STABILITY ANALYSIS

Power system transient stability has long been recognized as an important and problematic issue. As one of subcategories of rotor angle stability, transient stability is also called as large-disturbance rotor angle stability in the latest definition and classification of power system stability [4]. It is commonly concerned with the ability of the power system to maintain synchronism when subjected to a severe disturbance, such as a short circuit on a transmission line. The resulting system response involves large excursions of generator rotor angles and is influenced by the nonlinear power-angle relationship. Instability is usually in the form of aperiodic angular separation due to insufficient synchronizing torque, manifesting as first swing instability. In large power systems, transient instability may not always occur as first swing instability associated with a single mode; it could be a result of superposition of a slow inter-area swing mode and a local-plant swing mode causing a large excursion of rotor angle beyond the first swing [37]. It could also be a result of nonlinear effects affecting a single mode causing instability beyond the first swing.

Transient stability depends on both the initial operating state of the system and the severity of the disturbance. Categorized as short term phenomena, the time frame of interest in transient stability studies is usually 3 to 5 seconds following the disturbance. It may extend to 10–20 seconds for very large systems with dominant inter-area swings [4]. Up to now, methods for transient stability analysis can be categorized into time domain simulation and direct methods.

Time domain simulation is to analyze the nonlinear dynamic responses of the state variables of a power system, such as the generator rotor angles or real power outputs, via the solution of a set of differential-algebraic equations [37,38] describing

the electromechanical transients. Step-by-step numerical integration methods are used to solve the nonlinear ordinary differential equations with known initial values obtained by static power flow solution before the transients. A wide range of approaches has been reported in [39] for solving the corresponding differential-algebraic equations, depending on the numerical networks and modelling details used. The many possible schemes for the solution of the equations are characterized in [37].

Time domain simulation has been the most reliable and popular method for transient stability analysis in the industry. It is flexible in terms of different component modelling with complex details in power systems. Sufficient accurate results could be obtained even for large-scale systems with thousands of buses, branches, hundreds of generators and various controllers and relay protections. Besides, details of the time responses of dynamic parameters in the electromechanical transients could also be provided.

However, the large computation efforts and time consumption are recognized as one disadvantage of time domain simulation. For better accuracy and computation reliability, smaller steps are preferred generally, which induces more calculations. Many efforts have been made to improve the computation efficiency, in which parallel algorithms show their promising perspective with their development in decades, such as in [40-46]. In addition, large step simulations in time domain based on Taylor series expansions are studied for fast transient stability assessment [47-49].

Another commonly known disadvantage of time domain simulation is that it is incapable of providing a quantitative measure for the system stability or the stability margin. Moreover, prolonged transient simulation has to be taken to obtain reliable dynamic responses over a period of minutes. Although generator rotor angle limit is adopted as one of the criteria for practical application based on engineer experience [16], the threshold varies with different systems and is difficult to set universally. In [21], the coherency of generator rotor angles with respect to the centre of inertia (COI) is measured by six heuristic indices based on some numerical simulation experiments to predict the system stability. Some of the indices only use information

from the rotor angle first swing to reduce the computation efforts by the shortening of simulation period.

Direct methods are capable of determining the system stability "directly" without solving the complex differential-algebraic dynamic equation set. A function describing the system transient energy is computed at the end of the disturbance and compared with a critical (threshold) value of the energy for transient stability assessment. The difference between them is the energy margin, which is an indication of stability and of great interest in transient stability assessment.

Application of the energy function method to power system stability began with the early work of Magnusson [50] and Aylett [51], followed by a formal application of the more general Lyapunov's method by Gless [52], El-Abiad and Nagappan [53]. Direct methods has been academically appealing and received considerable attention since then. Much of the progress is summarized in [54-58]. Up to now, direct methods for transient stability analysis of power system are classified into two categories. One is based on transient stability energy function, including relevant or controlling instability equilibrium point (RUEP or CUEP) method [59-61], potential energy boundary surface (PEBS) method [62-64], boundary of stability region based controlling unstable equilibrium point (BCU) method [63,65]; the other is based on extended equal area criterion (EEAC) method [66-69].

Compared with time domain simulation, direct methods are less computational demanding, capable of providing a quantitative measure for the transient stability margin, and suitable for fast stability limit analysis using dynamic sensitivity techniques. However, the accuracy and reliability of direct methods is not guaranteed, for some instances due to the application of approximated critical transient margin with various assumptions, which cumber their widespread usage in the industry. More importantly, detailed models of the system components, including the synchronous machine, the excitation system dynamics, and various power electronics devices, often have to be included for realistic modelling of practical power systems, which will complicate the system model and increase the computation remarkably.

Although large amount of efforts and progress have been made over the years, the accuracy and reliability are in doubt while the enhanced direct methods become much more complicated and hence computational demanding.

Attempts, such as hybrid methods in [70,71], are taken to combine the time domain method and the TEF evaluation to produce stability indices using the concept of transient energy margin and simulated system responses. Though implementation difficulties have been encountered, this approach is promising.

I.2.2 OPTIMAL POWER FLOW WITH TRANSIENT STABILITY CONSTRAINTS

Optimal power flow (OPF), as a powerful tool to weaken the increasing exacerbated conflict between economy and security, was introduced originally as a "network constrained economic dispatch" by Carpentier [72] and formulated as optimal power flow by Dommel and Tinney [73]. The main purpose of an OPF program is to determine the optimal operating state of a power system by optimizing specific objectives while satisfying certain specified physical and operating constraints.

Practical on-line implementation of OPF is to be integrated into Energy Management System (EMS) in an automatic (closed loop) control mode [34]. Power system operating conditions are classified into five states: Normal, Alert, Emergency, In Extremis, and Restorative states [37]. The main goal of system operators in regional control centres or independent system operators (ISO) is to operate and maintain power systems in normal secure state with time-varied operating conditions. Power system state estimation is provided based on the collected measurements in the supervisory control and data acquisition (SCADA) system and on the assumed system status at the SCADA scan rate frequency. It will then be passed on to all the EMS application functions. For credible contingency analysis, on-line fast stability assessment is continuously triggered based on the current system snapshot for the next target window, 15-30 minutes. Preventive strategies based on OPF are expected to be triggered by changing operation state for the enhancement of the system

security from alert state to normal state.

Many research efforts have been made in preventive and corrective actions based on OPF for static security constrained economic dispatch and proved quite effective [1,28,29,74-80]. However, despite the idea of transient stability constrained OPF has been around for years, few effective solutions have as yet been proposed until now. The main obstacle faced is that the complexity involved for OPF with transient stability constraints is several orders of magnitude higher than that of traditional OPF with merely static constraints. Different from traditional constraints in static state, the add-on transient stability constraints are with the differential-algebraic equations (DAEs) for the dynamic transients, whose variables are usually defined in the functional space [31]. In particular, there are two major difficulties in tackling the problem of transient stability constrained OPF. The first is how to formulate the mathematical model, including the incorporation of transient stability constraints in OPF. If the transient stability constraints are introduced directly into OPF, the OPF will be a semi-infinite programming problem since the dimension of transient stability constraints is infinite. Traditional NLP methods for OPF study cannot handle SIP problems. The second is how to solve this problem effectively and efficiently.

So far, several attempts have been made to determine the OPF imbedded with transient stability constraints. Based on how the constraints are handled [14,26], they can be classified as "sequential" and "global" approaches.

- Sequential approach. This is a divide and conquer approach, in which the subproblems of OPF and transient stability analysis are solved in sequence separately [10,14,17-19,23,24,26,27,81,82]. In [10], an analytic sensitivity method is proposed based on EEAC and its application is prospected for transient security dispatch. In [14,19], generation shift scheme from critical machines based on the single machine equivalent (SIME) control is used to obtain near optimal solution. In [17,18,24,26,27,81,82], the sensitivities of the energy margin to system parameters, such as generation output, the total

system load, etc., are used to determine new schedules of stability limits or transmission interface power flow limits using optimization techniques. In [13], linear relationships between critical clearing time (CCT) and generator rotor angle, which is incorporated in OPF, is used for transient stability preventive control, although the relationships are not always true. In [13], generation is shifted from the most advanced generators to the least based on trajectory sensitivity, which is incorporated in OPF by the modification of generation output limits.

- Global approach. This is an integrated approach in which OPF with transient stability constraints is solved as a single problem [12,16,20,22,31,35,36,83,84]. In [12,16,20,22,35,83], transient stability constraints in a time domain are discretized into a set of algebraic (in)equations by specific time steps. Afterward, they are included in standard OPF program and solved. However, the number of the replacing constraints is proportional to the number of discretized intervals and tends to be large for good accuracy. The high-dimensional constraints may spoil the computational efficiency in the optimization. In order to keep the dimension of constraints lower, in [31,36], integration over the regions where the transient stability constraints are violated is used to replace the constraints. In [84], an algorithm based on control variable parameterization is implemented to solve the formulated dynamic-constrained optimization problem. But its application is still limited in a 9-bus system.

There are also some other methods applied in OPF with transient stability constraints, such as artificial neural network (ANN) [11,85].

It is noted that in the sequential approach, the transient stability constraints are not introduced directly into OPF. The true optimal solution may not be obtained. Sometimes, conservative solution is produced with the sacrifice in economic operation [31]. Conceptually, the global approach is more appealing as it handles the problem as a whole and hence is more capable to provide a true optimal solution,

which is more preferred by the system operator and the electric market participants. However, the global approach has to deal with the complicated problem of introducing transient stability constraints into OPF.

Mathematically, global transient stability constrained OPF is a SIP problem with finitely many decision variables for specific operating point and infinitely many transient stability constraints different from other finitely many static state constraints. Here, "infinite" constraints for transient stability are referred to that the stability should be satisfied in every time point in the whole studied transient. Obviously, the number of time points in transient is infinite. Therefore, standard programming methods fail to solve transient stability constrained OPF precisely and effectively. Instead, advanced SIP techniques play a very important role in the development of solution framework for a generic problem, which can be formulated as transient stability constrained OPF. Both the calculation of available transfer capability and dynamic security dispatch are two important problems in power system study, in which the satisfaction for transient stability is a must-do. In Chapter V and VI of this thesis, these two problems are modelled as SIP problems and solved respectively.

I.2.3 SEMI-INFINITE PROGRAMMING

A semi-infinite programming (SIP) problem is referred to an optimization problem with finitely many variables and, in contrast to finite optimization problems, infinitely many inequality constraints. SIP has been an exciting part of mathematical programming since the middle of the 20th century, such as in [86], standard convex program is formulated as a semi-infinite linear program.

There are numerous practical problems as well as theoretical problems naturally arising in optimal control, approximation theory, and engineering applications. The model contains at least one inequality constraint for each value of a parameter and the parameter, representing time, space, frequency etc., varies in a given domain and thus can be formulated as semi-infinite programs. In [87], a large class of

engineering design problems such as electronic circuit design, seismic-resistant structure design, and single-input single-output control systems design can be formulated as nonlinear semi-infinite programs. In [88], a survey of control system design via semi-infinite optimization is presented, in which typical control system design problem is transcribed into SIP problem and computational issues involved are discussed. In [89], engineering applications of SIP are reviewed and first order nondifferentiable optimization algorithms are constructed to solve the SIP problems. An overview of applications, algorithms and theories in this area is presented in [90].

So far there are three categories of numerical methods for solving semi-infinite programs: discretization methods, local reduction methods and exchange methods [91]. In the first category, a sequence of relaxed problems with a finite number of constraints is solved according to a predefined or adaptively controlled grid generation scheme [91-94]. The local reduction approach of the second category replaces a SIP problem by a locally equivalent problem with a finite number of implicitly defined inequality constraints or equivalently a system of nonlinear equations with finitely many unknowns [95-98]. In the third category, typical exchange methods consist of two phases: the purification phase providing an extreme point and the pivoting phase generating a sequence of linked extreme points leading to an optimal solution [90,99]. General remarks are presented for these three categories of methods in [90], in which fast convergence and fewer constraints in the related subproblems by reduced methods are notified.

Even though the theoretical and practical manifestations of the SIP model have been established, its application on the dynamic security constrained OPF is few and limited to two approaches in general up to now. One is based on discretization methods, such as in [12,16]. Further, in [22,35], multi-contingency transient stability constraints are incorporated. The other is based on transcription techniques of reduced methods, such as in [31,36]. However, the drawback of the former is the computational inefficiency due to the high-dimensional replacing constraints for the infinite constraints. Although the later can keep the dimension of constraints low by

transcription, it is not attractive either since it requires accurate integration over the regions where the infinite constraints are violated.

I.3 PRIMARY CONTRIBUTIONS

Security and economy must be reconciled with each other in modern deregulated power systems. The main objective of this research is to develop a novel methodology to deal with a category of problems related with both dynamic security and economy, which can be modelled as transient stability constrained OPF problems.

In summary, this thesis has made the following original contributions:

- Transient stability constrained OPF problems are generalized mathematically to be SIP problems with finitely many variables and finitely many constraints in time domain. Numerical methods for SIP are extended to locally reduce transient stability constraints to be finite-dimensional constraints based on L_1 and L_∞ norm. Thus transient stability constrained OPF is equivalently converted to an equivalent conventional OPF, which is solvable by conventional OPF methods.
- The direct primal dual interior point method, as a suitable nonlinear programming method, is used to solve the equivalent problem. Different from conventional OPF, the theoretical difficulties in forming the Jacobian and Hessian matrices of the transient stability constraints are overcome with the employment of implicit functions. The multi-local optimization subproblem in L_∞ norm local reduction method is solved by the application of intermediate value theorem for transient stability constraints according to its specific features.
- Effective measures are proposed to improve the performance of the implementation. The most effective section of transient stability constraints, as a novel concept, is proposed to reduce the functional space and hence to improve the computation efficiency remarkably, which is validated by

numerical tests. Besides, improved BFGS (Broyden-Fletcher-Goldfarb-Shanno) method is employed instead of Newton method to simplify the complicated derivation of Hessian matrix, in which only the difficult computation part of the Hessian matrix related to the transient stability constraints is updated approximately in BFGS formulation in each iterate.

- The calculation of dynamic available transfer capability (ATC) and dynamic security dispatch are formulated as transient stability constrained OPF problems in this thesis respectively. The effectiveness of the proposed methodology is validated for such categories of problems with dynamic security and economy considered. Multi-contingency cases are able to be dealt with simultaneously to obtain an economically secure solution for a credible contingency set.

I.4 ORGANIZATION OF THIS THESIS

This thesis consists of seven chapters.

This chapter, Chapter I, first states the background and motivation of this research, followed by the brief description on the current state of the art. A list of original contributions of this thesis is presented in section 3. Finally, the last section presents organization of the thesis.

In chapter II, conventional OPF problem is introduced. Dynamic power system model is described briefly for the transient stability assessment. Two indices based on rotor angle limit and PEBS concept, respectively, are proposed and compared with each other. Optimization of power flow with transient stability constraints is generalized as a SIP problem with the introduction of the proposed transient stability indices to the conventional OPF.

In chapter III, theoretical foundation and solution methods of SIP are presented and developed for the transformation of transient stability constraints in OPF problem. Firstly, preliminaries of SIP problems are introduced. Generalized KKT optimality conditions for SIP are extended. General scheme of the solution of SIP

problems is given based on discretization and local reduction methods, by which SIP problems are recast into equivalent nonlinear programming problems with a finite number of constraints under appropriate assumptions. In particular, L_1 and L_∞ penalty functions are employed for the implementation of local reduction. Transient stability constraints are locally reduced to be finite-dimensional constraints, which makes transient stability constrained OPF solvable through traditional nonlinear programming methods.

In chapter IV, the transient stability constrained OPF is solved by the direct nonlinear primal-dual interior point method. The theoretical difficulties in deriving the Jacobian and Hessian Matrices of the transient stability constraints are overcome based on implicate function and chain rule. Intermediate value theorem is applied to solve the local optimization subproblem in the local reduction of transient stability constraints. The overall algorithm is then presented. An improved BFGS method with superlinear convergence is exploited to avoid the complicated derivation of Hessian matrix. A new concept referred as "the most effective section" of transient stability constraints is proposed to alleviate the huge computational efforts and improve the convergence of the optimization calculation.

In chapter V, the study of transient stability constrained OPF is applied in the calculation of dynamic available transfer capability (ATC). The calculation of dynamic ATC is formulated as an OPF problem with security constraints, especially transient stability constraints. SIP techniques are employed and fully tested on the ATC calculation in the WSCC 9-bus and New England 39-bus systems.

In chapter VI, the study of transient stability constrained OPF is applied for dynamic security dispatch. Dynamic security dispatch is an effective preventive control to improve the security level of the systems by adjusting the controllable parameters. Dynamic security dispatch in this chapter is implemented as an extended OPF problem to minimize the economic cost and survive in credible contingencies as well. The effectiveness of the proposed method is fully validated in the New England 39-bus system. Multi-contingency is also considered in the dynamic security dispatch

for plural credible contingencies simultaneously.

Chapter VI gives the conclusion of this thesis and the possible future work.

Chapter II TRANSIENT STABILITY CONSTRAINED OPF

The demand for optimal power flow (OPF) tools has been on the increase since its initial formulation in the 1960's [72,73] for assessing state and recommended control actions for off-line and on-line studies. Transient stability, as one of the essential components of dynamic security assessment, has been noticed to be studied as constraints of OPF for years. In [34], it is recognized as a challenge in OPF study to propose optimal preventive or correction control schemes. In this chapter, the OPF problem is introduced briefly and the model of transient stability constrained OPF is formulated directly by the introduction of transient stability as one constraint in OPF.

II.1 FORMULATION OF CONVENTIONAL OPF PROBLEM

Optimal power flow (OPF) problem is formulated to obtain an optimal solution of a specific power system objective function by adjusting system parameters and controllable variables while satisfying a variety of equality and/or inequality constraints.

Although there are different OPF formulations for specific objectives and constraints, conventional OPF problem can be generalized as the following nonlinear programming problem:

$$\min f(\mathbf{x}_0, \mathbf{y}) \quad (2.1)$$

$$s.t. \quad \mathbf{g}(\mathbf{x}_0, \mathbf{y}) = \mathbf{0} \quad (2.2)$$

$$\mathbf{H}(\mathbf{x}_0, \mathbf{y}) \leq \mathbf{0} \quad (2.3)$$

where $\mathbf{x}_0 \in \mathbf{R}^{n_x}$ and $\mathbf{y} \in \mathbf{R}^{n_y}$ are the decision variable vectors of the system. Vector \mathbf{x}_0 is the time-dependent variable vector describing the static state of the system at a specified time instance (e.g. $t = 0$), including generation output, bus voltage, etc. Vector \mathbf{y} is time-independent and usually includes shunt capacitor, and the tap position of the transformer, etc, which is also stated as control variable related to

control actions. $f : \mathbf{R}^{n_x} \rightarrow \mathbf{R}$ is the OPF objective function, which is different with reference to various power system problems, such as unit commitment, reactive power dispatch, power market, etc. In this thesis, the detailed optimization problems of available transfer capability and dynamic security dispatch are studied as applications of OPF in the Chapter V and VI, respectively.

This nonlinear programming optimization problem is subjected to a number of equality and inequality constraints as follows:

- Equality constraints $\mathbf{g} : \mathbf{R}^{n_x+n_y} \rightarrow \mathbf{R}^{n_g}$

Active and reactive power flow balance in the system is formatted as polar coordinate form power flow equations as

$$P_{Gi} - P_{Di} - V_i \sum_{j \in I} V_j (G_{ij} \cos \theta_{ij} + B_{ij} \sin \theta_{ij}) = 0 \quad (2.4)$$

$$Q_{Gi} - Q_{Di} - V_i \sum_{j \in I} V_j (G_{ij} \sin \theta_{ij} - B_{ij} \cos \theta_{ij}) = 0 \quad (2.5)$$

where $i \in S_N$ is the index set of buses. P_{Gi} and Q_{Gi} are the active and reactive power generations at bus i . P_{Di} and Q_{Di} are the active and reactive power loads at bus i . V_i and θ_i are the voltage magnitude and its phase angle at bus i , and $\theta_{ij} = \theta_i - \theta_j$. $G_{ij} + jB_{ij}$ is the transfer admittance between bus i and j .

- Inequality constraints $\mathbf{H} : \mathbf{R}^{n_x+n_y} \rightarrow \mathbf{R}^{n_h}$

The steady-state operation limits of the system include the upper and lower limits of the generator outputs, bus voltage magnitudes, transformer taps, and power flow on transmission lines as

$$P_{Gi \min} \leq P_{Gi} \leq P_{Gi \max} \quad i \in S_G \quad (2.6)$$

$$Q_{Gi \min} \leq Q_{Gi} \leq Q_{Gi \max} \quad i \in S_R \quad (2.7)$$

$$V_{i \min} \leq V_i \leq V_{i \max} \quad i \in S_N \quad (2.8)$$

$$T_{i \min} \leq T_i \leq T_{i \max} \quad i \in S_T \quad (2.9)$$

$$P_{ij \min} \leq P_{ij} \leq P_{ij \max} \quad (i, j) \in S_{CL} \quad (2.10)$$

where S_G and S_R are the index sets of active and reactive power sources, respectively. S_T is the index set of transformers. T_i is the i -th transformer tap. S_{CL} is the index set of constrained transmission lines. P_{ij} is the active power flow on the transmission line $i - j$.

Clearly the OPF model (2.1-2.3) is with finitely many decision variables for static system performance and finitely many constraints. It can be solved by any appropriate standard nonlinear programming methods, such as interior point method, sequential quadratic programming (SQP), etc. Primal-dual interior point method is employed in this research and described in details in Chapter IV.

II.2 TRANSIENT STABILITY ASSESSMENT

Besides the constraints of steady-state operation in (2.2-2.3), more importantly, a practical power system should be operated to be able to dynamically survive when large disturbances or event disturbances occur, such as short-circuits, generator outages, sudden large load changes, etc. Therefore, transient stability is especially important to evaluate the practicability of the OPF solution. It is inevitably necessary to adopt a suitable transient stability index for inclusion in the OPF model.

II.2.1 POWER SYSTEM MODEL

Mathematically, power systems are compactly described by a set of non-linear differential-algebraic equations (DAEs)

$$\dot{\mathbf{x}}(t) = \mathbf{F}(\mathbf{x}(t), \mathbf{y}) \quad t \in T \quad (2.11)$$

$$\mathbf{G}(\mathbf{x}(t), \mathbf{y}) = \mathbf{0} \quad t \in T \quad (2.12)$$

The differential equation \mathbf{F} describes the dynamics associated with the generators, the excitation systems, the prime movers and the speed governors. The algebraic equation \mathbf{G} represents the network power balance equations. $\mathbf{x}(t)$ is the state variable vector including all dynamic components in the system, such as rotor angles of generators, which is time-dependent. \mathbf{y} is algebraic variable vector as

defined in (2.1-2.3), which are generally independent of transient stability analysis. $T = [t_0, t_{cl}) \cup (t_{cl}, t_e]$ is the studied transient process from the time t_0 of the occurrence of the disturbance to the clearing time t_{cl} and to the end of the study time t_e .

For each contingency, it should be noted that the dynamics of the disturbed system can generally be divided into three stages [37]:

- pre-disturbance at $t = t_0$

$$\mathbf{F}(\mathbf{x}(t), \mathbf{y}) = \mathbf{0} \quad (2.11.a)$$

$$\mathbf{G}(\mathbf{x}(t), \mathbf{y}) = \mathbf{0} \quad (2.12.a)$$

- during-disturbance for $t \in (t_0, t_{cl})$

$$\dot{\mathbf{x}}(t) = \mathbf{F}_1(\mathbf{x}(t), \mathbf{y}) \quad (2.11.b)$$

$$\mathbf{G}_1(\mathbf{x}(t), \mathbf{y}) = \mathbf{0} \quad (2.12.b)$$

- post-disturbance for $t \in (t_{cl}, t_e]$

$$\dot{\mathbf{x}}(t) = \mathbf{F}_2(\mathbf{x}(t), \mathbf{y}) \quad (2.11.c)$$

$$\mathbf{G}_2(\mathbf{x}(t), \mathbf{y}) = \mathbf{0} \quad (2.12.c)$$

Consider a power system consisting of ng generators and N buses. For simplicity, classical generator model for transient stability is used and load is modelled as constant impedance determined from initial (pre-disturbance) conditions. The dynamic model for the i -th synchronous generator can be formulated by the following differential equations:

$$\begin{cases} \dot{\delta}_i = \omega_i \\ \dot{\omega}_i = \frac{\omega_N}{M_i} [P_{mi} - P_{ei} - D_i \omega_i] \end{cases} \quad i \in \mathcal{S}_g \quad (2.13)$$

where

$$P_{ei} = \sum_{j=1}^{ng} E_i E_j (B_{ij} \sin \delta_{ij} + G_{ij} \cos \delta_{ij}). \quad (2.14)$$

P_{mi} and P_{ei} are the mechanical power input and electric power output of generator i respectively. E_i is the internal bus voltage of generator i . δ_i and ω_i are

rotor angle and rotor speed of generator i respectively. M_i is the moment of inertia of the generator i . ω_N is the base system radian frequency and $\omega_N = 2\pi f_0$. f_0 is the nominal system frequency. \mathcal{S}_g is the index set of generators. $Y_{ij} = G_{ij} + jB_{ij}$ is the admittance matrix for the reduced network with only the generator internal nodes preserved.

The power network is modeled by an algebraic equation

$$\mathbf{I} = \mathbf{Y}\mathbf{E} \quad (2.15)$$

where \mathbf{I} is the vector of node currents, which is also the generator currents.

Practically, time domain simulation is employed for transient stability assessment. The DAEs are solved by using step by step numerical integration techniques. Forth-order Runge-Kutta (R-K) method is adopted in this thesis for the numerical computation, see in Appendix C.

II.2.2 TRANSIENT STABILITY INDEX BASED ON ROTOR ANGLE LIMIT

Transient stability index based on rotor angle limit obtained from time-domain simulation is proposed here. For very stable cases, the rotor angle of each machine move coherently with the centre of inertia (COI) whose position is defined as

$$\delta_{COI} = \frac{\sum_{i=1}^{ng} M_i \delta_i}{M_T} \quad (2.16)$$

where $M_T = \sum_{i=1}^{ng} M_i$. In other word, the variation of each machine angle with reference to the COI will stay within a certain boundary. For unstable cases, there is at least one machine whose angle moves away from the COI and eventually lost of synchronism. Thus the transient stability index is defined as the deviation margin of rotor angles with respect to COI less a specified threshold as

$$h_i = \left| \delta_i - \delta_{COI} \right| - \delta_{\max} \leq 0 \quad i \in \mathcal{S}_g \quad (2.17)$$

in the study period T . δ_{\max} is the maximum allowable deviation of the rotor angle. For unstable cases, the simulation is terminated if one machine's angle reaches δ_{\max} degrees. Obviously, the smaller of the instability instant detected, the more

severe the contingency is.

Coherent indices based on rotor angle limits with respect to COI are proposed in [21]. It is found that rotor angle limit with respect to COI in the first swing has good accuracy and is consistent with a long period of time domain simulation. Thus shorter period for simulation could be used to reduce the computation efforts for stability assessment.

II.2.3 TRANSIENT STABILITY INDEX BASED ON PEBS

As an alternative approach to transient stability assessment, direct methods are capable of providing a quantitative measure for system transient stability margin. Power system under transient conditions can be described as a ball rolling on a bowled-shaped potential energy surface, which depends on the post-contingency network configuration. The stable equilibrium point (SEP) is surrounded by a set of unstable equilibrium points (UEP). The surface connecting all the UEPs is called potential energy boundary surface (PEBS). In [63], a theoretical foundation for the PEBS method is given for machines modelled classically. PEBS can be defined as *the locus of the local maxima of potential energy on all rays emanating from SEP* [59,105].

Furthermore, it is assumed that all unstable system trajectories cross the PEBS, whereas all stable trajectories remain inside the PEBS. The assumption is based on the recognition of the occurrence of transient instability when the system trajectories cross the potential energy maxima around the SEP with a residual kinetic energy. Remarkably, this test of stability is also valid for multi-swing instability. As illustrated in [54], both in the first and multi-swing instability cases, the PEBS is crossed by unstable trajectories.

Therefore, the transient stability constraints can be defined as to prevent the system trajectory crossing the PEBS. For the application of PEBS method, it is convenient to describe the transient behaviour of the system with the generator rotor angles expressed with respect to the COI. For instance, the equations of motion of

the i th generator becomes

$$\begin{cases} \dot{\tilde{\delta}}_i = \tilde{\omega}_i \\ M_i \dot{\tilde{\omega}}_i = P_{mi} - P_{ei} - \frac{M_i}{M_T} \cdot P_{COI} \end{cases} \quad (2.18)$$

where $P_{COI} = M_T \dot{\omega}_{COI} = \sum_{i=1}^{ng} (P_{mi} - P_{ei})$. $\tilde{\delta}$ and $\tilde{\omega}$ are the vector of rotor angles δ and rotor speed ω with reference to their COI respectively as

$$\tilde{\delta} = \delta - \delta_{COI} \quad (2.19)$$

$$\tilde{\omega} = \dot{\tilde{\delta}} - \dot{\delta}_{COI} = \omega - \omega_{COI} \quad (2.20)$$

and

$$\omega_{COI} = \frac{\sum_{i=1}^{ng} M_i \omega_i}{\sum_{i=1}^{ng} M_i} \quad (2.21)$$

$$\sum_{i=1}^{ng} M_i \tilde{\delta}_i = 0 \quad (2.22)$$

The potential energy is given as [57]

$$V_{PE}(\tilde{\delta}) = - \sum_{i=1}^{ng} \int_{\tilde{\delta}_i^s}^{\tilde{\delta}_i} f_i(\tilde{\delta}) d\tilde{\delta}_i \quad (2.23)$$

where $f(\tilde{\delta}) = [f_1, \dots, f_{ng}]$ is the vector of the accelerating power of rotors with the centre of inertia (COI) as reference in the scenario of credible contingency:

$$f_i(\tilde{\delta}) = P_{mi} - P_{ei} - \frac{M_i}{M_T} \cdot P_{COI} \quad i \in \mathbf{S}_g \quad (2.24)$$

$\tilde{\delta}^s$ is the vector of rotor angles δ^s at post-disturbance SEP with reference to their COI respectively as

$$\tilde{\delta}^s = \delta^s - \delta_{COI} \quad (2.25)$$

Assume the linear path for system trajectory, we have

$$\tilde{\delta} = \tilde{\delta}^s + \alpha (\tilde{\delta} - \tilde{\delta}^s) = \tilde{\delta}^s + \alpha \Delta \tilde{\delta} \quad (2.26)$$

and approximated potential energy

$$V_{PEapprox}(\tilde{\delta}) = -\sum_{i=1}^{ng} \int_0^{\alpha} f_i(\tilde{\delta}^s + \alpha\Delta\delta) \Delta\tilde{\delta}_i d\alpha \quad (2.27)$$

Thus mathematically, PEBS is deduced as

$$\frac{dV_{PEapprox}}{d\tilde{\delta}} = 0 \quad (2.28)$$

that is

$$-\sum_{i=1}^{ng} f_i(\tilde{\delta}^s + \alpha\Delta\delta) \Delta\tilde{\delta}_i = 0 \quad (2.29)$$

Therefore, PEBS is described as the following dot product.

$$P = \left[\mathbf{f}(\tilde{\delta}) \right]^T \cdot (\tilde{\delta} - \tilde{\delta}^s) = 0 \quad (2.30)$$

The application of PEBS is that the dot product (2.30) is negative inside the PEBS and positive outside. In [105], it is said *as long as the dot product evaluated is less than zero at each i^{th} time step of the discretized trajectory, the system is STABLE.*

Therefore, the transient stability index can be defined based on PEBS as

$$P = \left[\mathbf{f}(\tilde{\delta}) \right]^T \cdot (\tilde{\delta} - \tilde{\delta}^s) \leq 0 \quad (2.31)$$

II.2.4 REMARKS ON THE TWO INDICES OF TRANSIENT STABILITY

It is not easy to tell which index performs better for stability assessment and is more suitable to be introduced in OPF study. In this section, some general remarks are provided for the two indices of transient stability.

The index based on rotor angle limit has been widely adopted in many applications for its consistence with industry practice and acceptance for utility engineers. Firstly, with the lack of any generic methods, inequation (2.17) could be the most direct method for measuring the stability region of dynamic system [16]. Secondly, suppose the generators are approximately separated into two groups during the transient duration, then the well-known equal area criteria indicates that the relative rotor angle between the two groups of generators should always be smaller than the extreme 180 degrees, otherwise the system is unstable. Thirdly, a real-world power system should be operated such that any generator rotor angle will not be greater than a threshold (like the extreme case, 180 degrees). If a generator's rotor

angle is larger than such a threshold, the generator will be tripped off by out-of-step relay to protect it from being damaged [57].

The pitfall of index based on rotor angle limit is that the threshold is arbitrary in nature and would vary with different systems. If the threshold is too relaxed, systems may be unstable even if the limit has not been exceeded in the study period; on the contrary, if the threshold is too strict, the operation tends to be conservative and less economic. Moreover, from the optimization point of view, the index is an ng -dimensional vector, where ng is the number of machines, because the coherency of generator rotor angles with respect to COI should be maintained at each time step during dynamic simulation.

The situation gets better for index based on PEBS. This index can be regarded as a general criterion for different systems because it describes the performance of system. Another advantage is the dimension of this index is only one. The reason is that the PEBS criterion is referred to the whole system but not to each machine like rotor angle limit. Thus the dimension of transient stability constraint in OPF model is independent of the number of machines in the system if the constraint is based on PEBS criterion. However, the formulation of this index is more complicated, especially the computation of its derivative in the optimization process. It is also noted that the accuracy of PEBS method could be suffered with ill boundary surface and the assessment tends to be optimistic [56].

Power systems operation should be capable to survive in a set of credible contingencies. In this thesis, the criteria for transient stability are employed with reference to the two indices, rotor angle limit and PEBS, respectively. The criteria are introduced as transient stability constraints in OPF, which can be written compactly as

$$U^k(\mathbf{x}^k(t), \mathbf{y}^k) \leq 0 \quad (2.32)$$

where $k \in I_c$ and $U : \mathbf{R}^{n_x+n_y} \times T \rightarrow \mathbf{R}^{n_u}$. I_c is the index set of credible contingencies. Numerical comparison for the two kinds of indices is given in the later chapters.

II.3 TRANSIENT STABILITY CONSTRAINED OPF

The transient stability constrained OPF problem can be formulated as:

$$\min f(\mathbf{x}_0, \mathbf{y}) \quad (2.33)$$

$$s.t. \quad \mathbf{g}(\mathbf{x}_0, \mathbf{y}) = \mathbf{0} \quad (2.34)$$

$$\mathbf{H}(\mathbf{x}_0, \mathbf{y}) \leq \mathbf{0} \quad (2.35)$$

$$\mathbf{U}^k(\mathbf{x}^k(t), \mathbf{y}) \leq \mathbf{0} \quad t \in \mathbf{T}, k \in \mathbf{I}_c \quad (2.36)$$

where both variable vectors $\mathbf{x}_0 \in \mathbf{R}^{n_x}$ and $\mathbf{y} \in \mathbf{R}^{n_y}$, and functions $f: \mathbf{R}^{n_x} \rightarrow \mathbf{R}$, $\mathbf{g}: \mathbf{R}^{n_x+n_y} \rightarrow \mathbf{R}^{n_g}$ and $\mathbf{H}: \mathbf{R}^{n_x+n_y} \rightarrow \mathbf{R}^{n_H}$ are the same with the conventional OPF problem (2.1-2.3). $\mathbf{U}: \mathbf{R}^{n_x+n_y} \times \mathbf{T} \rightarrow \mathbf{R}^{n_u}$ is dynamic constraints to ensure the dynamic security of system disturbed by contingencies in the transient. It can be formulated either as (2.17) based on rotor angle limits or as (2.31) based on PEBS concept although the property of the constraint is different. $\mathbf{x} \in \mathbf{R}^{n_x}$ is a time-dependent variable vector related to the dynamic state of the system, such as the generation output, rotor angle, etc. \mathbf{x}_0 represents the initial value of \mathbf{x} at $t=0$.

Clearly, without inequality (2.36), the OPF model (2.33-2.35) is with finite optimal variables for static system performance and finite constraints. It can be solved by any appropriate standard programming method. The add-on transient stability constraints of inequality (2.36) become active in case instability is detected for the relative credible contingencies. An economically and securely viable operation is needed to be proposed by the solution of OPF (2.33-2.36) for the security and economy of the system.

However, inequality (2.36) for transient stability constraints is obviously different with the other conventional inequality constraints compactly describing as (2.35). Inequality (2.36) is infinite-dimensional in the functional space to ensure transient stability being satisfied during the transient period \mathbf{T} . In other word, even for single contingency, transient stability should be satisfied in every time point of the whole studied transient as shown in Figure II.1.

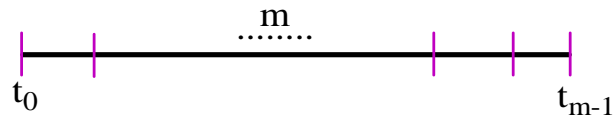


Figure II.1 Intuitionistic explanation for infinite-dimensional constraints

The transient period T is continuous and undividable, which causes the difference of the values of $U(x(t), y)$ due to the time-dependent variable $x(t)$ at different time t . Therefore, in the transient period T there are infinitely many constraints for transient stability for the infinitely many time points, or slices in Figure II.1, in the time domain.

Thus, mathematically, the OPF problem (2.33-2.36) is a semi-infinite programming (SIP) problem with finitely many optimal variables with infinitely many constraints for the introduction of transient stability constraints. Standard finite programming methods are incapable to handle this problem directly. The basic underlying difficulty in extending suitable standard algorithms of non-linear programming to the SIP case is to replace the infinitely many constraints of the latter by finite constraints. SIP methods should be implemented to transcribe the SIP problem appropriately into a finite programming problem. SIP is presented in chapter III and specifically employed for transient stability constrained OPF.

II.4 SUMMARY

This chapter deals with the formulation of transient stability constrained OPF.

Conventional OPF in static state is introduced firstly. Dynamic power system model is briefly presented for transient stability assessment. Two indices for transient stability based on rotor angle limit and PEBS concept are proposed. The properties of the two indices are compared theoretically. Optimization of power flow with transient stability constraints is generalized as a SIP problem, with finitely many variables and finitely many constraints, by introducing the proposed indices for

transient stability to the conventional OPF directly.

Chapter III SEMI-INFINITE PROGRAMMING AND TRANSFORMATION FOR TRANSIENT STABILITY CONSTRAINTS

This chapter presents the essential concepts for semi-infinite programming (SIP) problems in optimization theory, and describes numerical methods for the solution. The numerical methods are employed especially for the solution of transient stability constrained OPF.

Firstly, a few basic terms for mathematical analysis are defined as follows [101,106]:

- 1) A set $A \subset \mathbf{R}^n$ is open if and only if for every point $\mathbf{x}^* \in A$ there exists a $\rho > 0$ such that $\{\mathbf{x} \in \mathbf{R}^n \mid \|\mathbf{x} - \mathbf{x}^*\| \leq \rho\} \subset A$.
- 2) A set $A \subset \mathbf{R}^n$ is closed if and only if A^c is open, where c denotes the compliment.
- 3) A set $A \subset \mathbf{R}^n$ is bounded if and only if there exists a $\rho > 0$ such that $A \subset \{\mathbf{x} \in \mathbf{R}^n \mid \|\mathbf{x}\| \leq \rho\}$.
- 4) A set $A \subset \mathbf{R}^n$ is compact if and only if it is bounded and closed.
- 5) The interior of a set $A \subset \mathbf{R}^n$ is equal to the union of all open sets contained in A .
- 6) A set $A \subset \mathbf{R}^n$ has an interior if and only if the interior of A is non-empty.
- 7) A set $A \subset \mathbf{R}^n$ is convex if and only if for any $\mathbf{x}', \mathbf{x}'' \in A$ and $\lambda \in [0,1]$, $(\lambda \mathbf{x}' + (1-\lambda)\mathbf{x}'') \in A$.
- 8) A function is continuously differentiable if it has continuous derivatives.
- 9) A function $f : \mathbf{R}^n \rightarrow \mathbf{R}^m$ is Lipschitz continuous on the set $X \in \mathbf{R}^n$ if and only if there exists an $L < \infty$ such that $\|f(\mathbf{x}') - f(\mathbf{x}'')\| \leq L \|\mathbf{x}' - \mathbf{x}''\|$ for all $\mathbf{x}', \mathbf{x}'' \in A$.

III.1 PRELIMINARIES

Consider general SIP optimization problems of the form [107]

GSIP: minimize f on the feasible set M

with

$$M = \{ \mathbf{x} \in \mathbf{R}^n \mid g_i(\mathbf{x}, \mathbf{y}) \leq 0 \text{ for all } \mathbf{y} \in Y, i \in I; h_j(\mathbf{x}) = 0, j \in J \}$$

where I and J are finite index sets whereas the index set Y is of infinite cardinality and in many applications compact. $\mathbf{x}^* \in \mathbf{R}^n$ is called feasible for the programming problem if $\mathbf{x}^* \in M$ as

$$\begin{aligned} g_i(\mathbf{x}^*, \mathbf{y}) &\leq 0 \quad \forall \mathbf{y} \in Y, i \in I \\ h_j(\mathbf{x}^*) &= 0 \quad j \in J \end{aligned}$$

In full generality, Y is allowed to depend on the decision variable \mathbf{x} and described by functional constraints as

$$Y(\mathbf{x}) = \{ \mathbf{y} \in \mathbf{R}^m \mid u_k(\mathbf{x}, \mathbf{y}) \leq 0, k \in K; v_l(\mathbf{x}, \mathbf{y}) = 0, l \in L \}$$

with finite index sets K and L .

A simple but instructive example is given to illustrate the concept of general semi-infinite constraints.

Example 3.1

Take a simple general semi-infinite constraint

$$g(x, y) \leq 0, \quad \forall y \in Y$$

$$\text{and } Y(\mathbf{x}) = \{ \mathbf{y} \in \mathbf{R} \mid u(\mathbf{x}, \mathbf{y}) \leq 0 \}$$

with one real-value function g as an example. A simple index set Y is an interval in \mathbf{R} depending on x with reference to function u . If the decision variable x is also one-dimensional, then the restriction function g has two-dimensional arguments. An illustration for feasibility situation is sketched in Figure III.1, where the point x_1 is feasible, whereas x_2 and x_3 are not. ■

An important special case of general SIP arises if the infinite index set Y does

not depend on the decision variable x , i.e. $Y(x) \equiv Y$ where Y is some non-empty and compact set. In [100,107], problems of this type are called standard semi-infinite optimization problems. For instance, the constraint $g(x,y)$ in *Example 3.1* will become standard semi-infinite if Y is not dependent on x and merely an constant interval of $[a,b]$.

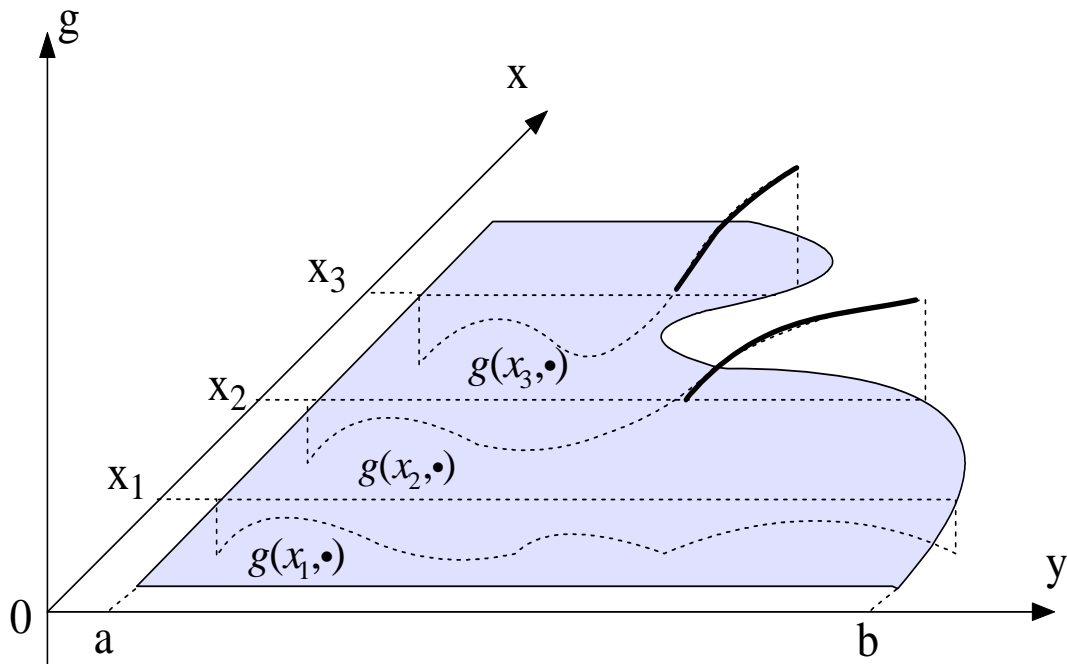


Figure III.1 Feasibility illustration under a standard semi-infinite constraint

A standard SIP problem is often written in the form of

$$SIP: \quad \min_{x \in \mathbf{R}^n} f(x) \tag{3.1}$$

$$s.t. \quad g(x,y) \leq 0 \quad \forall y \in Y \subset \mathbf{R}^p \tag{3.2}$$

where the objective function $f: \mathbf{R}^n \rightarrow \mathbf{R}$ and the constraint function $g: \mathbf{R}^n \times Y \rightarrow \mathbf{R}^{n_s}$ are both continuously differentiable in all arguments. $Y = \{y \in \mathbf{R}^p \mid u_k(y) \leq 0, k \in \mathbf{K}\}$ is defined as a Cartesian product of intervals for $p \geq 2$. The form of SIP problem can be reformulated easily in the case where a finite number of additional equality constraints are taken into the definition of the feasible set. However, the complexity of the problem will not be changed. Instead, they can be formatted as

inequalities as

$$h_j(\mathbf{x}) \geq 0 \text{ and } h_j(\mathbf{x}) \leq 0, \quad j \in \mathbf{J}.$$

For simplicity, equality constraints $h_j(\mathbf{x}) = 0, \quad j \in \mathbf{J}$ are not included in this form.

With reference to the model of transient stability constrained OPF (2.33-2.36) constructed in Chapter II, \mathbf{T} is constant and non-dependent on the decision variables \mathbf{x} and \mathbf{y} for the semi-infinite constraints \mathbf{U} . Thus the optimization of power flow with transient stability constraint is a standard SIP problem. Unless stated otherwise, all SIP problems afterwards in this chapter are in the standard format as (3.1-3.2).

The following are a simple example given to illustrate the concept of standard semi-infinite constraints.

Example 3.2

In this example, the feasibility set is defined as the unit disc in \mathbf{R}^2 as shown in Figure III.2,

$$D = \{ \mathbf{x} \in \mathbf{R}^2 \mid x_1^2 + x_2^2 \leq 1 \},$$

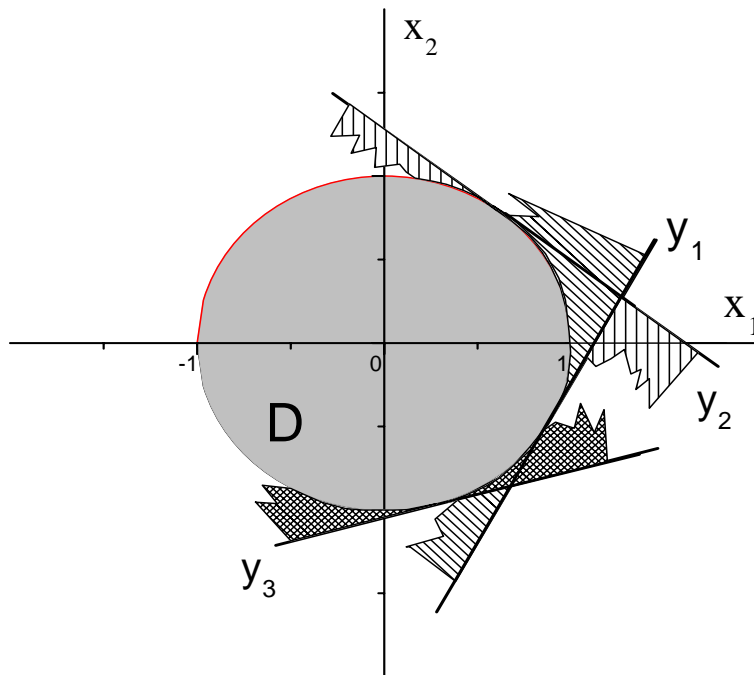


Figure III.2 The unit disc as intersection of infinitely many halfplanes

The feasibility set can also be described by means of infinitely many affine-linear inequality constraints:

$$\tilde{D} = \{ \mathbf{x} \in \mathbf{R}^2 \mid \mathbf{y}^T \mathbf{x} \leq 1, \forall \mathbf{y} \in Y \}$$

with

$$Y = \{ \mathbf{y} \in \mathbf{R}^2 \mid \|\mathbf{y}\|_2 \leq 1 \}.$$

In fact, this standard semi-infinite constraint describes D as the intersection of infinitely many halfplanes. Three of these halfplanes are depicted as examples in Figure III.2.

The SIP problem

$$\min \{ f(\mathbf{x}) \mid \mathbf{x} \in \tilde{D} \}$$

is able to be equivalently transcribed to a nonlinear programming problem

$$\begin{aligned} \min \quad & f(x_1, x_2) \\ \text{s.t.} \quad & x_1^2 + x_2^2 \leq 1 \end{aligned}$$

No doubt it is not necessary to search for a semi-infinite description of the feasibility set once a finite one can be presented. However, in some practices, only a semi-infinite description can be given. Thus SIP techniques have to be explored for those applications. ■

III.2 OPTIMALITY CONDITIONS

The primary concern in the practical study of optimization problems is with characterizing solution points and devising effective methods for finding them [106]. In this section optimality conditions are presented for nonlinear programming problems and extended to standard SIP problems.

III.2.1 OPTIMALITY CONDITIONS FOR NONLINEAR OPTIMIZATION

Consider a nonlinear programming (NLP) problem

$$\min_{\mathbf{x} \in \mathbf{R}^n} f(\mathbf{x}) \quad (3.3)$$

$$st. \quad \mathbf{g}(\mathbf{x}) \leq \mathbf{0} \quad (3.4)$$

$$\mathbf{h}(\mathbf{x}) = \mathbf{0} \quad (3.5)$$

where $\mathbf{g} = \{g_i\}$, $\mathbf{h} = \{h_j\}$, $i \in \mathbf{I}$ and $j \in \mathbf{J}$. Before deriving the first order optimality conditions, a few definitions are introduced with reference to [106].

Definition 3.1 Let $\mathbf{x}^* \in \mathbf{R}^n$ be feasible for the NLP problem. The inequality constraint $g_i(\mathbf{x})$ is active at \mathbf{x}^* if $g_i(\mathbf{x}^*) = 0$. The set of indices corresponding to active inequality constraints is written as

$$\mathbf{A}(\mathbf{x}^*) = \{i \in \mathbf{I} \mid g_i(\mathbf{x}^*) = 0\} \quad (3.6)$$

Of course, equality constraints are always active, but it is more preferred to account for their indices separately.

Definition 3.2 If the gradients of the active constraints at \mathbf{x}^* , $\{\nabla g_i, i \in \mathbf{A}(\mathbf{x}^*); \nabla h_j, j \in \mathbf{J}\}$, is linearly independent, the linear independence constraint qualification (LICQ) holds at \mathbf{x}^* .

\mathbf{x}^* is called a regular point in [106]. The LICQ assumption guarantees that the linearization of NLP around \mathbf{x}^* is differential-topologically equivalent to NLP in a neighbourhood of \mathbf{x}^* : the dimension of the manifold formed by the strictly feasible points in a neighbourhood of \mathbf{x}^* must remain the same after replacing each of the constraint surfaces by their tangent plane at \mathbf{x}^* .

The first order necessary conditions for optimality in constrained optimization problems involving both equality and inequality constraints are usually stated as the Karush-Kuhn-Tucker (KKT) conditions as below [106,108].

Theorem 3.1 First Order Necessary Optimality Conditions. Let \mathbf{x}^* be a local minimizer for (3.3-3.5). Assume the functions f , g_i and h_j are differentiable at \mathbf{x}^* for all $i \in \mathbf{I}$ and $j \in \mathbf{J}$ respectively. If the LICQ holds then there exist $\boldsymbol{\lambda}^* \in \mathbf{R}^m$, $\boldsymbol{\omega}^* \in \mathbf{R}^n$ such that $(\mathbf{x}^*, \boldsymbol{\lambda}^*, \boldsymbol{\omega}^*)$ solves the following system of (in)equalities,

$$\nabla f(\mathbf{x}^*) + \boldsymbol{\lambda}^{*T} \nabla \mathbf{g}(\mathbf{x}^*) + \boldsymbol{\omega}^{*T} \nabla \mathbf{h}(\mathbf{x}^*) = \mathbf{0} \quad (3.7)$$

$$g_i(\mathbf{x}^*) \leq 0 \quad \forall i \in \mathbf{I} \quad (3.8)$$

$$h_i(\mathbf{x}^*) = 0 \quad \forall i \in \mathbf{J} \quad (3.9)$$

$$\lambda_i^* = 0 \quad \forall i \in \mathbf{I} \setminus \mathbf{A}(\mathbf{x}^*) \quad (3.10)$$

$$\lambda_i^* \geq 0 \quad \forall i \in \mathbf{I} \quad (3.11)$$

The vector \mathbf{x}^* is called a KKT stationary point, and $(\mathbf{x}^*, \tilde{\boldsymbol{\lambda}}^*)$ is called a KKT pair with $\tilde{\boldsymbol{\lambda}}^* = (\boldsymbol{\lambda}^*, \boldsymbol{\omega}^*)^T$. The definition of \mathbf{x}^* as a KKT stationary point means that there exists vector of $\tilde{\boldsymbol{\lambda}}^*$ such that $(\mathbf{x}^*, \tilde{\boldsymbol{\lambda}}^*)$, as a KKT pair, satisfies the KKT (first-order necessary) conditions of local optimality. The KKT conditions can also be seen as an extension of the Lagrange multiplier theory for problems with equality constraints to problems with both equality and inequality constraints. $\boldsymbol{\lambda}^*$ and $\boldsymbol{\omega}^*$ are vectors of Lagrange multipliers for Lagrangian function

$$L(\mathbf{x}, \boldsymbol{\lambda}) = f(\mathbf{x}) + \boldsymbol{\lambda}^T \mathbf{g}(\mathbf{x}) + \boldsymbol{\omega}^T \mathbf{h}(\mathbf{x}) \quad (3.12)$$

The first-order (KKT) optimality conditions are sufficient for the global optimality of a feasible vector \mathbf{x}^* if f , g_i and h_j are differentiable convex functions.

The classical KKT conditions are developed from the Lagrange multiplier theory depending on the finite dimensionality of Euclidean space and the finiteness of the constraint set. In this thesis, the KKT conditions of finite-dimensional development are generalized and extended to programming problems in which the constraint functional is indexed by an infinite set.

III.2.2 OPTIMALITY CONDITIONS FOR SIP

In standard SIP problem (3.1-3.2), for convenience in notation, let

$$S = \{\mathbf{x} \mid \mathbf{g}(\mathbf{x}, \mathbf{y}) \leq \mathbf{0}, \mathbf{y} \in \mathbf{Y}\} \subset \mathbf{R}^n$$

be the feasible set. \mathbf{Y} is a non-empty and compact index set. Assume the functions f and \mathbf{g} are continuously differentiable with respect to \mathbf{x} everywhere on \mathbf{R}^n and

$\mathbf{R}^n \times \mathbf{R}^p$, respectively.

The Lagrange multiplier vector can be replaced with a measure on the infinite index set. Assume this measure is absolute continuous, it can be represented as a density function on the index set as pointed in [109]. Let $g = \{g_i\}$, $i \in I$, define $\lambda(I) = \lambda_i$ and $I_0(\mathbf{x}, \mathbf{y}) = \{i \in I \mid g_i(\mathbf{x}, \mathbf{y}) = 0\}$. The generalized Lagrangian function is written as

$$L(\mathbf{x}, \mathbf{y}, \lambda) = f(\mathbf{x}) + \int_I g_i(\mathbf{x}, \mathbf{y}) \lambda(di) \quad (3.13)$$

Associated with NLP is the generalized Lagrangian gradient

$$\nabla_x L(\mathbf{x}, \mathbf{y}, \lambda) = \nabla_x f(\mathbf{x}) + \int_I \nabla_x g_i(\mathbf{x}, \mathbf{y}) \lambda(di) = \mathbf{0}. \quad (3.14)$$

Suppose $\mathbf{x}^* \in S$ for the standard SIP problem (3.1-3.2), the generalized first-order conditions are

$$\nabla_x f(\mathbf{x}^*) + \int_I \nabla_x g_i(\mathbf{x}^*, \mathbf{y}) \lambda^*(di) = \mathbf{0} \quad (3.15)$$

$$\nabla_x g_i(\mathbf{x}^*, \mathbf{y}) \leq \mathbf{0} \quad (3.16)$$

$$\lambda^*(I') = 0 \quad \forall I' \subset I \setminus I_0(\mathbf{x}^*) \quad (3.17)$$

$$\lambda^*(I') \geq 0 \quad \forall I' \subset I \quad (3.18)$$

With reference to NLP, the first-order conditions are extended to standard SIP problem. However, it cannot be used directly for numerical algorithms.

The KKT type conditions are of interest in that the classical KKT conditions will be extended to a SIP problem in the next section by transcribing it equivalently (or approximately) to a general nonlinear programming problem with finitely many constraints.

III.3 SIP SOLUTION METHODS

Different methods exist to solve the SIP problem (3.1-3.2) numerically. One general scheme is to replace the original SIP problem by (a sequence of) finite programming problems with only a finite number of constraints. The known optimality conditions of finite optimization in section III.2 can then be

applied for SIP problems with specific assumptions and solved by appropriate linear or nonlinear programming algorithms.

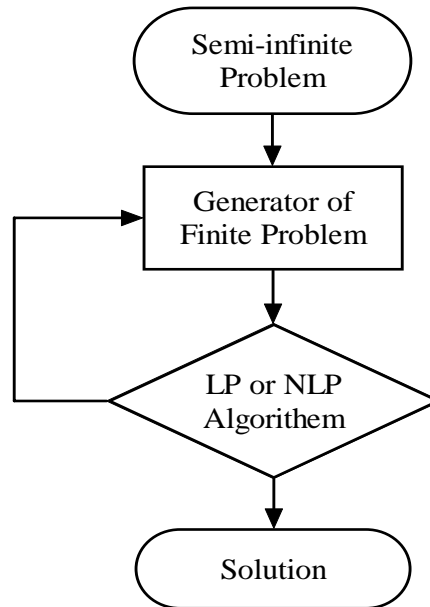


Figure III.3 General scheme to solve SIP problem

The general scheme of an algorithm for SIP is illustrated in the flowchart of Figure III.3. Depending on how the finite problems are generated, methods can be roughly classified into three categories: (1) discretization methods, (2) local reduction methods, and (3) exchange methods. In this thesis, only the first two methods are focused whilst exchanged methods are not encouraged due to its lower accuracy as pointed in [90].

III.3.1 DISCRETIZATION METHODS

Ordinary discretization is the most direct choice to describe or at least approximate the feasible set $S = \{x | g(x, y) \leq 0, y \in Y\}$ by imposing only finitely many constraints. By choosing $\bar{Y} \subset Y$, $|\bar{Y}| < \infty$, and replacing S by

$$S(\bar{Y}) = \{x | g(x, y) \leq 0, y \in \bar{Y}\},$$

the SIP problem (3.1-3.2) is approximate by

$$\min_{x \in \mathbf{R}^n} f(x) \tag{3.19}$$

$$st. \quad g(\mathbf{x}, \mathbf{y}) \leq \mathbf{0}, \quad \forall \mathbf{y} \in \bar{Y} \quad (3.20)$$

or

$$\min \left\{ f(\mathbf{x}) \mid \mathbf{x} \in S(\bar{Y}) \right\}. \quad (3.21)$$

Typically \bar{Y} is termed a grid. For a given step length vector $\mathbf{h}_i \in \mathbf{R}^p$ and $\mathbf{h}_i > \mathbf{0}$, $i = 1, \dots, m$, and a fixed $\mathbf{y}_0 \in \mathbf{R}^p$, the grid is defined as

$$G_h = \left\{ \mathbf{y} \mid (\mathbf{y} - \mathbf{y}_0)_i = \alpha_i \mathbf{h}_i, \quad \alpha_i \in \mathbf{Z}, \quad i = 1, \dots, m \right\} \quad (3.22)$$

and

$$\bar{Y} = Y \cap G_h. \quad (3.23)$$

This concept may be applied to general nonlinear problems. For $\mathbf{x}^* \in S(\bar{Y})$, the active set of \mathbf{y} , for which the constraints are active, is denoted as

$$\bar{A}(\mathbf{x}^*) = \left\{ \mathbf{y} \in Y \mid g(\mathbf{x}^*, \mathbf{y}_0 + \alpha_i \mathbf{h}_i) = \mathbf{0}, \quad \alpha_i \in \mathbf{Z}, \quad i = 1, \dots, m \right\}.$$

By the discretization of the infinite constraints into a sequence of finite-dimensional constraints

$$S(Y_{h_i}) = \left\{ \mathbf{x} \mid g(\mathbf{x}, \mathbf{y}_0 + \alpha_i \mathbf{h}_i) \leq \mathbf{0} \right\} \quad \alpha_i \in \mathbf{Z}, \quad i = 1, \dots, m. \quad (3.24)$$

the solution of the original program (3.1-3.2) can be obtained approximately by solving a sequence of problems (3.21).

For $\mathbf{x}^* \in S(\bar{Y})$, the KKT conditions for the discretized SIP problem are

$$\nabla_{\mathbf{x}} f(\mathbf{x}^*) + \sum_{i=1}^m \lambda_i^* \nabla_{\mathbf{x}} g(\mathbf{x}^*, \mathbf{y}_0 + \alpha_i \mathbf{h}_i) = \mathbf{0} \quad (3.25)$$

$$\lambda_i^* \nabla_{\mathbf{x}} g(\mathbf{x}^*, \mathbf{y}_0 + \alpha_i \mathbf{h}_i) \leq \mathbf{0} \quad \alpha_i \in \mathbf{Z}, \quad i = 1, \dots, m \quad (3.26)$$

$$\lambda_i^* \geq 0 \quad i = 1, \dots, m \quad (3.27)$$

Unfortunately, there is no guarantee for the existence of \bar{Y} , as a subset of Y , which yields identical set of solutions for the SIP (3.1-3.2) and the approximate problem (3.21). Also, if a finite sequence of finer and finer grids $\bar{Y}^{(n)}$ is used, it is not necessarily true that the accumulation points of solutions $\mathbf{x}^{*(n)}$ of (3.21) converge to the solution of (3.1-3.2). Thus the grids by discretization must be chosen with care

[90,101]. In [90], Theorem 3.2 is given for the question of identical value in the transformation for the infinite constraints.

Theorem 3.2 In Program (3.1-3.2) assume that Y is compact, both f and $g(\cdot, y)$ are convex with respect to x and all finite over \mathbf{R}^n , and the value of the program (3.1-3.2) is finite. Assume further that the following type of Slater condition holds in which there exists a x^* such that $g(x^*, y_i) < 0$, $i = 0, \dots, m$, for every set of $n+1$ points $y_0, \dots, y_n \in Y$ and $y_i = y_0 + \alpha_i h_i$. Then there exists $T_n = \{y_1, \dots, y_n\} \subset Y$ such that

- (i) the program (3.1-3.2) and its approximated program with T_n have the same value;
- (ii) there exist multipliers $\lambda_i \geq 0$, $i = 1, \dots, m$, such that the value of the program (3.1-3.2) is

$$\inf \left\{ f(x) + \sum_{i=1}^m \lambda_i g(x, y_i) \mid x \in \mathbf{R}^n \right\}.$$

It is noted that (ii) is basically a convex SIP Lagrangian duality result [90]. Obviously, a set T_n , even if its existence is known, will not be known explicitly, but usually is a result of a numerical solution of the problem.

Conceptual discretization method for SIP is presented as below.

Algorithm 3.1 Conceptual discretization method. For *Step* (i), one is given h^i , a selection $\bar{Y}_{h^i} \subset Y_{h^i}$ and a solution x^{*i} of the approximated problem (3.21) with $S(\bar{Y}_{h^i})$.

- (a) Set $h^{i+1} = (1/n_i)h^i$, $n_i \in \mathbf{N}$, $n_i \geq 2$.
- (b) Select $\bar{Y}_{h^{i+1}} \subset Y_{h^{i+1}}$ based on x^{*i} and \bar{Y}_{h^i} .
- (c) Compute a solution x^{*i+1} of the approximated problem (3.21) with $S(\bar{Y}_{h^{i+1}})$.
If x^{*i+1} is feasible with $S(\bar{Y}_{h^{i+1}})$ within a given accuracy then continue with (d), otherwise repeat (b).
- (d) If $i > i_0$, a pre-chosen number of refinement steps, then stop. Otherwise *Step* ($i + 1$).

An essential point with respect to efficiency is to use as much information as possible from previous grids when solving the approximated problem (3.21) with $S(\bar{Y}_{h^i})$. Since $Y_{h^i} \subset Y_{h^{i-1}}$, \mathbf{x}^{i-1} is generally a good starting point in solving the problem (3.21) with $S(\bar{Y}_{h^i})$. Besides, constraints from $S(Y_{h^i})$ should be reduced in *Step (b)* using information from previous grid. A convenient way of selecting $\bar{Y}_{h^i} \supset Y_{h^i}$ is as

$$\bar{Y}_{h^i} \supset Y_{h^i}^\rho := \left\{ \mathbf{y} \mid g(\mathbf{x}^{*i-1}, \mathbf{y}) \leq \rho, \mathbf{y} \in Y_{h^i} \right\} \quad (3.28)$$

with $\rho > 0$ being a chosen threshold. The choice of ρ in (3.28) is crucial: A larger ρ leads to more constraints for $S(\bar{Y}_{h^i})$ than necessary; whereas a smaller ρ may cause active parts of Y overlooked. It is demonstrated with examples in [91] that problems (with $m = 1, 2$) can be solved on very fine grids rather efficiently by these methods, requiring only the solution of a small number of finite problems with rather few constraints.

III.3.2 LOCAL REDUCTION METHODS

An exact, finite reformulation of (3.1-3.2) yields the following min-max program [101]:

$$\min_{\mathbf{x} \in R^n} f(\mathbf{x}) \quad (3.29)$$

$$s.t. \quad \max\{g(\mathbf{x}, \mathbf{y})\} \leq \mathbf{0}, \quad \forall \mathbf{y} \in Y \quad (3.30)$$

For standard SIP, $Y = \{\mathbf{y} \in R^p \mid u_k(\mathbf{y}) \leq 0, k \in \mathbf{K}\}$. The functions $f(\mathbf{x})$, $g(\mathbf{x}, \mathbf{y})$ and $u(\mathbf{y})$ are assumed continuously differentiable.

Let

$$\psi(\mathbf{x}) \triangleq \max_{\mathbf{y} \in Y} \{g(\mathbf{x}, \mathbf{y})\} \quad (3.31)$$

the problem (3.29-3.30) can be rephrased in the alternative form

$$\min_{\mathbf{x} \in R^n} f(\mathbf{x}) \quad (3.32)$$

$$s.t. \quad \psi(\mathbf{x}) \leq \mathbf{0} \quad (3.33)$$

Obviously, the feasible set is equivalently described by a finite set of restrictions as

$$S = \left\{ \mathbf{x} \in \mathbf{R}^n \mid \boldsymbol{\psi}(\mathbf{x}) \leq \mathbf{0} \right\} \quad (3.34)$$

Moreover, we assume the following holds.

Assumption 3.1 For a feasible solution $\mathbf{x}^* \in S$, the active points $\mathbf{y}^{*l} \in Y_0$, $l \in L$ and $L = \{1, \dots, r\}$, are optimal solutions of (3.31). $Y_0 = \{\mathbf{y} \in Y \mid g(\mathbf{x}, \mathbf{y}) = 0\}$ is a finite set of the active points. There exists a neighbourhood $U_{\mathbf{x}^*}$ of \mathbf{x}^* , neighbourhoods $U_{\mathbf{y}^{*l}}$ of \mathbf{y}^{*l} , and continuous mappings

$$\mathbf{y}^l : U_{\mathbf{x}^*} \rightarrow U_{\mathbf{y}^{*l}} \cap Y$$

such that

$$(i) \quad \mathbf{y}^l(\mathbf{x}^*) = \mathbf{y}^{*l}, \quad l \in L;$$

(ii) for every $\mathbf{x} \in U_{\mathbf{x}^*}$ and $l \in L$, $\mathbf{y}^l(\mathbf{x})$ is the only local solution of (3.31) in

$$U_{\mathbf{y}^{*l}} \cap Y.$$

With the assumption 3.1, there exists a neighbourhood $U_{\mathbf{x}^*}$ of \mathbf{x}^* such that for all $\mathbf{x} \in U_{\mathbf{x}^*}$ we have $\mathbf{x} \in S$ if and only if

$$G^l(\mathbf{x}) := g(\mathbf{x}, \mathbf{y}^l(\mathbf{x})) \leq 0 \quad (3.35)$$

Thus the so-called local reduction methods realize the local reduction of the SIP problem (3.1-3.2) to a finite dimensional optimization problem as

$$P_{red}(\mathbf{x}^*) \quad \min \left\{ f(\mathbf{x}) \mid G^l(\mathbf{x}) \leq 0, \quad l = 1, \dots, r; \quad \mathbf{x} \in U_{\mathbf{x}^*} \right\}. \quad (3.36)$$

If $G^l(\mathbf{x}^*) < 0$, $l = 1, \dots, r$, then \mathbf{x}^* is an interior point of S .

Theorem 3.3 Let $U_{\mathbf{x}^*}$ be a neighbourhood of $\mathbf{x}^* \in S$ as in (3.35). A point $\tilde{\mathbf{x}} \in U_{\mathbf{x}^*}$ is locally optimal for the original SIP (3.1-3.2) if and only if it is locally optimal for $P_{red}(\mathbf{x}^*)$.

Given Assumption 3.1, at least locally description of the feasible set of SIP is able to be presented in terms of finitely many constraints. However, it is noted that the finitely many constraints are defined only implicitly via solutions of a

parametric optimization problem (3.31). Thus it is difficult to formulate a given SIP as an ordinary optimization problem. Nevertheless, Theorem 3.3 allows the transfer of theory and methods of finite programming to SIP problems.

For feasible $\mathbf{x}^* \in S$ assume the set of active points Y_0 is nonempty. Clearly, any point $\mathbf{y}^{*l} \in Y_0$ is a global maximizer of the following parametric optimization problem

$$\max g(\mathbf{x}^*, \mathbf{y}) \quad (3.38)$$

$$s.t. \quad u_k(\mathbf{y}) \leq 0 \quad k \in \mathbf{K} \quad (3.39)$$

The active index set for (3.38)-(3.39) is written as

$$\mathbf{K}^l(\mathbf{x}^*, \mathbf{y}^*) = \{k \in \mathbf{K} \mid u_k(\mathbf{y}^*) = 0\}.$$

Assume LICQ holds on every active point of \mathbf{K}^l . The Lagrange function for (3.38)-(3.39) with respect to \mathbf{y}^{*l} is

$$\mathcal{L}^l(\mathbf{x}^*, \mathbf{y}, \boldsymbol{\lambda}) = g(\mathbf{x}^*, \mathbf{y}) - \sum_{k \in \mathbf{K}^l} \lambda_k^l u_k(\mathbf{y}). \quad (3.40)$$

According to the KKT conditions as stated in Theorem 3.1, there exist unique multipliers $\lambda_k^{l*} \geq 0$ such that

$$\nabla_{\mathbf{y}} \mathcal{L}^l(\mathbf{x}^*, \mathbf{y}^{*l}, \boldsymbol{\lambda}^{l*}) = \nabla_{\mathbf{y}} g(\mathbf{x}^*, \mathbf{y}^{*l}) - \sum_{k \in \mathbf{K}^l} \lambda_k^{l*} \nabla_{\mathbf{y}} u_k(\mathbf{y}^{*l}) = 0. \quad (3.41)$$

Moreover, if $\nabla_{\mathbf{y}\mathbf{y}} \mathcal{L}^l(\mathbf{x}^*, \mathbf{y}^{*l}, \boldsymbol{\lambda}^{l*})$ is negative definite on the tangent space

$$\mathbf{T}^l = \left\{ \mathbf{d} \mid \lambda_j^{l*} \nabla_{\mathbf{y}} h^j(\mathbf{y}^{*l})^T \mathbf{d} = 0, j \in \mathbf{K}^l \right\}, \quad (3.42)$$

the strong second order sufficient condition holds for \mathbf{y}^{*l} to be a strict local maximum of (3.38)-(3.39).

Theorem 3.4 Assume that Assumption 3.1 holds with continuously differentiable functions $\mathbf{y}^l : U_{\mathbf{x}^*} \rightarrow U_{\mathbf{y}^{*l}} \cap Y$, and strict complementary slackness of $\lambda_k^* > 0$ holds for (3.38)-(3.39). Moreover, there exists continuously differentiable $\boldsymbol{\lambda} : U_{\mathbf{x}^*} \rightarrow \mathbf{R}$ such that LICQ and the second order sufficient condition hold for all triples $(\mathbf{x}, \mathbf{y}(\mathbf{x}), \boldsymbol{\lambda}(\mathbf{x}))$, $\mathbf{x} \in U_{\mathbf{x}^*}$.

(i) The derivatives $\mathbf{y}'_x = \mathbf{y}'_x(\mathbf{x})$, $\boldsymbol{\lambda}'_x = \boldsymbol{\lambda}'_x(\mathbf{x})$ are uniquely determined by

$$\nabla_{\mathbf{y}\mathbf{y}} \mathcal{L}'(\mathbf{y}', \boldsymbol{\lambda}') \mathbf{y}'_x - \mathbf{U}'_x(\mathbf{y}') \boldsymbol{\lambda}'_x = -\nabla_{\mathbf{y}\mathbf{x}} g'(\mathbf{x}, \mathbf{y}') \quad (3.43)$$

$$\left(\mathbf{U}'_x(\mathbf{y}')\right)^T \mathbf{y}'_x = \mathbf{0} \quad (3.44)$$

with

$$\mathbf{U}'_x(\mathbf{y}') = \left(u_y^j(\mathbf{y}')\right)_{j \in K^l} \in \mathbf{R}^{p \times |K^l|} \quad (3.45)$$

(ii) The constraint functions $G^l(\mathbf{x}) = g(\mathbf{x}, \mathbf{y}'(\mathbf{x}))$ of the reduced problem are twice continuously differentiable in $U_{\mathbf{x}^*}$ and are given by

$$G^l_x(\mathbf{x}) = \nabla_{\mathbf{x}} g(\mathbf{x}, \mathbf{y}'(\mathbf{x})) \quad (3.46)$$

$$G^l_{\mathbf{x}\mathbf{x}}(\mathbf{x}) = \nabla_{\mathbf{x}\mathbf{x}} g^l(\mathbf{x}, \mathbf{y}'(\mathbf{x})) - \left(\nabla_{\mathbf{x}} \mathbf{y}'(\mathbf{x})\right)^T \nabla_{\mathbf{y}\mathbf{y}} \mathcal{L}'(\mathbf{y}'(\mathbf{x}), \boldsymbol{\lambda}'(\mathbf{x})) \left(\nabla_{\mathbf{x}} \mathbf{y}'(\mathbf{x})\right) \quad (3.47)$$

The proof of (i) uses the implicit function derivation and obvious continuity arguments. Equations (3.46) and (3.47) are derived from (i). Further relaxations of the related assumptions are possible to define reduced problems with G^l only Lipschitz continuous on the basis of $\mathbf{y}'(\mathbf{x})$, which may even be discontinuous [102].

For the SIP problem (3.1-3.2), its local reduced problem $P_{red}(\mathbf{x}^*)$ in (3.36) is a finite dimensional optimization problem. Its first order optimality conditions in a feasible solution \mathbf{x}^* are

$$\nabla_{\mathbf{x}} f(\mathbf{x}^*) + \sum_{l=1}^r \lambda^{l*} \nabla_{\mathbf{x}} G^l(\mathbf{x}^*) = \mathbf{0} \quad (3.48)$$

$$\lambda^{l*} \nabla_{\mathbf{x}} G^l(\mathbf{x}^*) \leq \mathbf{0} \quad l = 1, \dots, r \quad (3.49)$$

$$\lambda^{l*} \geq 0 \quad l = 1, \dots, r \quad (3.50)$$

in which $\nabla_{\mathbf{x}} G^l = G^l_x(\mathbf{x})$ as formulated in (3.46).

Conceptually, local reduction methods can be described as follows.

Algorithm 3.2 Conceptual reduction method. For *Step (i)*, one is given \mathbf{x}^i (not necessarily feasible).

(a) Determine $\mathfrak{A}(\mathbf{x}^i, \rho) = \{\mathbf{y}^1, \dots, \mathbf{y}^r\}$ with

$$\mathfrak{A}(\mathbf{x}^i, \rho) = \left\{ \mathbf{y} \in Y \mid g(\mathbf{x}^i, \mathbf{y}) \geq -\rho \right\} \cap \mathfrak{A}_0(\mathbf{x}^i), \quad (3.51)$$

in which $\mathfrak{A}_0(\mathbf{x}^i) = \left\{ \mathbf{y} \in Y \mid \mathbf{y} \text{ is a local maximizer of } g(\mathbf{x}^i, \mathbf{y}) \text{ over } Y \right\}$ and $\rho > 0$.

(b) Apply k_i steps of a finite programming algorithm to the reduced problem

$$\left(P_{red}(\mathbf{x}^i) \right) \quad \min \left\{ f(\mathbf{x}) \mid G^l(\mathbf{x}) \leq 0, l=1, \dots, r_i \right\} \quad (3.52)$$

with $G^l(\mathbf{x}) = g(\mathbf{x}, \mathbf{y}^l(\mathbf{x}))$. Let $\mathbf{x}^{i,j}$, $j=1, \dots, k_i$ be the iterates.

(c) Set $\mathbf{x}^{i+1} = \mathbf{x}^{i,k_i}$ and continue with *Step* ($i+1$).

Substep (a) is very costly as it requires a global search for maximizers of $g(\mathbf{x}^i, \mathbf{y})$ on $Y \subset \mathbf{R}^p$. The overall strategy should decrease the execution of this step as much as possible. For technical and practical reasons, it is convenient to focus attention on all local maximizers of $g(\mathbf{x}^i, \mathbf{y})$ that exceed a slightly negative threshold $-\rho$, rather than just the elements of $\mathfrak{A}(\mathbf{x}, 0)$. In a certain sense the costly global search for maximizers is replaced by the determination of $\mathfrak{A}(\mathbf{x}, \rho)$, which takes the whole clusters of points in the neighbourhoods of maximizers in Y . Substep (a) tacitly assumes that there are only finitely many maximizers of $\left(P_{red}(\mathbf{x}^i) \right)$. If this is not the case, a basic assumption for reduction fails to hold and another method (for instance, a discretization method, or L_1 penalty function presented in Section III.4) should be used. In substep (b), the parametric problem $\left(P_{red}(\mathbf{x}^i) \right)$ has also to be considered in evaluating the constraints G^l . Finite programming method can be performed efficiently, for instance, Newton methods, sequential quadratic programming (SQP) methods, etc., to solve the problem.

III.3.3 REMARKS ON NUMERICAL METHODS

Although it is difficult to determine which method should be selected for which type of problem, some general remarks are provided from restricted experiences on discretization methods and local reduction methods.

For either of discretization and local reduction method, the following

transcription of the SIP is involved in each iterate:

$$\min_{\mathbf{x} \in \mathbf{R}^n} f(\mathbf{x}) \quad (3.53)$$

$$st. \quad g(\mathbf{x}, \mathbf{y}) \leq 0, \quad \forall \mathbf{y} \in \bar{\mathbf{Y}}_i \quad (3.54)$$

where i is the current iteration, and $\bar{\mathbf{Y}}_i$ is a finite subset of the points in the interval \mathbf{Y} . Under suitable assumptions in III.3.1 and III.3.2, the sequence of solution values converges, via either of the two types of methods respectively, to the SIP minimum value, f_{SIP} , and every accumulation point of the sequence of solution points is a solution point of the SIP.

Discretization and reduction-based methods differ primarily in their selection of the finite set $\bar{\mathbf{Y}}_i$. Discretization methods mainly suffer from the drawback of the rapid growth of the dimension. When the index set \mathbf{Y} is higher-dimensional, i.e. $\mathbf{Y} \subset \mathbf{R}^p$, $p \geq 2$, the large-scale NLPs (3.19-3.20) have to be solved in successive iterations inefficiently with higher-dimensional constraints by discretization. In these cases, the methods become inefficient. Moreover, grid selection strategies for discretization should be tactically. However, one advantage is that weaker assumptions are required for the convergence of discretization methods to the solution of the original SIP problem.

Reduction methods have advantages to keep the cardinality of $\bar{\mathbf{Y}}_i$ low. The convergence to high accuracy is fast without increasing the dimension of the constraints in the subproblems between iterations. However, these methods make strong assumptions on the properties of the problem.

In this thesis, reduction methods are preferred to solve the transient stability constrained OPF with good convergence.

III.4 ALGORITHMS FOR SOLVING SIP

In this section practical algorithms based on local reduction are employed to solve the SIP problem. For a give $\rho > 0$ let $\mathfrak{A}(\mathbf{x}^*, \rho) = \{\mathbf{y}^{1*}, \dots, \mathbf{y}^{r*}\}$, which is defined in (3.51) as the set of local maximizers of g that take values not less than

$-\rho$. Assume that a finite set of functions $\{y^{l*}(\mathbf{x})\}$ exists such that each $y^{l*}(\mathbf{x}^*) = y^{l*}$ for all l is continuous at \mathbf{x}^* and $y^{l*}(\mathbf{x}) \in \mathcal{A}(\mathbf{x}, \infty)$ for all \mathbf{x} satisfying $\|\mathbf{x} - \mathbf{x}^*\| < \varepsilon$, $\varepsilon > 0$. Strictly, $y^{l*}(\mathbf{x})$ and r also depend on ρ although this dependence is kept implicit. The semi-infinite constraint, $g(\mathbf{x}, \mathbf{y}) \leq 0$, $\forall \mathbf{y} \in Y$, can be replaced by the finitely many constraints:

$$G^{l*}(\mathbf{x}) = g(\mathbf{x}, y^{l*}(\mathbf{x})) \leq 0, \quad l = 1, \dots, r(\mathbf{x}^*). \quad (3.55)$$

Although $G^{*l}(\mathbf{x})$ functions are important for theoretical purposes, $G^{*l}(\mathbf{x})$ and its derivatives are commonly evaluated only locally at $\mathbf{x} = \mathbf{x}^*$ in practical algorithms. The given \mathbf{x}^* is significant to trigger the searching process. In NLP the dependence on requiring good initial approximations is often successfully removed by employing exact penalty functions to force convergence from remote starting points. The superscript "*" is suppressed in the remaining chapter for compactness of notations.

III.4.1 EXACT PENALTY FUNCTIONS FOR SIP

Although less popular in the NLP context, exact penalty function is preferable for SIP problems [93]. The aim of the penalty function is to construct a function P , as a penalty function, such that any local solution to the original SIP problem is a local minimizer of the penalty function. A penalty function is exact if there exists a finite parameter value such that the solution of the penalty problem yields the exact solution to the original problem. Then the idea is to minimize the penalty function rather than solve the original SIP.

L_1 and L_∞ norm penalty functions are described in this part and then employed respectively in the later chapters. p -norm, $p \geq 1$, of vector $\mathbf{x} \in R^n$, $\mathbf{x} = \{x_i\}$, is defined as

$$\|\mathbf{x}\|_p := \left(\sum_{i=1}^n |x_i|^p \right)^{\frac{1}{p}}$$

Thus L_1 norm is defined as

$$\|\mathbf{x}\|_1 := \sum_{i=1}^n |x_i|$$

and L_∞ norm as

$$\|\mathbf{x}\|_\infty := \max(x_1, \dots, x_n).$$

With the introduction of penalty functions, the optimality conditions for NLP (3.7-3.11) or SIP (3.15-3.18) should be rewritten, in which the updated objective function is the original objective function plus penalty functions.

III.4.1.1 L_1 PENALTY FUNCTIONS

Penalty functions based on the L_1 norm of the constraint violations are commonly used. The analogue for the SIP case is the penalty function

$$P^1(\mathbf{x}, \mu) = f(\mathbf{x}) + \mu \sum_{l=1}^{r(\mathbf{x})} [G^l(\mathbf{x})]_+ \quad (3.56)$$

where $[G(\bullet)]_+$ denotes the maximum of $G(\bullet)$ and 0. Obviously, $P^1(\mathbf{x}, \mu) = f(\mathbf{x})$ if \mathbf{x} is feasible, i.e. $G^l(\mathbf{x}) \leq 0$, $l=1, \dots, r(\mathbf{x}^*)$. μ is a positive scalar such that any local solution to the SIP is a local minimizer of $P^1(\mathbf{x}, \mu)$ in the limit as $\mu \rightarrow +\infty$. However, the necessity of $\mu \rightarrow +\infty$ is not desirable for practical method for solving a SIP based on penalty function minimization.

In [103], an exact penalty function based on L_1 norm is constructed as an alternative

$$\hat{P}^1(\mathbf{x}, \mu) = f(\mathbf{x}) + \mu \frac{\sum_{j=1}^s \left(\int_{\Omega_j(\mathbf{x})} [g(\mathbf{x}, \mathbf{y})]_+ d\mathbf{y} \right)}{\sum_{j=1}^s \left(\int_{\Omega_j(\mathbf{x})} d\mathbf{y} \right)} \quad (3.57)$$

where $\Omega_j(\mathbf{x})$ is a finite set for a \mathbf{x} such that

- i) $\Omega_j(\mathbf{x}) \subseteq \mathbf{Y}$, $1 \leq j \leq s(\mathbf{x}) < \infty$,
- ii) $g(\mathbf{x}, \mathbf{y}) \geq 0$, $\forall \mathbf{y} \in \Omega_j(\mathbf{x})$ and $g(\mathbf{x}, \mathbf{y}) < 0$, $\forall \mathbf{y} \in \mathbf{Y} \setminus \left(\cup_{j=1}^s \Omega_j(\mathbf{x}) \right)$,
- iii) $\Omega_j(\mathbf{x}) \cap \Omega_k(\mathbf{x}) = \emptyset$ if $j \neq k$, and
- iv) $\Omega_j(\mathbf{x})$ is connected and non-trivial, i.e., $\int_{\Omega_j(\mathbf{x})} d\mathbf{y} > 0$.

Obviously, $\Omega_j(\mathbf{x})$ is empty if \mathbf{x} is feasible. In principle this is a generalization of

the L_1 exact penalty function for SIP, which has the advantage of not assuming a finite number of global maximizers of $G(\bullet)$ in each iterate. As argued in [103], it is essential to determine the normalizing denominator integral to make \hat{P}^1 be an exact penalty function.

However, in practice, the computation efforts involved by accurate evaluation of the integrals make \hat{P}^1 less attractive than L_∞ penalty functions as shown in the next section. Moreover, another disadvantage with this penalty function is it may be discontinuous. Examples of SIP problems for which discontinuities may cause difficulties can be found in [102,104]. These discontinuities can only occur at infeasible points but the consequent invalidity of convergence results for such problems makes this penalty functions inadvisable for general SIP problems.

III.4.1.2 L_∞ PENALTY FUNCTIONS

Exact penalty function for SIP based on L_∞ norm does not suffer the disadvantage of possible discontinuities at infeasible points. In [93], the exact penalty function is presented as

$$P^\infty(\mathbf{x}, \mu) = f(\mathbf{x}) + \mu \max_{\mathbf{y} \in Y} [g(\mathbf{x}, \mathbf{y})]_+ \quad (3.58)$$

Similarly as P^1 , $P^\infty(\mathbf{x}, \mu) = f(\mathbf{x})$ if \mathbf{x} is feasible, i.e., $g(\mathbf{x}, \mathbf{y}) \leq 0$. μ is a penalty parameter.

Practically, we can define

$$\mathfrak{A}(\mathbf{x}, \rho) = \{\mathbf{y} \in Y \mid g(\mathbf{x}, \mathbf{y}) \geq -\rho\} \cap \mathfrak{A}_0(\mathbf{x}) \quad (3.59)$$

where $\mathfrak{A}_0(\mathbf{x}) = \{\mathbf{y} \in Y \mid \mathbf{y} \text{ is a local maximizer of } g(\mathbf{x}, \mathbf{y}) \text{ over } Y\}$ and $\rho > 0$. $\mathfrak{A}(\mathbf{x}, \rho)$ can be expressed as

$$\mathfrak{A}(\mathbf{x}, \rho) = \{\mathbf{y}^k(\mathbf{x}) \mid k \in K(\mathbf{x})\} \quad (3.60)$$

where $K(\mathbf{x})$ is a subset of a finite index set of K and $\mathbf{y}^k(\mathbf{x})$ is continuous at \mathbf{x} . The cardinality of $K(\mathbf{x})$ may vary depending on \mathbf{x} and ρ . L_∞ norm penalty function can be replaced alternatively as

$$P^\infty(\mathbf{x}, \mu) = f(\mathbf{x}) + \mu \max_{k \in K(\mathbf{x})} \left[g(\mathbf{x}, \mathbf{y}^k(\mathbf{x})) \right]_+ \quad (3.61)$$

The computation related to the integration of violated constraints is avoided. However, a global maximizer and hence all local maximizers of $g(\mathbf{x}, \bullet)$ on Y have to be determined. Some other advantages are also presented in [102] with two-penalty-parameter exact penalty function based on L_∞ norm.

III.4.2 MULTI-LOCAL OPTIMIZATION SUBPROBLEM

Exact penalty functions have to be evaluated at each iterate and at each trial point. The calculation of an L_∞ exact penalty function at a point \mathbf{x}^* requires the solution of the global optimization problem

$$\max_{\mathbf{y} \in Y} \left[g(\mathbf{x}, \mathbf{y}) \right]_+. \quad (3.62)$$

In order to ensure convergence under appropriate conditions, all members of the set

$$\mathfrak{B}(\mathbf{x}^*, \rho) = \left\{ \mathbf{y} \in \mathfrak{M}(\mathbf{x}^*) \mid g(\mathbf{x}^*, \mathbf{y}) \geq \max_{\mathbf{y} \in Y} \left[g(\mathbf{x}^*, \mathbf{y}) \right]_+ - \rho \right\} \quad (3.63)$$

must be found for some pre-specified positive ρ , where $\mathfrak{M}(\mathbf{x}^*)$ is the set of local maximizers of $g(\mathbf{x}^*, \mathbf{y})$ over Y . If an L_1 exact penalty functions is employed, additional condition $\rho > \max_{\mathbf{y} \in Y} \left[g(\mathbf{x}^*, \mathbf{y}) \right]_+$ is needed to ensure convergence.

The problem (3.63) of finding all the global and near global maximizers is referred to as the multi-local optimization problem. However, there does not exist an algorithm which is able to detect a global maximizer of an arbitrary continuous function [93]. One common method for solving the multi-local optimization problem is to find coarse approximations to the local maximizers by comparison of function values of $g(\mathbf{x}, \bullet)$ on a uniform mesh over Y , and then to refine these approximations by an iterative procedure afterwards.

There are many methods of the computation of the unique local maximizer in a specific subregion of Y if Y is a one-dimensional set. In case Y has a dimension greater than one, all zeros of $\nabla_{\mathbf{y}} g(\mathbf{x}, \bullet)$ in the interior of Y have to be computed,

for example, by means of the BFGS quasi-Newton method, and all maximizers on the boundary of Y have to be specified separately.

The described ideas for multi-local maximizers includes the risk that not all local maximizers and therefore possibly not a true global maximizer are found without search more thoroughly parts of Y . The accuracy of local maximizers of $g(\mathbf{x}, \bullet)$ on Y obtained at an iteration \mathbf{x}^* may also give impact on the convergence. For the sake of simplicity, it is assumed here that all needed local maximizers are determined with sufficient accuracy and that hence algorithms which employ maximizers are always implementable in this respect. In the later chapters, these problems are solved practically.

III.4.3 ALGORITHM AND THE IMPLEMENTATION

In this section conceptual algorithms based on nonlinear programming methods are specified for their employment to solve the locally reduced problem from SIP as substep (b) in Algorithm 3.2.

Algorithm 3.3 Conceptual reduction method. For *Step (i)*, given \mathbf{x}^i

(a) Reduce the original SIP locally as

$$\min_{\mathbf{x} \in \mathbf{R}^n} f(\mathbf{x}) \quad (3.64)$$

$$s.t. \quad G(\mathbf{x}) \leq 0 \quad (3.65)$$

where $G(\mathbf{x})$ is either refer to the L_1 norm penalty term in (3.57) as

$$G(\mathbf{x}) = \frac{\sum_{j=1}^s \left(\int_{\Omega_j(\mathbf{x})} [g(\mathbf{x}, \mathbf{y})]_+ d\mathbf{y} \right)}{\sum_{j=1}^s \left(\int_{\Omega_j(\mathbf{x})} d\mathbf{y} \right)} \quad (3.66)$$

or the L_∞ norm penalty term in (3.61) as

$$G(\mathbf{x}) = \max_{k \in K(\mathbf{x})} \left[g(\mathbf{x}, \mathbf{y}^k(\mathbf{x})) \right]_+ \quad (3.67)$$

(b) Set $\mathbf{x}^{i,0} = \mathbf{x}^i$ and give $\lambda^{i,0}$. For $j = 1, \dots, k_i$ do (b₁)-(b₃).

(b1) Compute a solution $\mathbf{x}^{i,j}$ and an optimal multiplier vector $\boldsymbol{\lambda}^{i,j} \geq \mathbf{0}$ for

$$\nabla_{\mathbf{x}} L(\mathbf{x}^{i,j-1}, \boldsymbol{\lambda}^{i,j-1}) = \mathbf{0} \quad (3.68)$$

$$G(\mathbf{x}^{i,j-1}) = \mathbf{0} \quad (3.69)$$

where $L(\mathbf{x}, \boldsymbol{\lambda})$ is a Lagrange function

$$L(\mathbf{x}, \boldsymbol{\lambda}) = f(\mathbf{x}) + \boldsymbol{\lambda}^T \mathbf{G}(\mathbf{x}) \quad (3.70)$$

Most straightforwardly, Newton's method can solve the system (3.68-3.69) by solving the linearized version as below recursively.

$$\mathbf{H}^{i,j-1} \Delta \mathbf{x}^j + \nabla_{\mathbf{x}} G(\mathbf{x}^{i,j-1}) \Delta \boldsymbol{\lambda}^j = -\nabla L(\mathbf{x}^{i,j-1}, \boldsymbol{\lambda}^{i,j-1})^T \quad (3.71)$$

$$\nabla_{\mathbf{x}} \mathbf{G}(\mathbf{x}^{i,j-1}) \Delta \mathbf{x}^j = -\mathbf{G}(\mathbf{x}^{i,j-1}) \quad (3.72)$$

(b2) Compute step lengths, α_j and β_j , for $\mathbf{x}^{i,j}$ and $\boldsymbol{\lambda}^{i,j}$ respectively.

(b3) Let $\mathbf{x}^{i,j} = \mathbf{x}^{i,j-1} + \alpha_j \Delta \mathbf{x}^j$ and $\boldsymbol{\lambda}^{i,j} = \boldsymbol{\lambda}^{i,j-1} + \beta_j \Delta \boldsymbol{\lambda}^j$.

(c) Set $\mathbf{x}^{i+1} = \mathbf{x}^{i,k_i}$ and continue with *Step* ($i+1$).

Newton's method in substep (b1) will converge to the solution and the convergence will be of order at least two if the linearized system is nonsingular at the solution and the initial point is sufficiently close to the solution. In Newton's method, the matrix \mathbf{H} used in (3.71) is the Hessian matrix $\nabla_{\mathbf{x}}^2 L(\mathbf{x}, \boldsymbol{\lambda})$ of the Lagrange function (3.70) as

$$\nabla_{\mathbf{x}}^2 L(\mathbf{x}, \boldsymbol{\lambda}) = \nabla_{\mathbf{x}}^2 f(\mathbf{x}) + \sum_{l=1}^p \lambda_l \nabla_{\mathbf{x}}^2 G_l(\mathbf{x}). \quad (3.73)$$

However, it is not necessarily appropriate to use Hessian matrix exactly as $\nabla_{\mathbf{x}}^2 L(\mathbf{x}, \boldsymbol{\lambda})$. Quasi-Newton approximation to $\nabla_{\mathbf{x}}^2 L(\mathbf{x}, \boldsymbol{\lambda})$ can be employed to avoid complications arisen from second derivative methods but with some loss of efficiency. BFGS (Broyden-Fletcher-Goldfarb-Shanno) updating formula is used to provide quasi-Newton approximations for $\nabla_{\mathbf{x}}^2 L(\mathbf{x}, \boldsymbol{\lambda})$ [106,127]. An updated matrix \mathbf{B}_+ is computed to approximate Hessian matrix based on the formula

$$\mathbf{B}_+ = \mathbf{B} + \frac{\boldsymbol{\gamma}\boldsymbol{\gamma}^T}{d\boldsymbol{\gamma}^T} - \frac{(\mathbf{B}d)(d\mathbf{B})^T}{d^T \mathbf{B}d}. \quad (3.74)$$

where $\mathbf{d} = \Delta \mathbf{x}$ and $\boldsymbol{\gamma} = \boldsymbol{\gamma}^j$

$$\boldsymbol{\gamma}^j = \nabla_{\mathbf{x}} L(\mathbf{x}^{i,j}, \boldsymbol{\lambda}^{i,j}) - \nabla_{\mathbf{x}} L(\mathbf{x}^{i,j-1}, \boldsymbol{\lambda}^{i,j}). \quad (3.75)$$

III.5 TRANSFORMATION OF TRANSIENT STABILITY CONSTRAINTS

As constructed in Chapter II.3, the transient stability constrained OPF problem

$$\min f(\mathbf{x}_0, \mathbf{y}) \quad (3.76)$$

$$s.t. \quad \mathbf{g}(\mathbf{x}_0, \mathbf{y}) = \mathbf{0} \quad (3.77)$$

$$\mathbf{H}(\mathbf{x}_0, \mathbf{y}) \leq \mathbf{0} \quad (3.78)$$

$$\mathbf{U}^k(\mathbf{x}^k(t), \mathbf{y}) \leq \mathbf{0} \quad t \in \mathbf{T}, k \in \mathbf{I}_c \quad (3.79)$$

is a SIP problem due to the dynamic constraints (3.79) in transients. In this thesis, local reduction methods for SIP are employed to transform the transient stability constrained OPF into traditional OPF with finite-dimensional constraints.

Suppose only one credible contingency is considered, i.e. superscript k omitted in (3.79), to avoid much cumbersome notation. It is noted that transient stability constraint (3.79) with infinite dimension, based on either rotor angle limit as (2.17) or PEBS concept as (2.31), is associated to the DAEs (2.11-2.22) describing the dynamics in the transients. It is different from the defined form of standard SIP (3.1-3.2), in which the functional of infinite constraint is explicit. Thus the complexity of transient stability constrained OPF is increased due to the implicit representation of the infinite constraint in its functional space.

With $\mathbf{x}(t) = \mathbf{x}_0^*$ at $t=0$, $\mathbf{x}(t)$ can be obtained at $\forall t \in \mathbf{T}$ by solving the DAEs (2.11-2.22) with any suitable numerical integration method such as the implicit trapezoidal integration, see Appendix C. Thus for $\mathbf{x}(t)$, there exists $\boldsymbol{\varphi}(\mathbf{x}_0, \mathbf{y}, t)$ with implicit function theorem satisfying

$$\mathbf{x}(t) = \boldsymbol{\varphi}(\mathbf{x}_0, \mathbf{y}, t) = \mathbf{x}_0 + \int_0^t \mathbf{F}(\boldsymbol{\varphi}(\mathbf{x}_0, \mathbf{y}), \mathbf{y}) d\tau \quad t \in \mathbf{T} \quad (3.80)$$

After that, the substitution of (3.80) into the infinite constraint (3.79) yields:

$$U(\varphi(x_0, y, t), y) \leq 0 \quad (3.81)$$

or

$$U(x_0, y, t) \leq 0 \quad (3.82)$$

which is formatted explicitly for t , although (3.81) or (3.82) is not easy to be written explicitly in practice.

III.5.1 L_1 NORM LOCAL REDUCTION FOR TRANSIENT STABILITY CONSTRAINTS

Given a feasible solution (x_0^*, y^*) to (3.76)-(3.79), the rewritten infinite constraint (3.82) is reduced locally based on L_1 norm as

$$q_i(x_0^*, y^*) = \int_0^{t_e} [u_i(x_0^*, y^*, t)]_+ dt \leq 0 \quad (3.83)$$

where $Q = \{q_i\}$ and $U = \{u_i\}$, $i = 1, \dots, m$. $[\bullet]_+$ is defined as $\max\{\bullet, 0\}$. m is different depending on the type of transient stability index being adopted. If infinite constraint (3.79) is based on rotor angle limit, m is equal to the number of machines, i.e. n_g ; whereas based on PEBS concept, m is one.

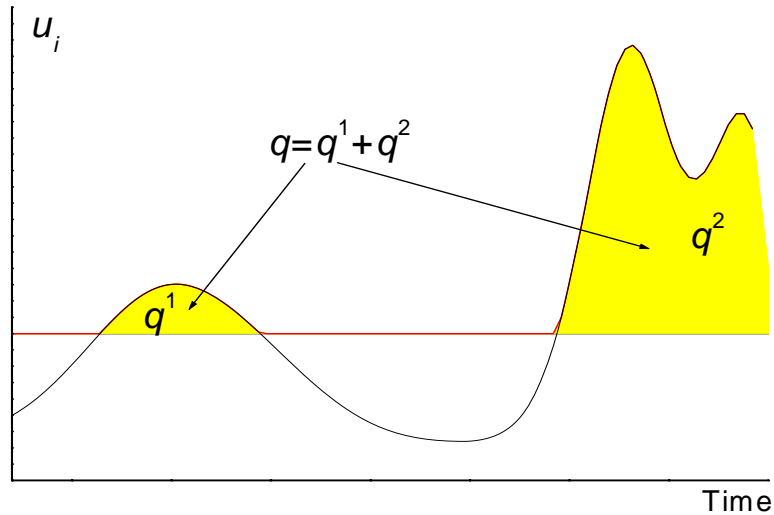


Figure III.4 Intuitionistic explanation for L_1 norm local reduction

Here, interpretation is given by taking the index based on rotor angle limit as an example. The rotor angle of each generator with respect to the COI must keep below the allowed upper limit δ_{\max} . Equivalently, this stability requirement can be fulfilled by reducing the shadowed area q , as shown in Figure III.4, to zero. The area, which can be composed of separated sub-areas like q^1 and q^2 as shown in Figure III.4, is enclosed by the swing curve and the allowed threshold δ_{\max} . This equivalence is represented mathematically as the integration on the time intervals corresponding to the swing curve beyond the threshold δ_{\max} being zero as (3.83).

Generally, in power systems the original transient stability constraint is not a hard constraint. That is to say, some tolerant violations in transients can be accepted if the system is able to reach a secure steady-state operation condition finally. Thus, a slightly positive tolerance ρ rather than 0 is introduced to relax the strictness of (3.83) as

$$q_i(\mathbf{x}_0^*, \mathbf{y}^*) = \int_0^{t_e} \left[u_i(\mathbf{x}_0^*, \mathbf{y}^*, t) \right]_+ dt - \rho \leq 0 \quad i = 1, \dots, m \quad (3.84)$$

From the technical and practical aspects, this relaxation might improve the convergence property of the optimization [93].

III.5.2 L_∞ NORM LOCAL REDUCTION FOR TRANSIENT STABILITY CONSTRAINTS

Let $(\mathbf{x}_0^*, \mathbf{y}^*)$ denote a feasible solution to problem (3.76)-(3.79). For infinite constraint u_i , the i -th element of vector \mathbf{U} in (3.82), we define

$$E_i(\mathbf{x}_0^*, \mathbf{y}^*) = \left\{ t \in \mathbf{T} \mid u_i(\mathbf{x}_0^*, \mathbf{y}^*, t) - \rho > 0 \right\} \cap E_{i0}(\mathbf{x}_0^*, \mathbf{y}^*) \quad (3.85)$$

where

$$E_{i0}(\mathbf{x}_0^*, \mathbf{y}^*) = \left\{ t \in \mathbf{T} \mid t \text{ is a local maximizer of } u_i \text{ on } \mathbf{T} \right\}. \quad (3.86)$$

For the same reason as given in section III.5.1, all local maximizers of $u_i(\mathbf{x}_0^*, \mathbf{y}^*, t)$ that exceed a slightly positive tolerance ρ rather than 0 are focused on in (3.85). Thus $E_i(\mathbf{x}_0^*, \mathbf{y}^*)$ is the set of active points. It is composed of the local maximizers for the violated constraint u_i on the time domain \mathbf{T} .

As the illustration in Figure III.5, assume $E_i(\mathbf{x}_0^*, \mathbf{y}^*)$ is expressed as

$$E_i(\mathbf{x}_0^*, \mathbf{y}^*) = \left\{ t_k(\mathbf{x}_0^*, \mathbf{y}^*) \mid k \in K(\mathbf{x}_0^*, \mathbf{y}^*) \right\} \quad (3.87)$$

where $K(\mathbf{x}_0^*, \mathbf{y}^*)$ is a subset of a finite index set of K and $t_k(\mathbf{x}_0^*, \mathbf{y}^*)$ is continuous at $(\mathbf{x}_0^*, \mathbf{y}^*)$. The cardinality of $K(\mathbf{x}_0^*, \mathbf{y}^*)$ may vary depending on $(\mathbf{x}_0^*, \mathbf{y}^*)$. Strictly, $t_k(\mathbf{x}_0^*, \mathbf{y}^*)$ and $K(\mathbf{x}_0^*, \mathbf{y}^*)$ also depend on ρ although this dependence is implicit.

After that, the semi-infinite constraints (3.79) can be replaced by

$$q_i(\mathbf{x}_0^*, \mathbf{y}^*) = \max_{k \in K(\mathbf{x}_0^*, \mathbf{y}^*)} \left[u_i(\mathbf{x}_0^*, \mathbf{y}^*, t_k(\mathbf{x}_0^*, \mathbf{y}^*)) \right]_+ \leq 0 \quad (3.88)$$

where the tolerance ρ has been taken into account in u_i in (3.85). The expression of $q_i(\mathbf{x}_0^*, \mathbf{y}^*)$ is the infinity norm of the i -th infinite constraint of inequation (3.79) violations. Tacitly $q_i(\mathbf{x}_0^*, \mathbf{y}^*)$ is with finite dimension because the index set $K(\mathbf{x}_0^*)$ is finite. The practical implementation to obtain the multi-local maximizers in (3.88) is described in the next chapter.

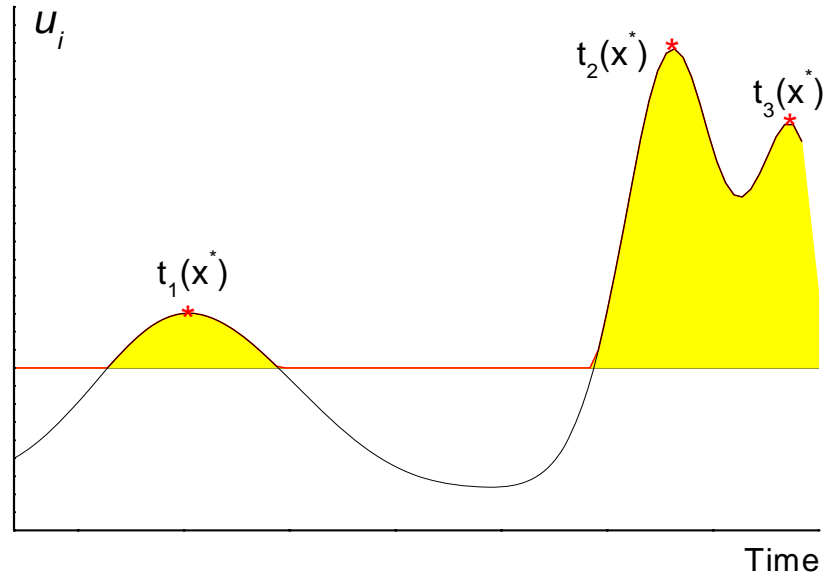


Figure III.5 Intuitionistic explanation for L_∞ norm local reduction

III.5.3 REFORMULATED TRANSIENT STABILITY CONSTRAINED OPF

Using local reduction methods for SIP, transient stability constrained OPF can be reformulated as the following traditional NLP problem:

$$\min f(\mathbf{x}_0, \mathbf{y}) \quad (3.89)$$

$$s.t. \quad \mathbf{g}(\mathbf{x}_0, \mathbf{y}) = \mathbf{0} \quad (3.90)$$

$$\mathbf{H}(\mathbf{x}_0, \mathbf{y}) \leq \mathbf{0} \quad (3.91)$$

$$\mathbf{Q}^k(\mathbf{x}_0^k, \mathbf{y}) \leq \mathbf{0} \quad k \in \mathcal{C} \quad (3.92)$$

where $\mathbf{Q} : \mathbf{R}^{n_x+n_y} \rightarrow \mathbf{R}^{n_u}$ in (3.92) can be formatted as either (3.84) by L_1 norm or (3.88) by L_∞ norm. Obviously, the equivalent programming problem (3.89-3.92) has a finite number of optimal variables and a finite number of constraints. The replacement of constraint (3.92) for the original (3.79) allows extending theory and methods of standard finite programming to the original SIP problem. The solution implementation for this problem is presented in Chapter IV. It is noted that the dimension of finite constraints \mathbf{Q} in (3.92) is equal to n_u , the dimension of the original infinite constraints \mathbf{U} in (3.79). Thus the total dimension of the optimization is kept lower than that of discretization methods, such as in [12,16].

In this study, the research is focused on the modelling of transient stability constrained OPF. The higher order generator models and more complicated controllers, such as AVR, are not included in the framework of transient stability constrained OPF although there is no theoretical limitation for such extension. Therefore, optimal solutions obtained in this framework could be somewhat conservative because some of the insecure operating points detected could be secure in practice due to the fast actions of controllers.

III.6 SUMMARY

The general scheme to solve SIP problems is introduced in this chapter and extended to the solution of transient stability constrained OPF.

Preliminaries of SIP problems are introduced. The extension of KKT optimality conditions of NLP is generalized to SIP. After that, general scheme is given to solve the SIP numerically. By using discretization and local reduction methods, SIP problems are recast into equivalent nonlinear programming problems with a finite number of constraints under appropriate assumptions. Conceptual algorithms are described. The properties of the two numerical methods are illustrated and compared.

Transient stability constrains are local reduced by L_1 and L_∞ norm local reduction methods to finite-dimensional constraints. Thus the original transient stability constrained OPF is converted into an equivalent NLP problem with finitely many variables and finitely many constraints. The transformation makes it solvable by conventional OPF methods.

Chapter IV IMPLEMENTATION OF TRANSIENT STABILITY CONSTRAINED OPF

IV.1 INTRODUCTION

With the use of local reduction based SIP methods, transient stability constrained OPF can be equivalently formulated as the following nonlinear program:

$$\min f(\mathbf{x}_0, \mathbf{y}) \quad (4.1)$$

$$s.t. \quad \mathbf{g}(\mathbf{x}_0, \mathbf{y}) = \mathbf{0} \quad (4.2)$$

$$\mathbf{H}(\mathbf{x}_0, \mathbf{y}) \leq \mathbf{0} \quad (4.3)$$

$$\mathbf{Q}(\mathbf{x}_0, \mathbf{y}) \leq \mathbf{0} \quad (4.4)$$

where $\mathbf{Q}: \mathbf{R}^{n_x+n_y} \rightarrow \mathbf{R}^{n_Q}$ in (4.4) represents transient stability constraints defined based on either rotor angle limit as in (2.17) or PEBS concept as in (2.31). No matter it is formatted by L_1 norm as in (3.84) or by L_∞ norm as in (3.88), the equivalent nonlinear programming problem (4.1-4.4) has a finite number of optimal variables and a finite number of constraints. Thus it is possible to extend theory and methods of standard finite programming to the original SIP problem.

Generally, OPF problem is non-convex and there are multiple local minima in the feasible region, and these different local minima are reached from different initial points. The non-convexity may even prevent a particular method of solution from reaching a true local or global minimum. Many attempts to overcome this problem have been published, employing the various optimization techniques, traditionally, such as nonlinear programming (NLP) [73,110,111], successive linear programming (SLP) [28,112], or successive quadratic programming (SQP) algorithms [113-114], etc. The development of numerical analysis techniques and programming methods, particularly interior point methods, allows large-scale problems in power systems to be solved with reasonable computational effort.

Since Karmarkar's fundamental paper of interior point method appeared in 1984 [115], many interior point methods for linear programming and quadratic programming have been proposed, and also extended for nonlinear programming. Extensive numerical computation has shown that the primal-dual path-following method is one of the best that is known up to now [116]. In essence, the theoretical foundation for the primal-dual path-following method comprises three crucial building blocks: Newton's method for solving nonlinear equations and hence for unconstrained optimization, Lagrange's method for optimization with equality constraints, and logarithmic barrier method for optimization with inequality constraints [117-126].

In this chapter, a direct primal-dual nonlinear interior point method is employed to solve the local reduced SIP programming problem of OPF.

IV.2 DIRECT NONLINEAR PRIMAL-DUAL INTERIOR POINT METHOD

By the introduction of slack variable vectors $\mathbf{u} \in \mathbf{R}^{n_H}$ and $\mathbf{v} \in \mathbf{R}^{n_Q}$, where $\mathbf{u}, \mathbf{v} \geq \mathbf{0}$, to (4.3) and (4.4), the previous inequation constraints in the nonlinear programming problem (4.1-4.4) can be converted to the following equation constraints

$$\mathbf{H}(\mathbf{x}_0, \mathbf{y}) + \mathbf{u} = \mathbf{0} \quad (4.5)$$

$$\mathbf{Q}(\mathbf{x}_0, \mathbf{y}) + \mathbf{v} = \mathbf{0} \quad (4.6)$$

The nonnegative feature of the slack variables can be eliminated by the employment of the logarithmic barrier method. The Lagrange function for the nonlinear programming problem (4.1-4.2) together with (4.5-4.6) can then be obtained as following by the introduction of Lagrangian multiplier to equation (4.2) and (4.5-4.6).

$$L = f(\mathbf{x}_0, \mathbf{y}) - \mathbf{y}_g^T \mathbf{g}(\mathbf{x}_0, \mathbf{y}) - \mathbf{y}_u^T (\mathbf{H}(\mathbf{x}_0, \mathbf{y}) + \mathbf{u}) - \mathbf{y}_v^T (\mathbf{Q}(\mathbf{x}_0, \mathbf{y}) + \mathbf{v}) - \mu \sum_j \ln u_j - \mu \sum_j \ln v_j \quad (4.7)$$

where y_g , y_u and y_v are the Lagrangian multiplier vectors, $y_u, y_v \leq \mathbf{0}$. μ is the barrier parameter and $\mu \geq 0$. Based on the Fiacco and McCormick's theorem [127], μ is enforced to decrease towards zero as the iterations progress.

Based on the Karush-Kuhn-Tucker optimality condition for a stationary point $(\mathbf{x}_0, \mathbf{y})$, a set of nonlinear equations can be derived from (4.7) as

$$L_{x_0} = \nabla_{x_0} f(\mathbf{x}_0, \mathbf{y}) - \nabla_{x_0} \mathbf{g}(\mathbf{x}_0, \mathbf{y}) y_g - \nabla_{x_0} \mathbf{H}(\mathbf{x}_0, \mathbf{y}) y_u - \nabla_{x_0} \mathbf{Q}(\mathbf{x}_0, \mathbf{y}) y_v = \mathbf{0} \quad (4.8)$$

$$L_y = \nabla_y f(\mathbf{x}_0, \mathbf{y}) - \nabla_y \mathbf{g}(\mathbf{x}_0, \mathbf{y}) y_g - \nabla_y \mathbf{H}(\mathbf{x}_0, \mathbf{y}) y_u - \nabla_y \mathbf{Q}(\mathbf{x}_0, \mathbf{y}) y_v = \mathbf{0} \quad (4.9)$$

$$L_{y_g} = \mathbf{g}(\mathbf{x}_0, \mathbf{y}) = \mathbf{0} \quad (4.10)$$

$$L_{y_u} = \mathbf{H}(\mathbf{x}_0, \mathbf{y}) + \mathbf{u} = \mathbf{0} \quad (4.11)$$

$$L_{y_v} = \mathbf{Q}(\mathbf{x}_0, \mathbf{y}) + \mathbf{v} = \mathbf{0} \quad (4.12)$$

$$L_u = \mathbf{U} Y_u e_u + \mu e_u = \mathbf{0} \quad (4.13)$$

$$L_v = \mathbf{V} Y_v e_v + \mu e_v = \mathbf{0} \quad (4.14)$$

where \mathbf{U} , \mathbf{V} , \mathbf{Y}_u , and \mathbf{Y}_v are diagonal matrices with the element u_i , v_i , y_{ui} , and y_{vi} . $e_u = [1, \dots, 1]^T \in \mathbf{R}^{n_H}$ and $e_v = [1, \dots, 1]^T \in \mathbf{R}^{n_Q}$. $\nabla_{\alpha} f(\mathbf{x}_0, \mathbf{y})$, $\nabla_{\alpha} \mathbf{g}(\mathbf{x}_0, \mathbf{y})$, $\nabla_{\alpha} \mathbf{H}(\mathbf{x}_0, \mathbf{y})$ and $\nabla_{\alpha} \mathbf{Q}(\mathbf{x}_0, \mathbf{y})$ are the sub-Jacobian matrices of $f(\mathbf{x}_0, \mathbf{y})$, $\mathbf{g}(\mathbf{x}_0, \mathbf{y})$, $\mathbf{H}(\mathbf{x}_0, \mathbf{y})$ and $\mathbf{Q}(\mathbf{x}_0, \mathbf{y})$ respectively, $\forall \alpha \in \{\mathbf{x}_0, \mathbf{y}\}$.

By applying Newton's method to the KKT condition (4.8-4.14), the corresponding set of linear correction equation can be derived in sequence as

$$-L_{x_0 0} = \mathbf{a}_{11} \Delta \mathbf{x}_0 + \mathbf{a}_{12} \Delta \mathbf{y} - \nabla_{x_0} \mathbf{g}(\mathbf{x}_0, \mathbf{y}) \Delta y_g - \nabla_{x_0} \mathbf{H}(\mathbf{x}_0, \mathbf{y}) \Delta y_u - \nabla_{x_0} \mathbf{Q}(\mathbf{x}_0, \mathbf{y}) \Delta y_v \quad (4.15)$$

$$-L_{y 0} = \mathbf{a}_{21} \Delta \mathbf{x}_0 + \mathbf{a}_{22} \Delta \mathbf{y} - \nabla_y \mathbf{g}(\mathbf{x}_0, \mathbf{y}) \Delta y_g - \nabla_y \mathbf{H}(\mathbf{x}_0, \mathbf{y}) \Delta y_u - \nabla_y \mathbf{Q}(\mathbf{x}_0, \mathbf{y}) \Delta y_v \quad (4.16)$$

$$-L_{y_g 0} = -\nabla_{x_0} \mathbf{g}(\mathbf{x}_0, \mathbf{y}) \Delta \mathbf{x}_0 - \nabla_y \mathbf{g}(\mathbf{x}_0, \mathbf{y}) \Delta \mathbf{y} \quad (4.17)$$

$$-L_{y_u 0} = \nabla_{x_0} H(\mathbf{x}_0, \mathbf{y}) \Delta \mathbf{x}_0 + \nabla_y H(\mathbf{x}, \mathbf{y}) \Delta \mathbf{y} + \Delta \mathbf{u} \quad (4.18)$$

$$-L_{y_v 0} = \nabla_{x_0} Q(\mathbf{x}_0, \mathbf{y}) \Delta \mathbf{x}_0 + \nabla_y Q(\mathbf{x}_0, \mathbf{y}) \Delta \mathbf{y} + \Delta \mathbf{v} \quad (4.19)$$

$$-L_{u0} = U \Delta \mathbf{y}_u + Y_u \Delta \mathbf{u} \quad (4.20)$$

$$-L_{v0} = V \Delta \mathbf{y}_v + Y_v \Delta \mathbf{v} \quad (4.21)$$

where $L_{x_0 0}$, L_{y_0} , $L_{y_g 0}$, $L_{y_u 0}$, $L_{y_v 0}$, L_{u0} and L_{v0} are the values at a point of expansion and denote the residuals of equations (4.8-4.14). In (4.15-4.16),

$$\mathbf{a}_{11} = \nabla_{x_0 x_0}^2 f(\mathbf{x}_0, \mathbf{y}) - \nabla_{x_0 x_0}^2 \mathbf{g}(\mathbf{x}_0, \mathbf{y}) \mathbf{y}_g - \nabla_{x_0 x_0}^2 H(\mathbf{x}_0, \mathbf{y}) \mathbf{y}_u - \nabla_{x_0 x_0}^2 Q(\mathbf{x}_0, \mathbf{y}) \mathbf{y}_v \quad (4.22)$$

$$\mathbf{a}_{12} = \nabla_{x_0 y}^2 f(\mathbf{x}_0, \mathbf{y}) - \nabla_{x_0 y}^2 \mathbf{g}(\mathbf{x}_0, \mathbf{y}) \mathbf{y}_g - \nabla_{x_0 y}^2 H(\mathbf{x}_0, \mathbf{y}) \mathbf{y}_u - \nabla_{x_0 y}^2 Q(\mathbf{x}_0, \mathbf{y}) \mathbf{y}_v \quad (4.23)$$

$$\mathbf{a}_{22} = \nabla_{yy}^2 f(\mathbf{x}_0, \mathbf{y}) - \nabla_{yy}^2 \mathbf{g}(\mathbf{x}_0, \mathbf{y}) \mathbf{y}_g - \nabla_{yy}^2 H(\mathbf{x}_0, \mathbf{y}) \mathbf{y}_u - \nabla_{yy}^2 Q(\mathbf{x}_0, \mathbf{y}) \mathbf{y}_v \quad (4.24)$$

$$\mathbf{a}_{21} = \mathbf{a}_{12} \quad (4.25)$$

where $\nabla_{\alpha\beta}^2 f(\mathbf{x}_0, \mathbf{y})$, $\nabla_{\alpha\beta}^2 \mathbf{g}(\mathbf{x}_0, \mathbf{y})$, $\nabla_{\alpha\beta}^2 H(\mathbf{x}_0, \mathbf{y})$ and $\nabla_{\alpha\beta}^2 Q(\mathbf{x}_0, \mathbf{y})$ are sub-Hessian matrices of $f(\mathbf{x}_0, \mathbf{y})$, $\mathbf{g}(\mathbf{x}_0, \mathbf{y})$, $H(\mathbf{x}_0, \mathbf{y})$ and $Q(\mathbf{x}_0, \mathbf{y})$ respectively, $\forall \alpha, \beta \in \{\mathbf{x}_0, \mathbf{y}\}$.

The correction equations can be reduced by eliminating $(\Delta \mathbf{u}, \Delta \mathbf{v}, \Delta \mathbf{y}_u, \Delta \mathbf{y}_v)$ to handle inequality constraints efficiently. According to (4.18-4.21),

$$\Delta \mathbf{u} = -L_{y_u 0} - \nabla_{x_0} H(\mathbf{x}_0, \mathbf{y}) \Delta \mathbf{x}_0 - \nabla_y H(\mathbf{x}_0, \mathbf{y}) \Delta \mathbf{y} \quad (4.26)$$

$$\Delta \mathbf{v} = -L_{y_v 0} - \nabla_{x_0} Q(\mathbf{x}_0, \mathbf{y}) \Delta \mathbf{x}_0 - \nabla_y Q(\mathbf{x}_0, \mathbf{y}) \Delta \mathbf{y} \quad (4.27)$$

$$\Delta \mathbf{y}_u = -U^{-1} \left[L_{u0} - Y_u \left(L_{y_u 0} + \nabla_{x_0} H(\mathbf{x}_0, \mathbf{y}) \Delta \mathbf{x}_0 + \nabla_y H(\mathbf{x}_0, \mathbf{y}) \Delta \mathbf{y} \right) \right] \quad (4.28)$$

$$\Delta \mathbf{y}_v = -V^{-1} \left[L_{v0} - Y_v \left(L_{y_v 0} + \nabla_{x_0} Q(\mathbf{x}_0, \mathbf{y}) \Delta \mathbf{x}_0 + \nabla_y Q(\mathbf{x}_0, \mathbf{y}) \Delta \mathbf{y} \right) \right] \quad (4.29)$$

After that, the reduced correction equations are obtained as

$$\begin{bmatrix} \bar{a}_{11} & \bar{a}_{12} & -(\nabla_{x_0} \mathbf{g})^T \\ \bar{a}_{21} & \bar{a}_{22} & -(\nabla_y \mathbf{g})^T \\ -\nabla_{x_0} \mathbf{g} & -\nabla_y \mathbf{g} & \mathbf{0} \end{bmatrix} \begin{bmatrix} \Delta x_0 \\ \Delta y \\ \Delta y_g \end{bmatrix} = \begin{bmatrix} \mathbf{B}_1 \\ \mathbf{B}_2 \\ -L_{y_g \theta} \end{bmatrix} \quad (4.30)$$

where

$$\bar{a}_{11} = a_{11} - (\nabla_{x_0} \mathbf{H})^T (U^{-1} Y_u) \nabla_{x_0} \mathbf{H} - (\nabla_{x_0} \mathbf{Q})^T (V^{-1} Y_v) \nabla_{x_0} \mathbf{Q} \quad (4.31)$$

$$\bar{a}_{12} = a_{12} - (\nabla_{x_0} \mathbf{H})^T (U^{-1} Y_u) \nabla_y \mathbf{H} - (\nabla_{x_0} \mathbf{Q})^T (V^{-1} Y_v) \nabla_y \mathbf{Q} \quad (4.32)$$

$$\bar{a}_{21} = \bar{a}_{12} \quad (4.33)$$

$$\bar{a}_{22} = a_{22} - (\nabla_y \mathbf{H})^T (U^{-1} Y_u) \nabla_y \mathbf{H} - (\nabla_y \mathbf{Q})^T (V^{-1} Y_v) \nabla_y \mathbf{Q} \quad (4.34)$$

$$\mathbf{B}_1 = -L_{x_0 \theta} - \nabla_{x_0} \mathbf{H} \left[U^{-1} (L_{u\theta} - Y_u L_{y_u \theta}) \right] - \nabla_{x_0} \mathbf{Q} \left[V^{-1} (L_{v\theta} - Y_v L_{y_v \theta}) \right] \quad (4.35)$$

$$\mathbf{B}_2 = -L_{y\theta} - \nabla_y \mathbf{H} \left[U^{-1} (L_{u\theta} - Y_u L_{y_u \theta}) \right] - \nabla_y \mathbf{Q} \left[V^{-1} (L_{v\theta} - Y_v L_{y_v \theta}) \right] \quad (4.36)$$

It is obvious that the coefficient matrix of the reduced correction equation (4.30) is symmetrical. Variable inequality constraints including the functional inequality are eliminated. Thus the size of (4.30), which is determined only by the number of variables and equality constraints, is much smaller than that of (4.15-4.21).

Traditionally, the corrections at each iteration can thus be readily obtained for the primal variables and dual variables. However, the calculation of the Jacobian and Hessian matrices is fairly complex due to the introduction of transient stability constraints (4.4) and is the main obstacle in solving the transient stability constrained OPF effectively.

IV.3 JACOBIAN AND HESSIAN MATRICES

The calculation of the Jacobian and Hessian matrices of transient stability constraints (4.4) is based on which norm the local reduction is taken.

IV.3.1 LOCAL REDUCTION BASED ON L_1 NORM

Based on L_1 norm local reduction as addressed in III.5.1, the semi-infinite

constraint of transient stability (4.4) is represented as

$$q_i(\mathbf{x}_0, \mathbf{y}) = \int_0^{t_e} [u_i(\mathbf{x}_0, \mathbf{y}, t)]_+ dt \leq 0, \quad \forall q_i \in \mathcal{Q} \quad (4.37)$$

The elements in Jacobian and Hessian matrices of transient stability constraints (4.37) can be represented respectively as

$$\frac{\partial q_i}{\partial \alpha} = \int_0^{t_e} \frac{\partial \max\{0, u_i(\mathbf{x}_0, \mathbf{y}, t)\}}{\partial \alpha} dt \quad (4.38)$$

$$\frac{\partial^2 q_i}{\partial \alpha \partial \beta} = \int_0^{t_e} \frac{\partial^2 \max\{0, u_i(\mathbf{x}_0, \mathbf{y}, t)\}}{\partial \alpha \partial \beta} dt \quad (4.39)$$

where α and β are any elements in the vector \mathbf{x}_0 or \mathbf{y} . Unless the transient stability constraints are satisfied in the functional space \mathcal{T} , i.e. $u_i(\mathbf{x}_0, \mathbf{y}, t) \leq 0$ and $\frac{\partial q_i}{\partial \alpha} = 0$, $\frac{\partial^2 q_i}{\partial \alpha \partial \beta} = 0$, the difficulty in calculating (4.38-4.39) lies in how to determine the first and second partial derivative of $u_i(\mathbf{x}_0, \mathbf{y}, t)$ with respect to α and β . Based on the chain rule for compound function and implicit derivative techniques, the derivations of $u_i(\mathbf{x}_0, \mathbf{y}, t)$ are formatted as

$$\frac{\partial u_i}{\partial \alpha} = \frac{\partial u_i}{\partial \mathbf{x}_t} \cdot \frac{\partial \mathbf{x}_t}{\partial \alpha} \quad (4.40)$$

$$\frac{\partial^2 u_i}{\partial \alpha \partial \beta} = \frac{\partial^2 u_i}{\partial \mathbf{x}_t^2} \cdot \frac{\partial \mathbf{x}_t}{\partial \beta} \cdot \frac{\partial \mathbf{x}_t}{\partial \alpha} + \frac{\partial u_i}{\partial \mathbf{x}_t} \cdot \frac{\partial^2 \mathbf{x}_t}{\partial \alpha \partial \beta} \quad (4.41)$$

Apparently, it is convenient to obtain $\frac{\partial u_i}{\partial \mathbf{x}_t}$ and $\frac{\partial^2 u_i}{\partial \mathbf{x}_t^2}$ in (4.40) and (4.41) directly in that $u_i(\mathbf{x}_0, \mathbf{y}, t) \equiv u_i(\mathbf{x}(t), \mathbf{y})$ is an explicit function of $\mathbf{x}(t)$, formatted compactly as \mathbf{x}_t . However, $\mathbf{x}_t = \boldsymbol{\varphi}(\mathbf{x}_0, \mathbf{y}, t)$, as defined in (3.80), is not an explicit function of either \mathbf{x}_0 or \mathbf{y} , and the calculation of $\frac{\partial \mathbf{x}_t}{\partial \alpha}$ and $\frac{\partial^2 \mathbf{x}_t}{\partial \alpha \partial \beta}$ needs further derivation.

By differentiating (2.11) with respect to α , we obtain:

$$\frac{d}{dt} \left(\frac{\partial \mathbf{x}_t}{\partial \alpha} \right) = \frac{\partial \mathbf{F}}{\partial \mathbf{x}_t} \cdot \frac{\partial \mathbf{x}_t}{\partial \alpha} + \frac{\partial \mathbf{F}}{\partial \alpha} \quad (4.42)$$

where $\frac{\partial \mathbf{F}}{\partial \mathbf{x}_t}$ and $\frac{\partial \mathbf{F}}{\partial \alpha}$ can be calculated directly in that $\mathbf{F}(\mathbf{x}(t), \mathbf{y})$ is an explicit function of \mathbf{x}_t and \mathbf{y} . Thus it is recognized that (4.42) is a set of ordinary time-varying differential equations with $\frac{\partial \mathbf{x}_t}{\partial \alpha}$ as variables with initial value

$$\frac{\partial x_{i0}}{\partial \alpha} = \begin{cases} 1, & \alpha = x_{i0} \\ 0, & \text{others} \end{cases} \quad (4.43)$$

Furthermore, by differentiating (4.42) with respect to β , we obtain:

$$\frac{d}{dt} \left(\frac{\partial^2 \mathbf{x}_t}{\partial \alpha \partial \beta} \right) = \frac{\partial^2 \mathbf{F}}{\partial \mathbf{x}_t^2} \cdot \frac{\partial \mathbf{x}_t}{\partial \beta} \cdot \frac{\partial \mathbf{x}_t}{\partial \alpha} + \frac{\partial \mathbf{F}}{\partial \mathbf{x}_t} \cdot \frac{\partial^2 \mathbf{x}_t}{\partial \alpha \partial \beta} + \frac{\partial^2 \mathbf{F}}{\partial \alpha \partial \beta} \quad (4.44)$$

Using the same tricks as in (4.42), $\frac{\partial \mathbf{F}}{\partial \mathbf{x}_t}$, $\frac{\partial^2 \mathbf{F}}{\partial \mathbf{x}_t^2}$ and $\frac{\partial^2 \mathbf{F}}{\partial \alpha \partial \beta}$ can be calculated directly, and thus, (4.44) is a set of ordinary time-varying differential equations with $\frac{\partial^2 \mathbf{x}_t}{\partial \alpha \partial \beta}$ as variables with initial value

$$\frac{\partial^2 x_{i0}}{\partial \alpha \partial \beta} = 0 \quad (4.45)$$

Afterwards the time dependent $\frac{\partial \mathbf{x}_t}{\partial \alpha}$ and $\frac{\partial^2 \mathbf{x}_t}{\partial \alpha \partial \beta}$ can be solved by integrating the ordinary differential equations (4.44) and (4.45), using the Runge-Kutta method for example. See in Appendix C.

Finally, $\frac{\partial q_i}{\partial \alpha}$ and $\frac{\partial^2 q_i}{\partial \alpha \partial \beta}$ in (4.42) and (4.44) can be obtained by numerical integration methods such as the trapezoidal rule, and the Jacobian and Hessian matrices of transient stability constraints $\mathbf{Q}(\mathbf{x}_0, \mathbf{y})$ is now computable.

IV.3.2 LOCAL REDUCTION BASED ON L_∞ NORM

Based on L_∞ norm local reduction as addressed in III.5.2, the semi-infinite

constraint of transient stability (4.4) is represented as

$$q_i(\mathbf{x}_0, \mathbf{y}) = \max_{k \in K(\mathbf{x}_0, \mathbf{y})} \left[u_i(\mathbf{x}_0, \mathbf{y}, t_k(\mathbf{x}_0, \mathbf{y})) \right]_+ \leq 0, \quad \forall q_i \in \mathbf{Q} \quad (4.46)$$

Before the calculation of the Jacobian and Hessian matrices of transient stability constraints (4.46), it is noted that the global or near global maximizer should be detected among all the local maximizers of u_i , which is referred to as a multi-local optimization problem.

For given $(\mathbf{x}_0, \mathbf{y})$, all zeros of $\frac{du_i}{dt}$ in the interior of \mathbf{T} have to be computed together with all maximizers on the boundary of \mathbf{T} . Thanks to one-dimensional characteristic of the functional space \mathbf{T} , in principal, the global maximizers is able to be detected coarsely by comparison of function values of u_i on a uniform mesh over \mathbf{T} composed of step by step integration of (2.11) with appropriate stepsize. However, practically, the mesh has to be subtle enough to prevent omitting the global maximizer, which will increase computation efforts.

In this thesis, the detection of global maximizer is accomplished by function value comparison among all zeros of $\frac{du_i}{dt}$ in the interior of \mathbf{T} and all maximizers on the boundary of \mathbf{T} . Take the transient stability constraints defined in (2.17) as an example, for generator i , all the local maximizers satisfy

$$\frac{dh_i}{dt} = \omega_i - \omega_{COI} = 0 \quad (4.47)$$

and

$$\omega_{COI} = \frac{\sum_{i=1}^{ng} M_i \omega_i}{\sum_{i=1}^{ng} M_i} \quad (4.48)$$

It is noted that the absolute value of $\frac{du_i}{dt}$ could be much larger than zero, except

at zeros of $\frac{du_i}{dt}$, if u_i is steep over T . Thus merely based on the value of $\frac{du_i}{dt}$ is not a reliable criterion to determine zeros of $\frac{du_i}{dt}$.

Theorem 4.1 Intermediate Value Theorem

Suppose an interval $I = [a, b] \in \mathbb{R}$, and $f : I \rightarrow \mathbb{R}$ is a continuous function. For a real value σ , there exist $c \in (a, b)$ satisfying $f(c) = \sigma$ if $f(a) < \sigma < f(b)$ or $f(b) < \sigma < f(a)$.

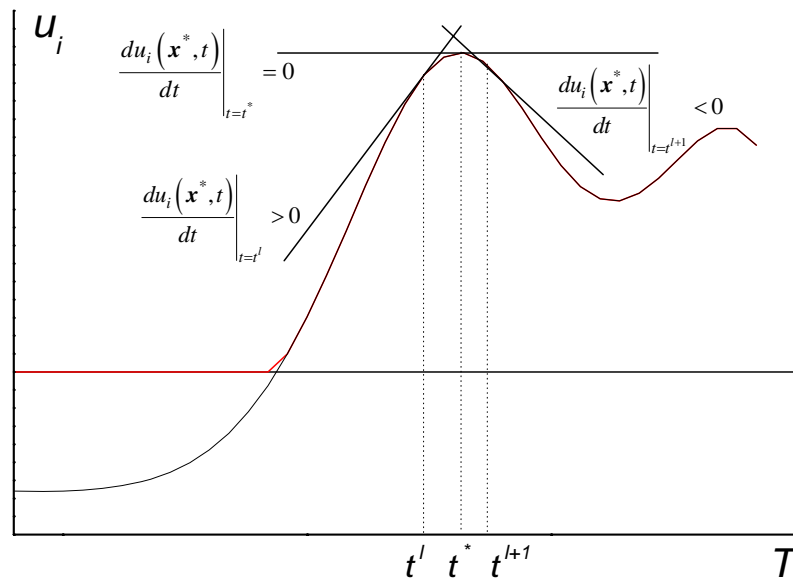


Figure IV.1 Intuitionistic explanation for local maximizer detection

According to intermediate value theorem, zeros of $\frac{du_i(\mathbf{x}^*, t)}{dt}$ are able to be positioned between t^l and t^{l+1} if $\left. \frac{du_i(\mathbf{x}^*, t)}{dt} \right|_{t=t^l}$ and $\left. \frac{du_i(\mathbf{x}^*, t)}{dt} \right|_{t=t^{l+1}}$ have opposite signs as illustrated in Figure IV.1, i.e. $\left. \frac{du_i(\mathbf{x}^*, t)}{dt} \right|_{t=t^l} \cdot \left. \frac{du_i(\mathbf{x}^*, t)}{dt} \right|_{t=t^{l+1}} < 0$. After

that, the local maximizer t^* is approximated by the larger based on the comparison between $u_i(\mathbf{x}^*, t^l)$ and $u_i(\mathbf{x}^*, t^{l+1})$ if at least one of them is positive, which means the relative constraint is violated; otherwise the local maximizer of $u_i(\mathbf{x}^*, t)$ can only be positioned approximately by reducing the distance between t^l and t^{l+1} . These approximations can be refined by iterative procedures afterwards if higher accuracy is needed. If $u_i(\mathbf{x}^*, t)$ is nearly constant over the mesh in \mathbf{T} , then most function evaluations will be redundant. Larger stepsize can be used to reduce the redundant computation.

Now that the global maximizer of u_i is able to be detected, implicit derivative techniques employed in IV.3.1 can also be used here to compute the derivatives $\frac{\partial q_i}{\partial \alpha}$ and $\frac{\partial^2 q_i}{\partial \alpha \partial \beta}$. Finally, the Jacobian and Hessian matrices of transient stability constraints $\mathcal{Q}(\mathbf{x}_0, \mathbf{y})$ is computable.

IV.4 OVERALL IMPLEMENTATION OF THE ALGORITHM

The overall implementation of the primal-dual interior point method for the transient stability constrained OPF is as follows:

- a) Initialization: input system parameters, the initial value of primal-dual variables, required convergence accuracy ε_1 and ε_2 , for complementary gap G_{gap} and the maximal mismatch of power flow M_{max} respectively, etc. Set the iteration counter $k = 0$, the maximal iteration number and damping factor $\sigma \in (0, 1)$. Here, complementary gap

$$G_{gap} = -\sum_{i=1}^{n_H} y_{ui} u_i - \sum_{i=1}^{n_Q} y_{vi} v_i \quad (4.49)$$

is employed instead of duality gap. The reason is that the value of duality gap may not be positive because the primal and dual variables are not feasible [120].

- b) Test whether transient stability constraints, formulated based on either rotor angle limit or PEBS concept, are satisfied. If yes, set FLAG=0, and go to next step; otherwise, set FLAG=1 and jump to step (e).
- c) Check whether convergence precisions are satisfied. Compute G_{gap} and M_{max} . If both G_{gap} and M_{max} are satisfied, then the output optimal solution is obtained and go to the final step (i); otherwise, go to the next step.
- d) Compute the barrier penalty parameter

$$\mu = \frac{\sigma G_{gap}}{n_H + n_Q} \quad (4.50)$$

- e) If FLAG=1, locally reduce the original SIP problem based on L_1 or L_∞ norm and calculate the Jacobian and Hessian matrices of transient stability constraints Q according to the proposed method in IV. 3; otherwise, if FLAG=0, set the Jacobian and Hessian matrices of Q to be zero.
- f) Formulate the linear correction equations (4.30). Solve the correction equations, obtain the correction direction $\Delta \mathbf{x}_0$, $\Delta \mathbf{y}$ and $\Delta \mathbf{y}_g$. Substitute into (4.26-4.29), $\Delta \mathbf{u}$, $\Delta \mathbf{v}$, $\Delta \mathbf{y}_u$ and $\Delta \mathbf{y}_v$ are obtained.
- g) Determine the step lengths $step_p$ and $step_d$ for the primal and dual variables respectively.

$$step_p = 0.9995 \min \left\{ 1.0, \min_i \left\{ \frac{-\alpha_i}{\Delta \alpha_i}, \text{ if } \Delta \alpha_i < 0 \right\} \right\}, \alpha \in \mathbf{x}_0, \mathbf{y}, \mathbf{u}, \mathbf{v} \quad (4.51)$$

$$step_d = 0.9995 \min \left\{ 1.0, \min_i \left\{ \frac{-\beta_i}{\Delta \beta_i}, \text{ if } \Delta \beta_i < 0 \right\} \right\}, \beta \in \mathbf{y}_u, \mathbf{y}_v \quad (4.52)$$

The constant, 0.9995, is chosen to prevent nonnegative variables, \mathbf{u} and \mathbf{v} , from being zero. Because of this feature, the logarithmic barrier functions are continuous and differentiable. Moreover, during the algorithm, there is no need to evaluate any barrier function, $\ln(\bullet)$.

h) Update primal and dual variables

$$\begin{bmatrix} \mathbf{x}_0 \\ \mathbf{y} \\ \mathbf{u} \\ \mathbf{v} \end{bmatrix}^{(k+1)} = \begin{bmatrix} \mathbf{x}_0 \\ \mathbf{y} \\ \mathbf{u} \\ \mathbf{v} \end{bmatrix}^{(k)} + step_p \cdot \begin{bmatrix} \Delta \mathbf{x}_0 \\ \Delta \mathbf{y} \\ \Delta \mathbf{u} \\ \Delta \mathbf{v} \end{bmatrix}^{(k)} \quad (4.53)$$

$$\begin{bmatrix} \mathbf{y}_g \\ \mathbf{y}_u \\ \mathbf{y}_v \end{bmatrix}^{(k+1)} = \begin{bmatrix} \mathbf{y}_g \\ \mathbf{y}_u \\ \mathbf{y}_v \end{bmatrix}^{(k)} + step_d \cdot \begin{bmatrix} \Delta \mathbf{y}_g \\ \Delta \mathbf{y}_u \\ \Delta \mathbf{y}_v \end{bmatrix}^{(k)} \quad (4.54)$$

Set $k = k + 1$, jump back to step (b).

i) Output the optimal solution and stop.

It is noted that Newton based method can only converge to a local minimal solution. Starting from different initial points, for example, as x_1^0 and x_2^0 shown in Fig. IV.2, Newton method may converge to different local optimal solutions x^* and x^{**} respectively, which may not be the global optimal solution. Therefore, global solution should be found by using advanced global programming methods [128] or triggering the process from different starting points in case more economical solutions are expected; however, this is beyond the scope of this research.

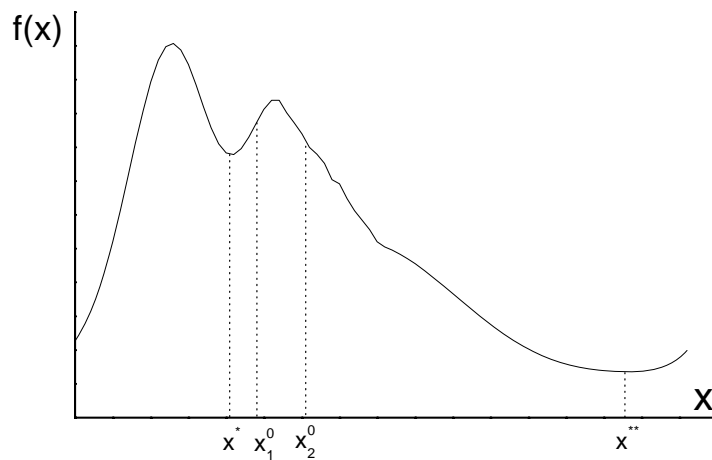


Figure IV.2 Optimal solutions obtained from different starting points

IV.5 IMPROVED BFGS METHOD

Most often, Hessian matrix in Newton's method is not easy to derive. Its computation becomes much more difficult for semi-infinite constraints for transient stability due to the involvement of complicated implicit function relationships for the transcribed infinite dimensional constraints based on local reduction methods.

In Newton's method a quadratic approximation is used instead of a linear approximation of the function $F(\mathbf{x})$. The next approximate solution is obtained at a point that minimizes the quadratic function

$$F(\mathbf{x}_{k+1}) = F(\mathbf{x}_k + \Delta\mathbf{x}_k) = F(\mathbf{x}_k) + \mathbf{g}_k^T \Delta\mathbf{x}_k + \frac{1}{2} \Delta\mathbf{x}_k^T \mathbf{H}_k \Delta\mathbf{x}_k \quad (4.55)$$

Hence, the obtained sequence is

$$\mathbf{x}_{k+1} = \mathbf{x}_k - \mathbf{H}_k^{-1} \mathbf{g}_k^T \quad (4.56)$$

which needs the calculation of Jacobian matrix \mathbf{g}_k and Hessian matrix \mathbf{H}_k .

To avoid the complex derivation of \mathbf{H} , the idea of quasi-Newton methods can be adopted to update an approximation of \mathbf{H} as the iteration progresses. Suppose

$$\mathbf{H} = \mathbf{C} + \mathbf{A} \quad (4.57)$$

where \mathbf{C} is the computed part and \mathbf{A} is the approximated part. Generally, \mathbf{C} is much easier to be obtained than \mathbf{A} . Thus, quasi-Newton methods tend to exploit this structure by updating \mathbf{A} only [129]. Hence,

$$\mathbf{H}_+ = \mathbf{C}_+ + \mathbf{A}_+ \quad (4.58)$$

the updated Hessian matrix is approximated by the combination of the exact computation of the computed part \mathbf{C} and approximated part \mathbf{A} .

Broyden-Fletcher-Goldfarb-Shanno (BFGS) method [106,129] is a kind of quasi-Newton method with superlinear convergence. Different from the traditional update for the whole Hessian matrix by BFGS, here, we adopt a special case of a result from [130] in the BFGS formulation, and name it as the improved BFGS method. Only the approximated part \mathbf{A} of Hessian matrix is calculated as

$$\mathbf{A}_+ = \mathbf{A}_c + \frac{\boldsymbol{\gamma}_k \boldsymbol{\gamma}_k^T}{\mathbf{d}_k \boldsymbol{\gamma}_k^T} - \frac{\mathbf{A}_c \mathbf{d}_k \mathbf{d}_k^T \mathbf{A}_c}{\mathbf{d}_k^T \mathbf{A}_c \mathbf{d}_k} \quad (4.59)$$

where

$$\mathbf{d}_k = \mathbf{x}_{k+1} - \mathbf{x}_k \quad (4.60)$$

$$\boldsymbol{\gamma}_k = \mathbf{g}_{k+1} - \mathbf{g}_k \quad (4.61)$$

The quasi-Newton iteration defined by (4.59) exists and converges superlinearly to \mathbf{x}^* . This result is given as theorem 4.3.2 in [129].

Generally, quasi-Newton method is to approximate the true Hessian matrix \mathbf{H} by updating an approximated matrix from iteration to iteration incorporating the most recent gradient information. Since only the approximated part of the true Hessian matrix is updated by the improved BFGS method, more information of the true Hessian matrix is preserved. As a result, the final approximated Hessian matrix for the whole programming is remarkably closer to the true one than that by traditional BFGS method. Therefore, the performance of the programming will be better than the traditional ones.

In the OPF model proposed in this thesis, obviously, the Hessian matrix for traditional OPF problem is much easier to compute than the one with transient stability constraints introduced. Thus, the accurate Hessian matrix for the conventional programming (4.1-4.3) is computed directly as \mathbf{C} ; whilst the Hessian matrix related with transient stability constraint (4.4) is approximated as \mathbf{A} . In other words, the sum of \mathbf{C} and \mathbf{A} would be the Hessian matrix for the whole programming problem (4.1-4.4) if \mathbf{A} is close enough to the true one.

IV.6 MEASURES TO IMPROVE COMPUTATION EFFICIENCY

The computational burden in the proposed method is much heavier than the conventional OPF due to the involvement of transient stability constraints. It is very necessary to improve the efficiency and reduce the computational efforts for practical use of the proposed method. The semi-infinite transient stability constraints are

required to be satisfied in the study period $(0, t_e]$. The following two remarks can be drawn:

- 1) Let $t_1, t_2 \in (0, t_e]$, and $t_1 > t_2$. If the system fails to satisfy transient stability constraints in $(0, t_2]$, which means that there exist $u_i(\mathbf{x}(t), \mathbf{y}) > 0$, $u_i \in U$, $t \in (0, t_2]$ as in (3.79), then the system fails to satisfy transient stability constraints in $(0, t_1]$ as well, which means that $u_i(\mathbf{x}(t), \mathbf{y}) > 0$, $t \in (0, t_1]$.
- 2) Discretize the study time interval $(0, t_e]$ into a time sequence $\mathbf{T} = \{T_1, T_2, \dots, T_m\}$, $T_i = (0, t_i]$, with step length Δh , where $t_i < t_j$ and $0 < i < j \leq m$. If the system satisfies transient stability constraints in T_{i-1} , but not satisfies in T_i , which means $u_i(\mathbf{x}(t), \mathbf{y}) \leq 0$, $\forall t \in T_{i-1}$ and $u_i(\mathbf{x}(t), \mathbf{y}) > 0$, $t \in T_i$, then we define the constraints in the time interval T_i as the most effective section of transient stability constraints.

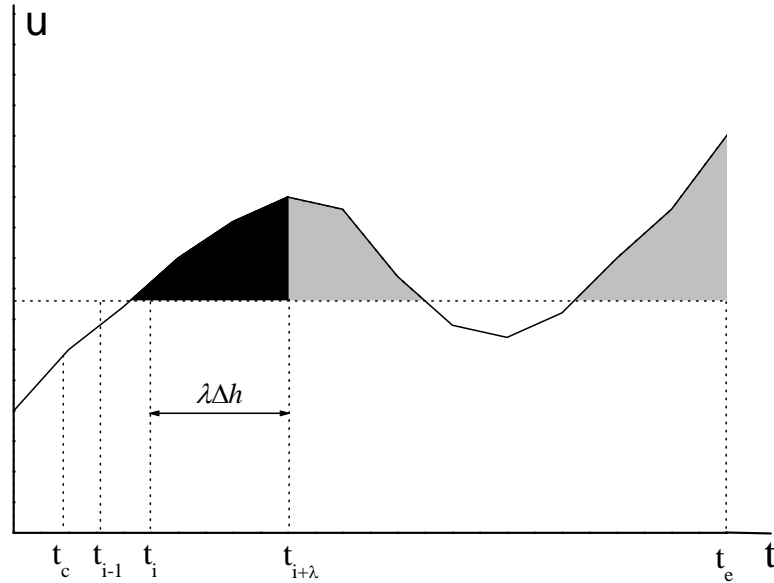


Figure IV.3 Intuitionistic explanation of transient stability constraints

By replacing the transient stability constraints in its whole functional space with its most effective section, the computation burden can be reduced considerably during the optimization process since it is not necessary to take the overall transient

behaviour in T_{nt} into account if transient instability occurs at $t = t_i < t_e$. However, in order to improve the convergence of the optimization, it would be better to reasonably expand the most effective section to strengthen the transient stability constraints. As illustrated in Figure IV.2, λ steps were extended after the time interval T_i which is the most effective section of transient stability constraints.

Since only the most effective section $T_{i+\lambda}$ of transient stability constraints is introduced in the optimization, the computation efforts are reduced considerably. However, it should be noted that the locally reduced semi-infinite constraints may vary from iteration to iteration in the optimization generally. Therefore, it is necessary to determine whether and when the instability will occur in each iterate. Based on the numerical test results, the instability instant t_i , the first time that the transient stability constraints are violated, is found to move toward t_e gradually with the optimization process progressing. This indicates the system security for a given contingency has been improved to cover the whole period $(0, t_e]$ associated with the optimization procedure.

IV.7 SUMMARY

This chapter deals with the implementation of solving transient stability constrained OPF.

The direct nonlinear primal-dual interior point method is employed to solve the locally reduce SIP problem. The theoretical difficulties in forming the Jacobian and Hessian matrices of the transient stability constraints are overcome using implicit relationship between the transient stability constraints and the DAEs for the dynamic performance. In the L_∞ norm local reduction, the multi-local maximizers are easily detected by intermediate value theorem. After that, the overall algorithm is presented.

Moreover, an improved BFGS method, a quasi-Newton method with superlinear convergence, is exploited to avoid the complicated derivation of Hessian matrix. The Hessian matrix is splitting into two parts: one is easier to obtain exactly for

conventional OPF and the other is more difficult to derive for transient stability constraints. Only the difficult part is approximated by BFGS updating.

Finally, a new concept referred as "the most effective section" of transient stability constraints is proposed to alleviate the huge computational efforts and improve the convergence of the optimization calculation.

Chapter V CALCULATION OF AVAILABLE TRANSFER CAPABILITY

In this chapter, the calculation of available transfer capability (ATC) is investigated as an application of transient stability constrained OPF.

V.1 INTRODUCTION

ATC is not only a technical index for the safe operation of power grid, but also a market signal that reflects the capability of more commercial activities between interconnected transmission networks in power market as well. Although earlier study of transfer capability could be traced back to decades ago, such as in [17], the demand and application of ATC calculation did not attract researchers' attention until the electric industry started deregulation and open access. In US, FERC mandated the order 888 and 889 in 1996, which claim that the public utility had to open their transmission grid for market participants and required that the ATC information of the transmission networks should be calculated and posted on Open Access Same-time Information System (OASIS). Shortly later in the same year, North America Electric Reliability Council (NERC) presents a comprehensive definition for ATC in [131] at the first time. After that, a framework for ATC definition and evaluation is established for interconnected electric network in North America [132]. The calculation of ATC is employed practically in North America from then on [133].

According to NERC's definition, ATC is the transfer capability remaining in the physical transmission network for further commercial activity over and above already committed uses [132]. Numerically, ATC is the transfer capability deduced from the Total Transfer Capability (TTC) less the Transmission Margin (TM) and the sum of existing transmission commitments (ETC) as

$$ATC = TTC - ETC - TM \quad (5.1)$$

Particularly, TTC is defined as the amount of electric power that can be transferred over a specific interface or a corridor of the interconnected transmission network whilst all the reliability conditions are satisfied. TM is defined as the amount of transmission transfer capability reserved for the uncertainties in the system operation. It is composed of Transmission Reliability Margin (TRM) and Capacity Benefit Margin (CBM). TRM is defined as that amount of transmission transfer capability necessary to ensure that the interconnected network is secure under a reasonable range of uncertainties in system conditions. CBM is defined as that amount of transmission transfer capability reserved by load serving entities to ensure access to generation from interconnected systems to meet generation reliability requirements. It is recognized that different transmission systems, such as individual systems, power pools, sub-regions and regions, identify their different TRM and CBM procedures used to establish transfer margins as necessary. Without the consideration of TM, the value of ATC is the TTC less the basic case power flow. As a result, the calculation of TTC will be focused in this thesis to determine ATCs in interconnected transmission networks.

The definition of TTC between any two areas or across particular paths or interfaces is direction specific. TTC is the amount of electric power that can be transferred over the interconnected transmission network in a reliable manner. For existing or planned system configurations with normal (pre-contingency) operating procedures in effect, all facility loadings are required to be within normal ratings and all voltages within normal limits. The electric systems should be capable of absorbing the dynamic power swings, and remaining stable, following a disturbance that results in the loss of any single electric system element, such as a transmission line, transformer, or generating unit. Depending on the variation in operation conditions, the most stringent operation limits may shift among thermal, voltage and transient stability limits over time. Nevertheless, the determination of TTC has to respect to the strictest of them. Thus the calculation of ATC can be formulated as an OPF problem with the objective to maximize the transfer capability over some

specific interfaces of interconnected networks and security constraints.

Since the loss and control cost associated with transient instability is very expensive, transient stability, as an important constraint, is necessary to be included in the OPF modelling for the calculation of ATC so that the system is able to survive in credible contingencies. However, the involvements of OPF based ATC calculation with transient stability constraints are much more complicated than that of the conventional OPF problem so that traditional programming methods cannot solve this SIP problem directly. In this thesis, the calculation of ATC is modelled as an SIP problem and solved by SIP methods.

V.2 MODELLING OF ATC

The calculation of ATC depends on the determination of the total or maximal transfer capability (TTC) of the network so that all the operation and security constraints are satisfied. Thus, the calculation of ATC is modelled as an OPF problem as

$$\min f(\mathbf{x}_0, \mathbf{y}) \quad (5.2)$$

$$s.t. \quad \mathbf{g}(\mathbf{x}_0, \mathbf{y}) = \mathbf{0} \quad (5.3)$$

$$\mathbf{H}(\mathbf{x}_0, \mathbf{y}) \leq \mathbf{0} \quad (5.4)$$

$$\mathbf{U}(\mathbf{x}(t), \mathbf{y}) \leq \mathbf{0} \quad (5.5)$$

where $f(\mathbf{x}_0, \mathbf{y})$ is the objective function of TTC in specific interface. $\mathbf{g}(\mathbf{x}_0, \mathbf{y})$ is equality constraints for power flow balance. Inequality constraints $\mathbf{H}(\mathbf{x}_0, \mathbf{y})$ are the steady-state operation limits of the system including the upper and lower limits of the generator outputs, bus voltage magnitudes, transformer taps, and power flow on transmission lines, etc. Inequality constraints $\mathbf{U}(\mathbf{x}(t), \mathbf{y})$ are the semi-infinite constraints for transient stability. Therefore, the calculation of ATC is eventually determined by the strictest limit of all these security constraints, including steady-state or transient security limits. $\mathbf{U}(\mathbf{x}(t), \mathbf{y})$ can be locally reduced based on L_1 or L_∞

norm penalty functions respectively. Primal-dual interior point method is used to solve the transcribed finite programming problem.

The objective of ATC computation is to determine the maximal transfer capability of the network. For OPF study, generally, the objective is to find minimal. Therefore, $f(\mathbf{x}_0, \mathbf{y})$ is defined in this thesis as the negative ATC over some specific interfaces between interconnected networks. One interface is generally composed of transmission lines in the cut set for individual networks respectively. As shown in Figure V.1, the interface of area i , $i=1, \dots, N$, to other areas is its cut set Γ_{Ti} .

Transfer capability is the measure of the ability of interconnected electric systems to reliably transfer power from one area to another over the interface in between under specified system conditions. The units of transfer capability are in terms of electric power, generally expressed in megawatts (MW). In this context, "area" may be an individual electric system, power pool, control area, subregion, or a portion of any of these.

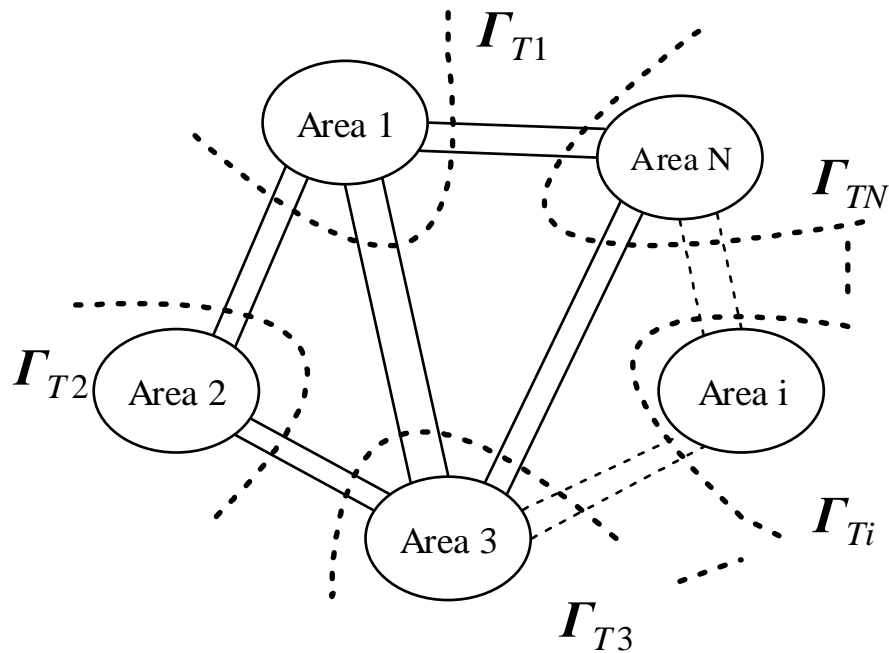


Figure V.1 Interconnected systems and their respective transmission interfaces

Before the calculation of transfer capability, Assumption 5.1 and Theorem 5.1 are given with reference to [134].

Assumption 5.1 For the transfer capability from area i to j ,

- 1) The base case of the system operation is specific, no matter whether it is existing or planned.
- 2) All loads in area i are the same with the power flow in base case and fixed.
- 3) All generation outputs in area j are the same with the power flow in base case and fixed.
- 4) All of the loads and generation outputs in the other interconnected areas, except area i and j , are the same with the power flow in base case and fixed.
- 5) The increase of the loads in area j will lead to the increase of the generation output in area i until any limit of system operation is reached.

Theorem 5.1 If Assumption 5.1 holds, without the consideration of transmission loss, the following six formulations of maximal transfer capability from area i to j are equal:

1) Maximize the sum of all generation outputs in area i , i.e. $f_1 = \max\left(\sum_{k \in \Gamma_{Gi}} P_{Gk}\right)$.

2) Maximize the sum of all active loads in area j , i.e. $f_2 = \max\left(\sum_{l \in \Gamma_{Lj}} P_{Ll}\right)$.

3) Maximize the sum of all generation outputs in area i and all active loads in area j , i.e. $f_3 = \max\left(\sum_{k \in \Gamma_{Gi}} P_{Gk} + \sum_{l \in \Gamma_{Lj}} P_{Ll}\right)$.

4) Maximize the sum of output active power in the interface Γ_{Ti} of area i , i.e.

$$f_4 = \max\left(\sum_{ij \in \Gamma_{Ti}} P_{ij}\right).$$

Here, "output" refers to the power flows out from all

the sources of the interface Γ_{Ti} .

- 5) Maximize the sum of input active power in the interface Γ_{Tj} of area j , i.e.

$$f_5 = -\max\left(\sum_{ji \in \Gamma_{Tj}} P_{ji}\right). \text{ Here, "input" refers to the power flows into the sinks}$$

of the interface Γ_{Tj} .

- 6) Maximize the sum of output active power in the interface Γ_{Ti} of area i and input active power in the interface Γ_{Tj} of area j , i.e.

$$f_6 = \max\left(\sum_{ij \in \Gamma_{Ti}} P_{ij} - \sum_{ji \in \Gamma_{Tj}} P_{ji}\right).$$

where for area k , $k = 1, \dots, N$, its interface with other areas is Γ_{Tk} , generator bus set is Γ_{Gk} , loading bus set is Γ_{Lk} .

The objective function of ATC can be selected from the six formulations in Theorem 5.1. In this thesis, the fourth formulation of the sum of output active power in the interface Γ_{Ti} of area i is employed.

V.3 CASE STUDY AND DISCUSSIONS

The proposed algorithms for the calculation of ATC are fully tested on the WSCC 9-bus and the New England 39-bus system.

V.3.1 WSCC 9-BUS SYSTEM

The full system parameters of WSCC 9-bus system are detailed in Appendix A and [135]. This system consists of 3 generators, 9 buses, 3 load points, and 6 transmission lines. Bus 1 is the slack bus, and the system base is 100 MVA. For the evaluation of the purposed method, this 9-bus system is partitioned into A and B subsystems as shown in Figure V.2. The interconnected interface consists of line 7-5 and 9-6 with transfer direction as illustrated in Figure V.2. The objective function is selected as the TTC in the interface. The base case power flow across this interface is

1.4778 pu.

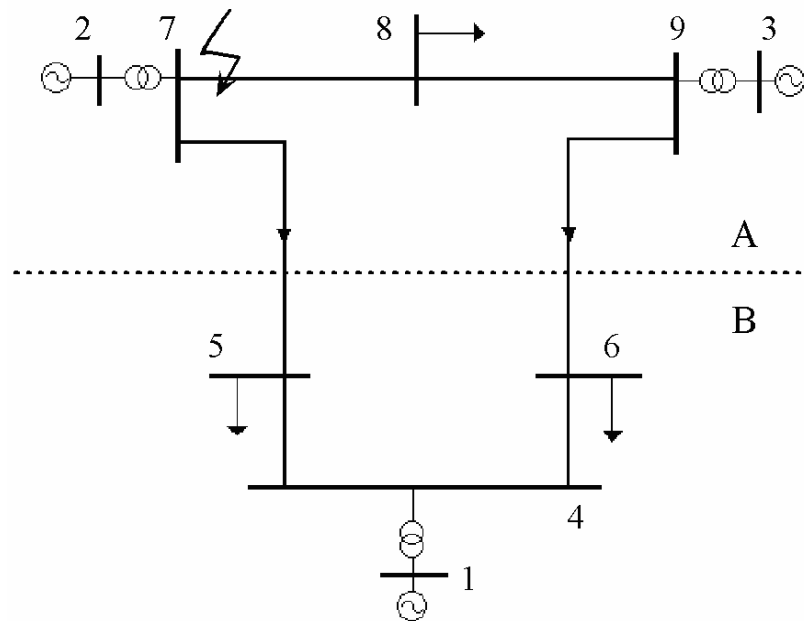


Figure V.2 One line diagram of the WSCC 9-bus system

For simplicity, only one single contingency is considered here. It consists of a three-phase fault occurred near bus 7 at the end of line 8-7. The fault is subsequently cleared at $t = 0.18s$ with line 8-7 tripped.

V.3.1.1 VALIDATION TEST

Three methods are employed here to validate the proposed ATC computation by comparison with each other. Method 1 is the conventional OPF optimization without the consideration of transient stability constraints. Both Method 2 and 3 include transient stability constraints for the specific contingency based on rotor angle limit with the threshold $\delta_{\max} = 120^\circ$ relaxed by $\rho = 0.01$. The transient period under study is 1.5 sec with integration time step length of 0.01 sec. Here, 1.5 second is selected based on the recommendation from [21] to ensure the system stability during the first swing. Method 3, as an enhancement to the Method 2, uses the proposed concept of the most effective section of transient stability constraints with

$\lambda = 6$, as defined in Section IV.6. Local reduction based on L_1 norm is applied here to transcribe semi-infinite constraints in Method 2 and 3. Convergence accuracies ε_1 and ε_2 in all the three methods, for complementary gap G_{gap} and the maximal mismatch of power flow M_{max} respectively, are set to 10^{-3} .

Table V.1 Optimal results obtained with the WSCC 9-bus system

Method	TTC (p.u.)	Increase of TTC (%)	ATC (p.u.)	Iteration Counter
1	2.1113	42.87	0.6335	10
2	1.9878	34.51	0.5100	106
3	2.0068	35.80	0.5290	21

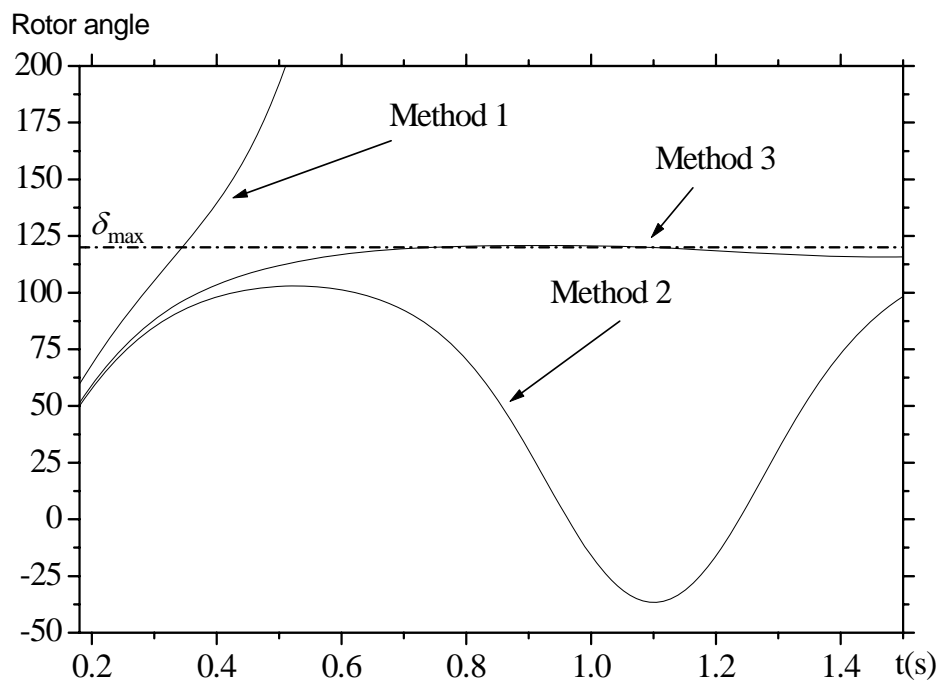


Figure V.3 Comparison between swing curves of generator 2 based on optimization by Method 1, 2 and 3

Table V.1 shows the optimization results obtained by the three methods. Figure V.3 shows the largest rotor swing curves, which belongs to generator 2, in the

credible contingency according to the operation conditions by the three methods.

In the absence of any transient stability constraints, the TTC by Method 1 is 2.1113 pu, 42.87% increase compared with the base case. However, the optimized system is transient insecure and will become unstable after about 0.4 sec for the given contingency as illustrated in Figure V.3; whereas, the systems optimized by Method 2 and 3 can meet the security requirement and remain transient stable under the same contingency, but with the expense of 0.1235 pu and 0.1045 pu decrease in TTC compared with the optimal result by Method 1, respectively. Most often, the decreased TTC, which is able to survive dynamically, can be regarded as a social optimal solution since system security is guaranteed and the aggregate benefit is maximized.

V.3.1.2 NUMERICAL ANALYSIS

The changes of the complementary gap, maximum power flow mismatch, and instability instant in the optimization by Method 2 and 3 for WSCC 9-bus system are plotted in Figure V.4 and V.5, respectively.

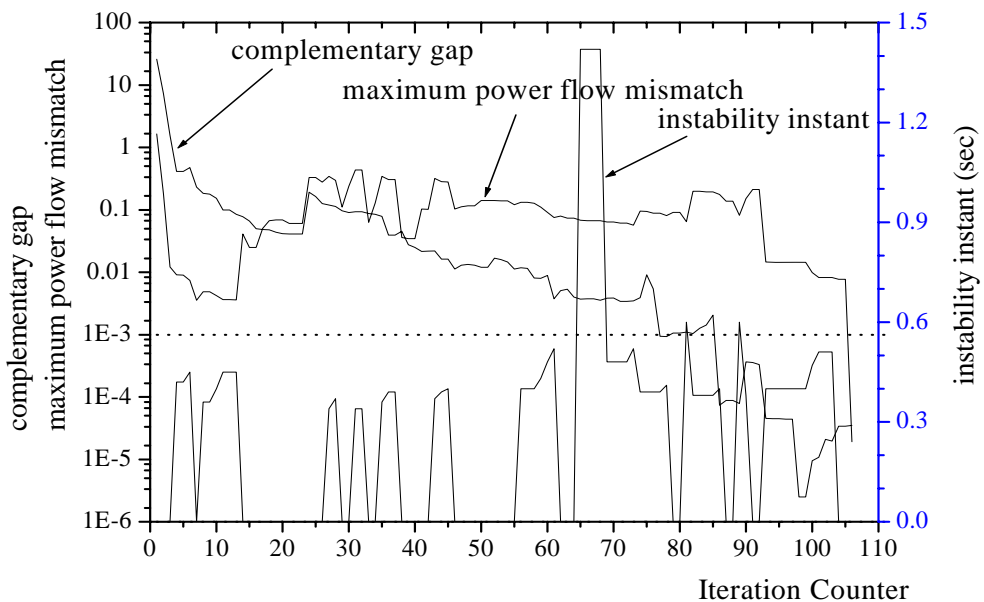


Figure V.4 Change of maximum power flow mismatch, complementary gap and instability instant in the calculation by Method 2

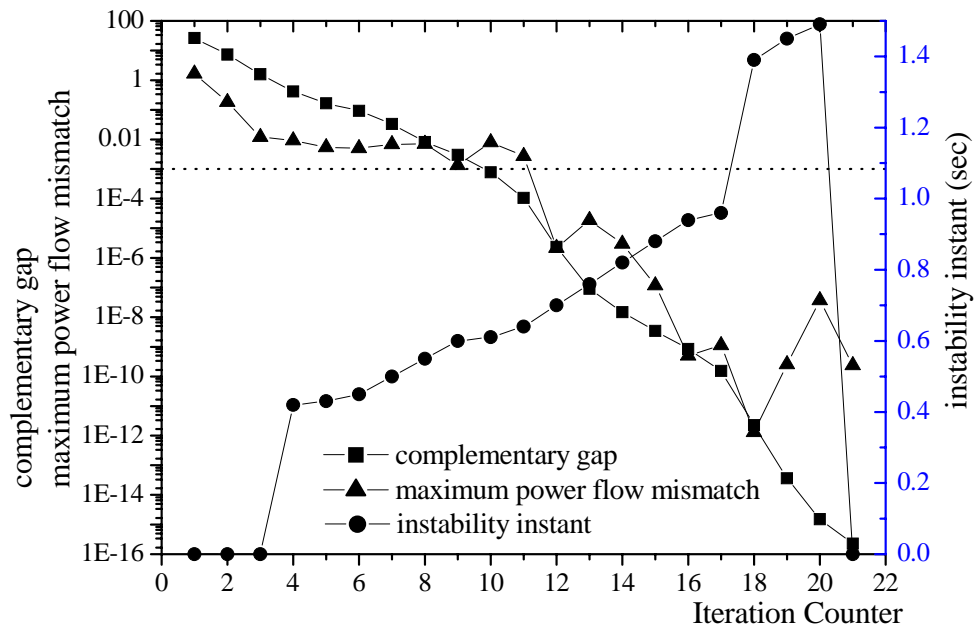


Figure V.5 Change of maximum power flow mismatch, complementary gap and instability instant in the calculation by Method 3

The "instability instant" referred in the figures is the time when the rotor angle of any generator first passes the maximum allowable angle δ_{\max} . For the convenience of the plotting, the instability instant is set to zero if the system is transient stable for the whole period of study, i.e. all transient stability constraints are satisfied.

Although both Method 2 and Method 3 take the transient stability constraints into consideration, the optimization results produced by Method 2 and 3 are not quite the same as illustrated in the WSCC 9-bus system. As illustrated in Figure V.4, the complementary gap and the maximum power flow mismatch are disturbed seriously whenever there is a violation of transient stability constraints. Most often those disturbances caused by the transient stability constraints are large enough to spoil the optimization process and even make the optimization become infeasible. On the contrary, Method 3 introduces transient stability constraints gently iteration by iteration using the most effective section concept. As illustrated in Figure V.5, the complementary gap, maximum power flow mismatch and instability instant do not

fluctuate as frequently as the ones in Method 2. This indicates that the optimization process progresses nicely to reach the optimum.

As for the computation efficiency, Method 3 is more efficient than Method 2 because of its better convergence property. Much less number of iterations is required to obtain the optimum solution using Method 3. According to the results of WSCC 9-bus system, the iteration counter in Method 3 is 21, just about one-fifth of that in Method 2.

Moreover, the computation efforts in each iteration in Method 3 is greatly reduced since only the most effective section is computed instead of the whole transient stability simulation period. As shown in Figure V.6, area C is the most effective section of transient stability constraints in each iterate, whose upper boundary is the instability instant. Area B is an extension of the most effective section of area C. Compared with Method 2, which requires the calculation in area A, B and C, only the calculation in area B and C are needed in Method 3. Therefore, even if Method 2 and 3 have the same number of iterations, the computation efforts of Method 3 are still much less than that of Method 2.

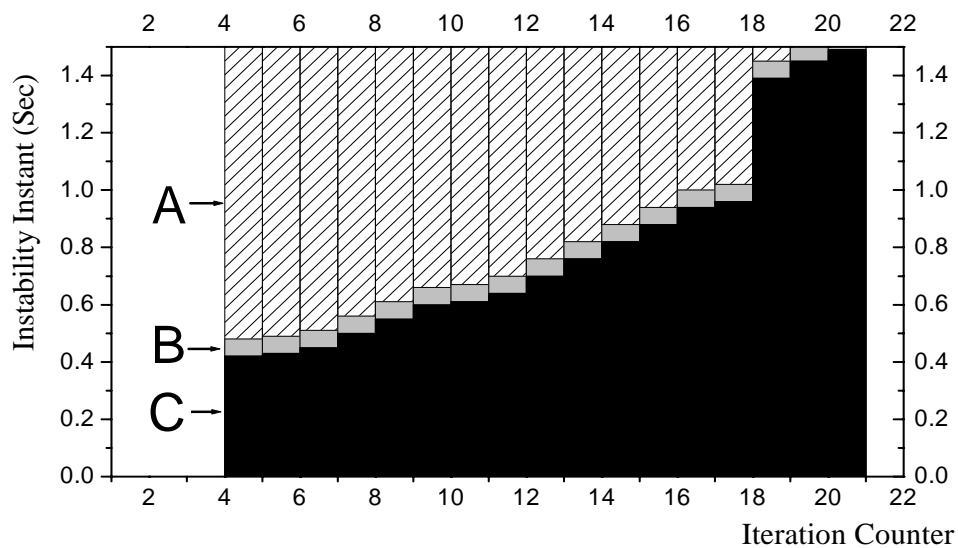


Figure V.6 Computation related to transient stability by Method 3

For the WSCC 9-bus system, Method 3 produces better results than Method 2 as

shown in Table V.1. This can be explained as follows. Firstly, the computation accuracy of Method 3 near the end of the optimization process is better than that of Method 2. When the optimization by Method 2 was completed, the complementary gap and maximum power flow mismatch were 3.52×10^{-5} and 1.91×10^{-5} , respectively; whereas for Method 3, the convergence accuracies have already been satisfied in the 11th and 12th iteration, while transient stability constraints were still violated. Further iterations are then needed to satisfy all the stability constraints. At the end of the optimization process, the complementary gap and maximum power flow mismatch are improved to 2.27×10^{-16} and 2.40×10^{-10} , respectively, which are order of magnitude better than those obtained by Method 2. Secondly, the larger TTC by Method 3 is obtained by driving the operation point much closer to the stability limit than Method 2, as illustrated in Figure V.3. It is noted that the closer to the stability limit, the higher risk will be for the operation. Therefore, longer simulation period should be taken for better checking of transient stability after first swing.

V.3.1.3 NUMERICAL COMPARISON BETWEEN ROTOR ANGLE LIMIT AND PEBS

In this section, the performances of transient stability constraints based on rotor angle limit and PEBS are compared using the Method 3 solution approach. The transient period under study is set to 2.0 sec in this study to ensure the transient stability in a longer time scale in case of the instability after the first swing.

Larger TTC can be obtained by relaxing the rotor angle limits. With the rotor angle limit varied from 120 to 180 degree, the TTC increased from 1.7932 pu to 2.0068 pu as shown in Figure V.7. TTC stops to increase once the threshold is over 140 degree. This means the effect of transient stability constraints in OPF will remain more or less the same once the limit is set over a certain threshold value.

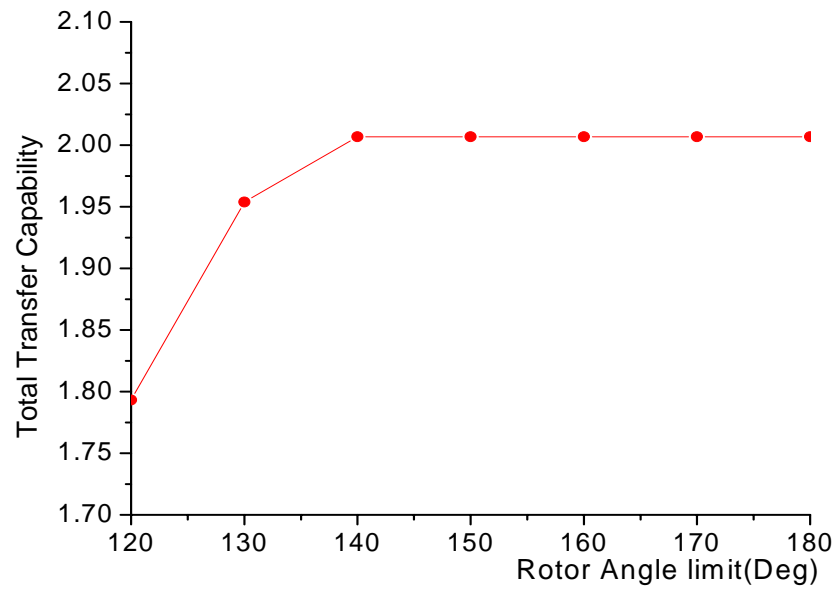


Figure V.7 Optimization results with different rotor angle limits

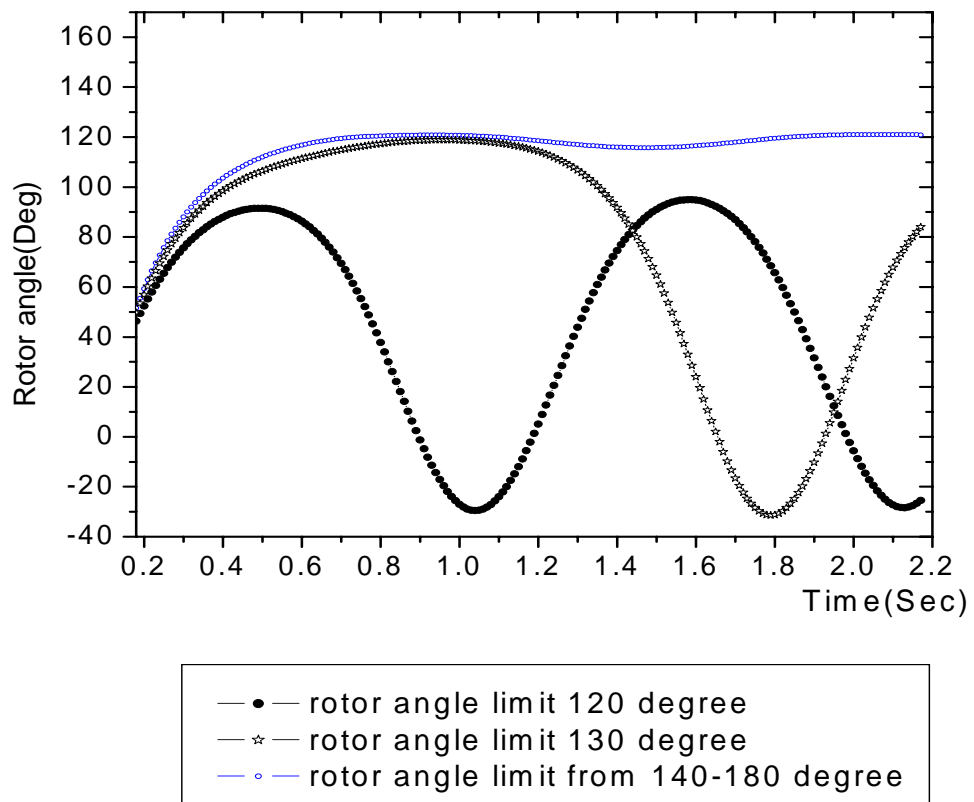


Figure V.8 Simulation based on different rotor angle limits

However, it is noted that, numerically, although transient stability is satisfied in all cases with threshold from 120 to 180 degree, the first swings are heavily distorted as shown in Figure V.8. From an operation point of view, simulation responses with stricter thresholds of 120 and 130 degree are preferred since the system obtained with over 140 degree threshold is too close to the stability limit. This indicates that how to appropriately set the rotor angle limit and set longer study period for transients are important issues in OPF. Up to now, there is no uniform policy to set the rotor angle limit for different systems. If the threshold is too relaxed, systems may not be stable enough although there is no violation in the study period; on the contrary, if the threshold is too strict, the operation tends to be conservative and less economic. Besides, numerical experiments show that sometimes the threshold value of rotor angle deviation could not absolutely indicate how much the system stability or instability is. In another word, the satisfaction for threshold value of 120 degree could not always be more reliable than that for 180 degree.

TTC is calculated and compared with transient stability constraints defined by PEBS with the same contingency. BFGS method is employed to update the Hessian matrix approximately due to the complex formulation of transient stability constraints based on PEBS. The obtained TTC is 1.7576 pu, 18.93% increase compared with the base case. The optimal result is comparable with that defined based on rotor angle limit of 130 degree. Transient stability constraints are satisfied as illustrated in Figure V.9, in which the dot product curve remains negative in the study period of [0, 2] sec. Transient stability can also be recognized according to the swing curve with reference to COI as shown in Figure V.10.

Obviously, the advantage of PEBS approach is that it can be regarded as a uniform criterion to transient stability constraints for different systems. However, in

this case, it makes the obtained TTC somewhat more conservative compared with that defined by rotor angle limit of 130 degree. There is no guarantee that the obtained optimal results always be conservative. If an aggressive optimal solution, which can spoil the stability, obtained based on PEBS, rotor angle limit has to be used instead.

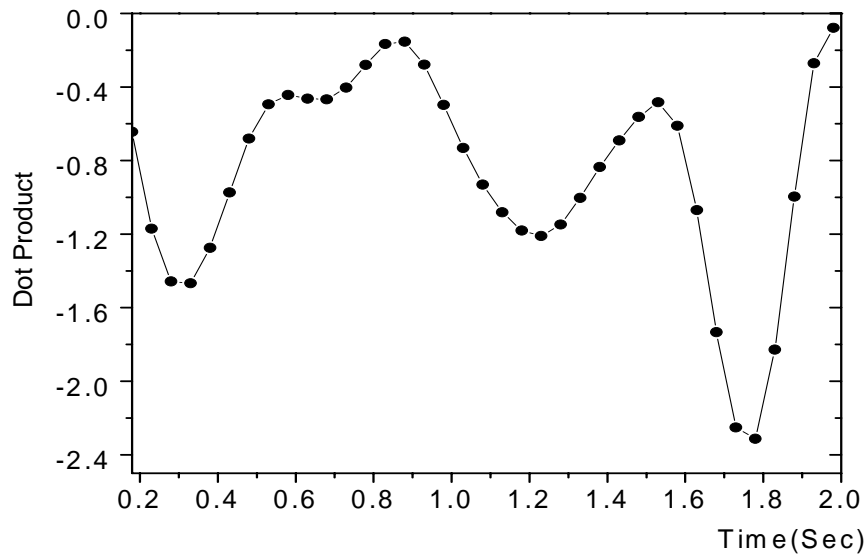


Figure V.9 Dot product variation curve

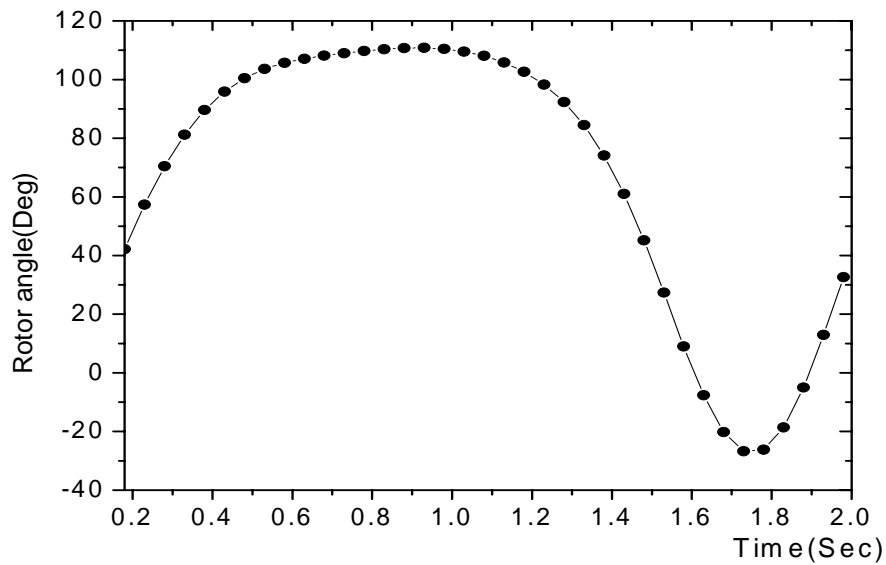


Figure V.10 Swing curve based on the results by PEBS

V.3.2 NEW ENGLAND 39-BUS SYSTEM

The New England 39-bus system as shown in Figure V.11 is selected as a larger test system for the proposed method. It comprises 10 generators, 39 buses, 34 lines and 12 transformers. Bus 1 is selected as the slack bus, and the system base is 100 MVA. Details of this system are listed in Appendix B and also can be found in [55].

The OPF model is to determine the TTC with transient stability maintained. The 39-bus system is separated into two areas as shown in Figure V.11 with the power transfer from the upper area to the lower area. The interconnected interface is composed of line 12-11, 12-13 and 36-37.

For the validation of the optimization results, only a single contingency is considered. This contingency consists of a three-phase fault occurred near bus 36 at the end of line 35-36. The fault is subsequently cleared at $t = 0.1s$ with line 35-36 tripped.

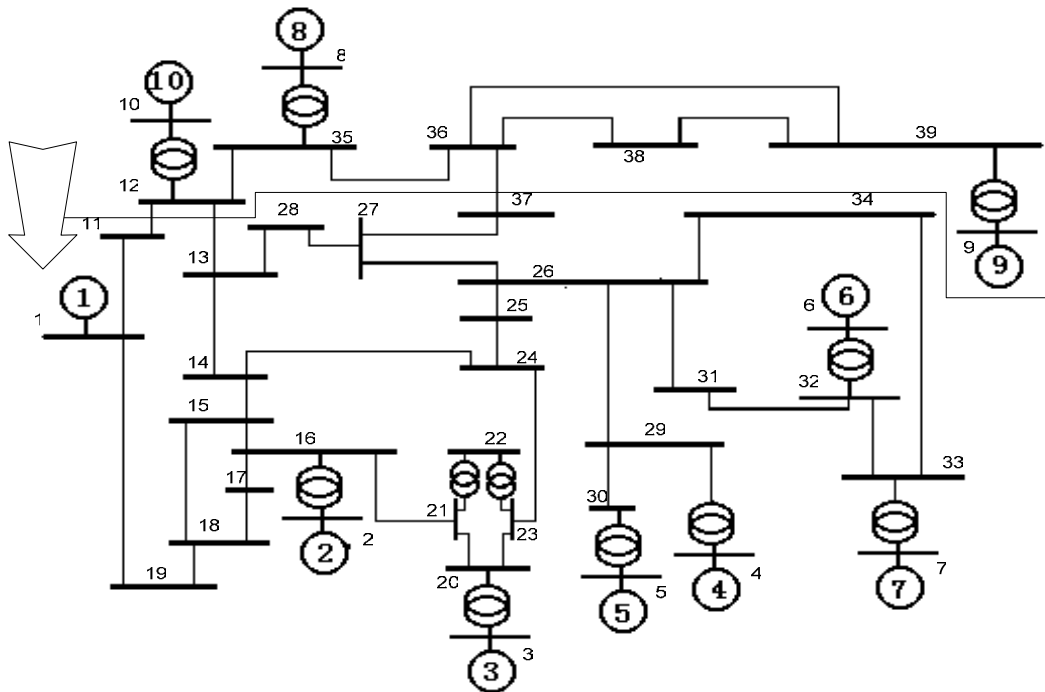


Figure V.11 One line diagram of New England 39-bus system

Table V.2 shows the resulted system transfer capabilities. Method 1 is the conventional OPF without the consideration of transient stability constraints; whilst Method 2 is the optimization with transient stability constraints defined by PEBS.

Table V.2 Optimization results obtained with New England 39-bus system

Method	1	2
TTC (p.u.)	20.98	12.59

There is a large difference between the optimal results by Method 1 and 2. In this case, with consideration of the creditable contingency, the TTC reduces to about 60% of that without any transient stability constraints.

However, when the contingency occurs, the performance of the two optimal solutions is also very different. As the dot product plotted in Figure V.12 and V.13 for Method 1 and 2, the optimal solution by Method 2 is secure even if the contingency occurs since the dot product in Figure V.13 remains negative in the study period of [0,2] sec. The effectiveness of method 2 can also be demonstrated by the comparison based on dynamic simulations. Figure V.14 and V.15 are the plots of rotor angles with reference to generator 1 by Method 1 and 2, respectively. Obviously, the difference of rotor angles increases and the system becomes unstable as shown in Figure V.14; whilst in Figure V.15 the rotors reach their maximum and then decrease. Further simulation in a longer period showed that the system remains stable.

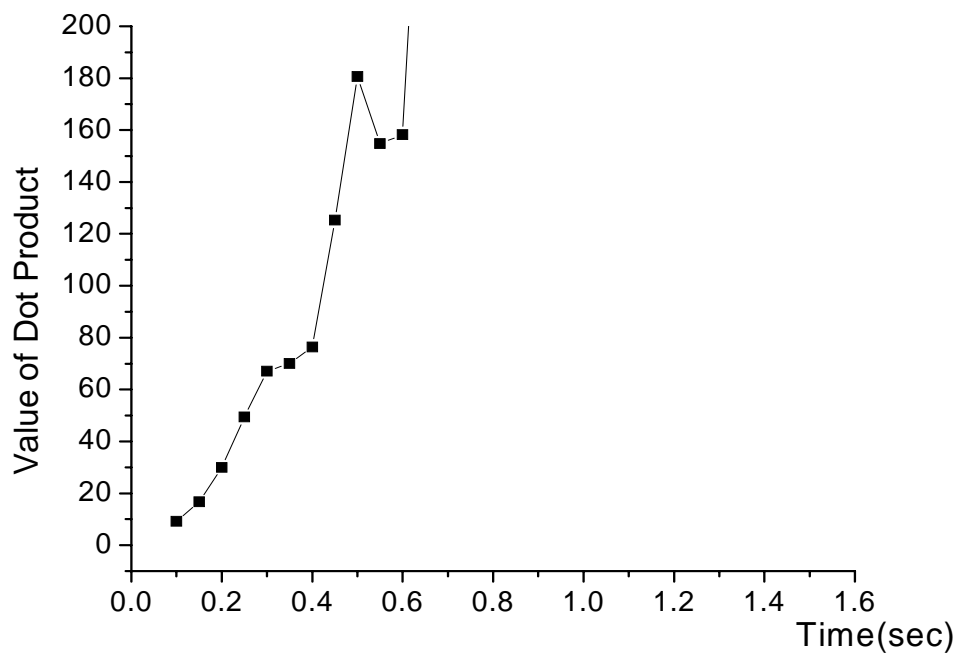


Figure V.12 Dot product variation curve for Method 1

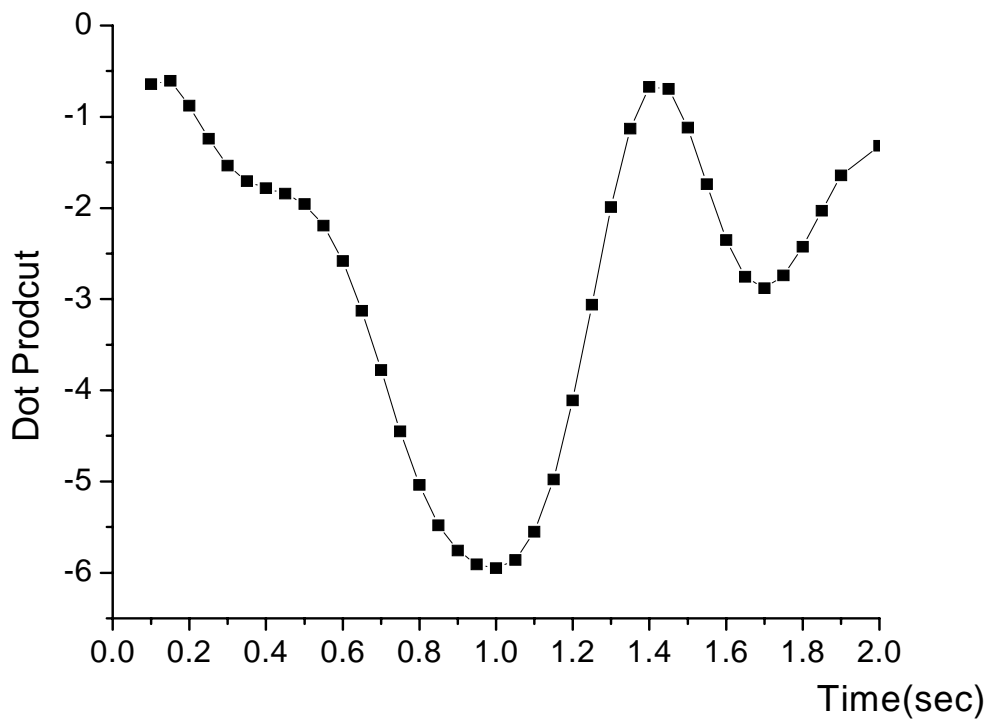


Figure V.13 Dot product variation curve for Method 2

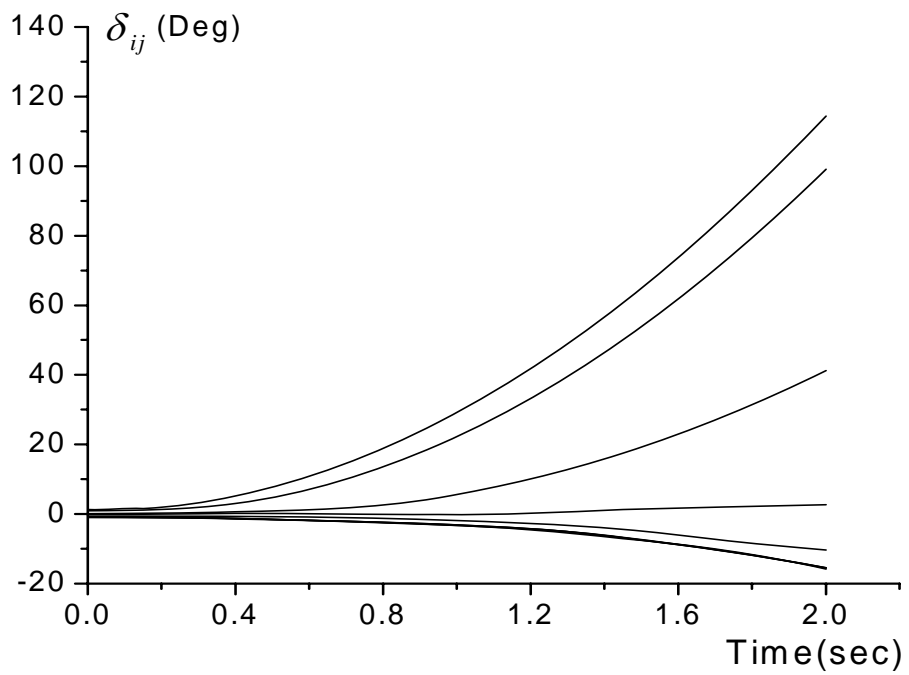


Figure V.14 Swing curves for Method 1

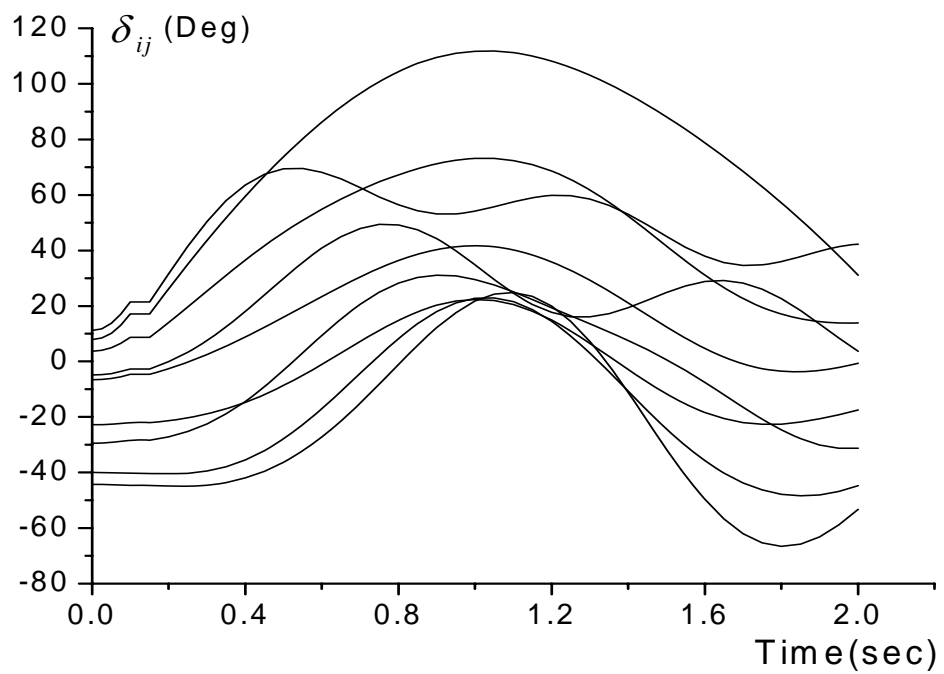


Figure V.15 Swing curves for Method 2

With transient stability constraints, OPF solution by Method 2 is indeed able to meet the security requirement and is transient stable under the credible contingency. It should also be noticed that there is 8.39 pu, about 40%, reduction in transfer capability by Method 2 compared with Method 1. The significance to consider the transient stability in OPF study is clearly demonstrated. Without transient stability constraints consideration, the system operator may be seriously misled. The reduction in TTC could be regarded as the economical sacrifice for the consideration of security, or the cost for the secure guarantee.

V.4 SUMMARY

In this chapter, the calculation of ATC is formulated as an OPF problem with security constraints, especially transient stability constraints. SIP techniques are employed to solve this problem. The proposed methods for the calculation of ATC are fully tested on WSCC 9-bus and New England 39-bus systems. The necessity of transient stability involvement in OPF is illustrated in the case study. The good performances of the most effective section of transient stability constraints are presented based on numerical comparison. Transient stability constraints based on rotor angle limits and PEBS are also compared based on the numerical results. The improved BFGS method is used in the case study to avoid complex Hessian matrix derivation.

Chapter VI DYNAMIC SECURITY DISPATCH

In this chapter, a new methodology for dynamic security dispatch is presented to reconcile the possible conflict between economy and dynamic security in the optimization.

VI.1 INTRODUCTION

Security dispatch is to provide economic operation in the presence of a specific list of contingencies. With increasing economical pressure and intensified transactions, especially in competitive environment, to maintain dynamic security of the economic operation to an acceptable level becomes more important and complicated [1]. Appropriate strategies of preventive control or remedial actions should be triggered for dynamic security enhancement if credible dangers of instability are detected.

Basic formulation for dynamic security dispatch is presented preliminarily in [136]. The usual cost function is augmented by including transient stability indices across selected cut sets. A trade-off between optimal economy and steady-state and dynamic security is obtained by optimization. Similarly, in [137], instability index is defined with potential energy and algebraic interpretations. Insecurity cost is assigned together with the total system cost. After that, optimal dispatch is taken for real power scheduling.

Generation rescheduling has long been recognized as an effective means to alleviate power system insecurity. For several decades, many efforts, for example, in [8,10,13,14,21,23-25], have been made for dynamic security dispatch via preventive control and generation rescheduling. In [10,24,25], sensitivities of the energy margin to system parameters, such as generation output, are proposed for generation rescheduling. In [10], sensitivity with respect to generation power is studied based on extended equal area criterion and a related transient stability margin. Economic

dispatch algorithm is remarked to be extended to transient stability dispatch. In [24], generation rescheduling is carried out by the combination between transient stability constraints and optimization techniques based on the sensitivities of the energy margin. In [25], preventive generation rescheduling is taken based on a structure preserving energy margin sensitivity-based analysis to stabilize a transiently unstable power system. In [8,23], trajectory sensitivities are calculated to provide a preventive rescheduling scheme. In [23], optimal dynamic security constrained rescheduling is resolved by introducing power constraints for transient stability, which is produced based on trajectory sensitivities for credible contingencies. In [8], the sensitivity trajectory of the most critical rotor angle, defined as a good coherent index, with respect to the generation outputs is addressed to determine the rescheduling.

Unlike sensitivity methods, in [21], dynamic security dispatch is accomplished by the improvement of the coherence of machines according to the variation rate of generator speeds at fault clearing time. Optimization should be taken into account for the ultimate rescheduling. In [14], generation rescheduling is implemented via shifting generation from critical machines to noncritical machines, the amount of which depends on the size of stability margin determined by the single machine equivalent hybrid transient stability method. In [13], transient stability preventive control is carried out by generation rescheduling using the linear relationships, which is not always true, between critical clearing time and generator rotor angles.

In reality dynamic security dispatch appears to be an extended OPF problem with add-on dynamic security constraints. The basic idea is to find the OPF solution with the objective of economic cost subjected to transient stability constraints. Mathematically, the extended OPF can be formulated as an SIP problem with finite dimension for optimal variables but infinite dimension for dynamic security constraints in time domain as in [12,16,20,22,31,35,36]. In this thesis, the strategies of dynamic security dispatch are implemented based on stability constrained OPF model with local reduction method.

VI.2 MODELING OF DYNAMIC SECURITY DISPATCH

Dynamic security dispatch is modelled as an OPF problem as

$$\min f(\mathbf{x}_0, \mathbf{y}) \quad (6.1)$$

$$s.t. \quad \mathbf{g}(\mathbf{x}_0, \mathbf{y}) = \mathbf{0} \quad (6.2)$$

$$\mathbf{H}(\mathbf{x}_0, \mathbf{y}) \leq \mathbf{0} \quad (6.3)$$

$$\mathbf{U}(\mathbf{x}(t), \mathbf{y}) \leq \mathbf{0} \quad (6.4)$$

Other than the objective function $f: \mathbf{R}^{n_x+n_y} \rightarrow \mathbf{R}$, all the other definitions of the variables and functions in (6.1-6.4) are similar with the general formulation (2.33-2.36).

The OPF objective function, $f(\mathbf{x}_0, \mathbf{y})$, is selected as the fuel cost. Generally, the fuel cost curve can be approximated by a quadratic function of generator active power output as

$$f(\mathbf{P}_G) = \sum_{i=1}^{ng} (a_i P_{Gi}^2 + b_i P_{Gi} + c_i) \quad (6.5)$$

where $\mathbf{P}_G = \{P_{Gi}\}$, $i \in \mathbf{I}_g$ is the vector of generation active power output. \mathbf{I}_g is the index set of generators. ng is the total number of generators. a_i , b_i , and c_i are fuel cost curve coefficients of the i -th generator respectively.

Clearly Inequality (6.4) is infinite-dimensional in the functional space. Thus, mathematically, dynamic security dispatch problem (6.1-6.4) is a SIP problem with finitely many optimal variables with infinitely many constraints, and hence cannot be solved directly by standard finite programming methods. Instead, SIP techniques are employed based on local reduction method to transform the SIP problem into a finite programming problem.

It is noted that a large number of credible contingencies should be taken into consideration to guarantee secure operation of the system. It is necessary to screen out the very stable contingencies for dynamic security dispatch so as to reduce computation efforts in the optimization. In addition, multi-contingency in many cases should be considered for practical dynamic security dispatch.

VI.3 CASE STUDY AND DISCUSSIONS

The proposed model and solution for dynamic security dispatch is illustrated on the New England 39-bus system. The full system parameters are available in Appendix B. The output limits and coefficients of quadratic fuel cost function of generators are referred to MATPOWER [138] and listed in Appendix B. Synchronous machines are represented with classical models. All loads are modelled as constant power in the load flow calculation and as constant impedance in the transient stability simulation with initial value set by the load flow solution. L_∞ norm local reduction method is used to transcribe the semi-infinite transient stability constraints.

Two different loading conditions are tested in this study. One is the base loading conditions with the load as detailed in Appendix B and [55]. The other is heavy loading conditions in which all loads are increased by 20% from the base value.

The proposed methodology has been implemented in C language running under Windows XP using a Pentium 4 2.4 GHz computer.

VI.3.1 BASE LOADING CONDITIONS

In the absence of any transient stability constraints, conventional OPF is performed to obtain the pre-rescheduling dispatch solution. The total fuel cost is 36,119 \$/hr for this base loading condition, and the computation time is 2.27 sec with 14 iterations in total. The generation active power outputs are reported in Table VI.1.

Dynamic simulations are then performed to determine whether the system could survive in credible contingencies with such scheduling of generation. The credible contingencies are permanent three-phase faults to ground at the end of line. The faults are subsequently cleared by switching out of the faulty line. In all simulations, the transient period under study is 3 sec with integration time step of 0.01 sec. The rotor angle deviation threshold with respect to the COI is set to 120 degree with ρ being 10% of this threshold. Credible contingencies leading to different patterns of

instability are selected here for illustrating how the proposed method could optimally reschedule generation to ensure economic and secure operation of the power system.

Table VI.1 Comparison between generation pre-rescheduling and rescheduling
in base loading conditions

Generators	pre-rescheduling (MW)	Case A (MW)	Case B (MW)	Case C (MW)
1	968.4	992.4	1089.0	984.5
2	577.7	666.7	615.8	551.6
3	574.2	497.4	597.1	607.0
4	563.0	577.3	550.0	594.5
5	562.7	543.5	531.5	526.3
6	567.3	595.2	597.2	590.5
7	564.5	561.0	574.1	568.6
8	554.5	561.9	535.8	613.7
9	909.2	845.7	812.1	808.0
10	350.0	350.0	285.9	350.0
Total cost (\$/hr)	36,119	36,338	36,690	36,334
Iterate counter	14	13	16	14
CPU time (sec)	2.27	60.58	116.92	86.88

Case A:

In this case the fault is applied at bus 13 and cleared by tripping line 12-13 at $t_{cl} = 0.24$ sec which is a slightly larger than the critical clearing time of 0.23 sec. With the pre-rescheduling operation point, the rotor angle of generator 5 with respect

to COI is over the threshold in the second swing at about 2.5 sec after the fault occurs as shown in Figure VI.1. Although the violation is gentle, dynamic security dispatch based on the proposed methodology is triggered to eliminate this dynamic violation.

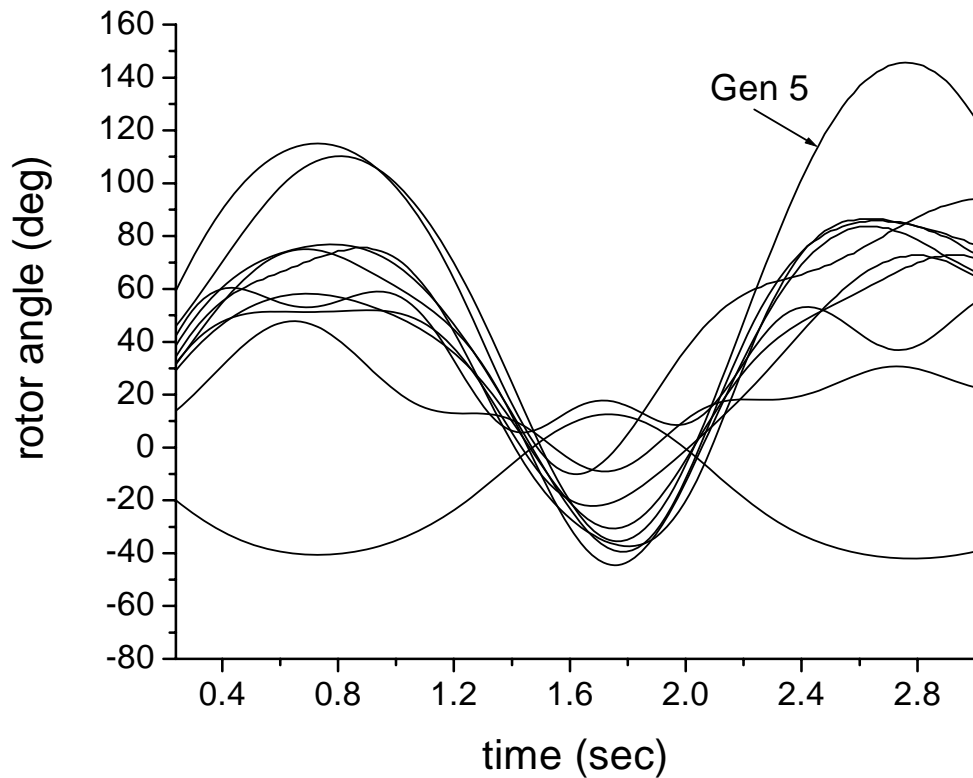


Figure VI.1 Swing curves with pre-rescheduling for Case A

The rescheduled generation active power outputs are reported in Table VI.1. Compared with the pre-rescheduling conditions, the total fuel cost is increased to 36,338 \$/hr. As shown in Figure VI.2 for plots of swing curves, the deviation of generator 5 with respect to COI is kept less than the threshold and all generators remain in synchronism with each other throughout the study period. This illustrates that the OPF solution obtained by the proposed approach is able to dynamically survive in the contingency, and the fuel cost increase of 219 \$/hr, i.e. 0.6%, can be

regarded as the dispatch cost for keeping the system stable.

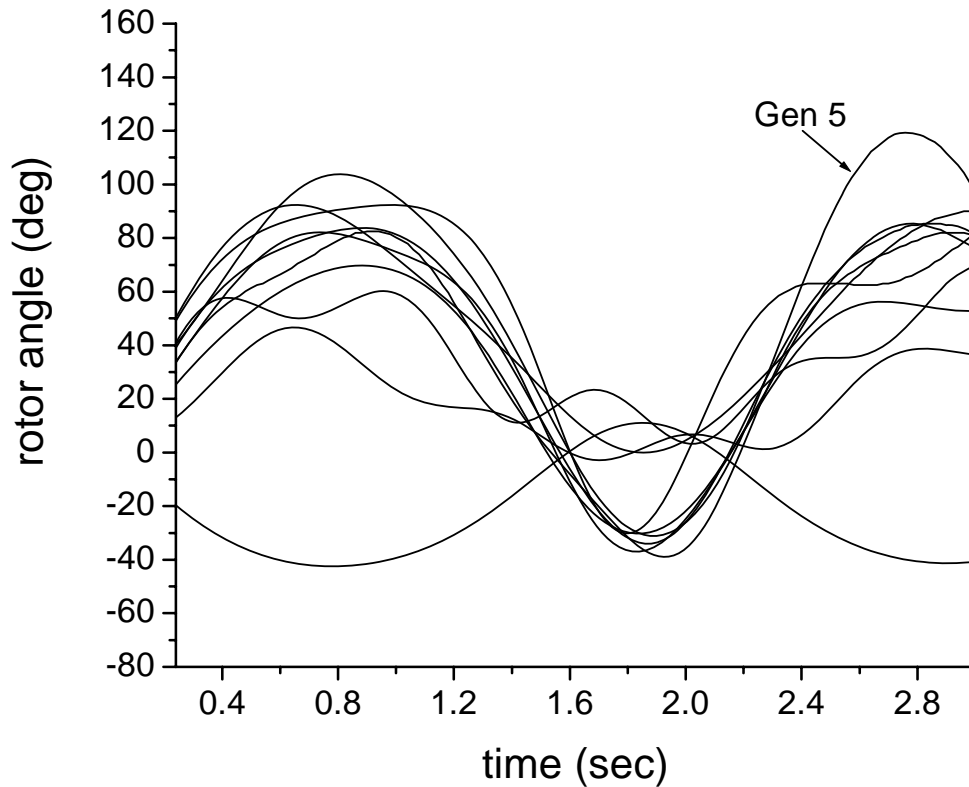


Figure VI.2 Swing curves after rescheduling for Case A

Case B:

With the same fault as Case A but cleared at $t_{cl} = 0.28$ sec, i.e. this case is significantly more severe than Case A as shown in Figure VI.3. When the contingency occurs, the system behaves unstable with generator 1, which has the largest inertia, separated from other machines.

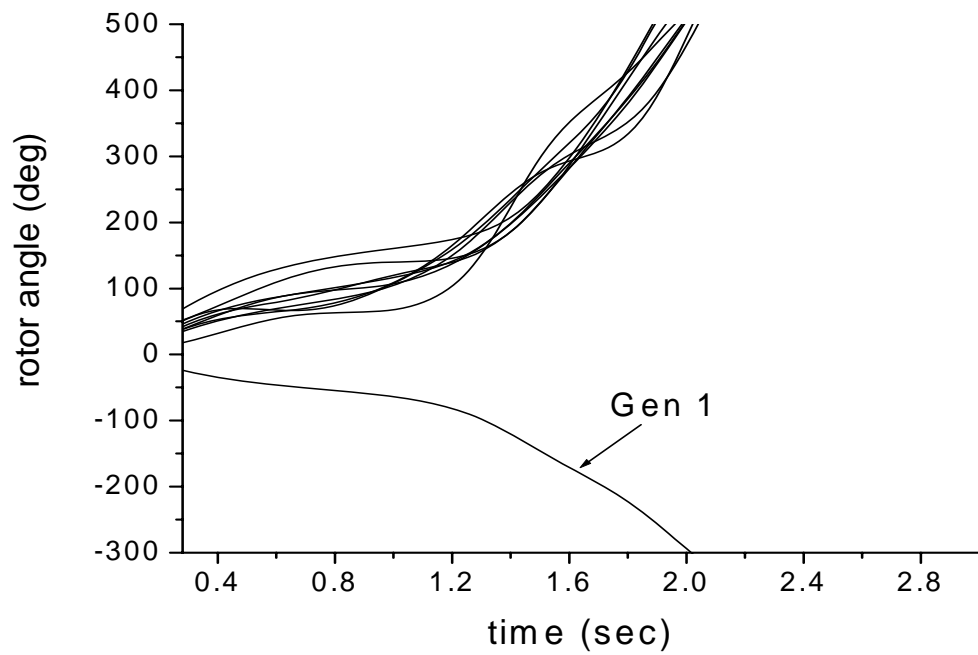


Figure VI.3 Swing curves with pre-rescheduling for Case B

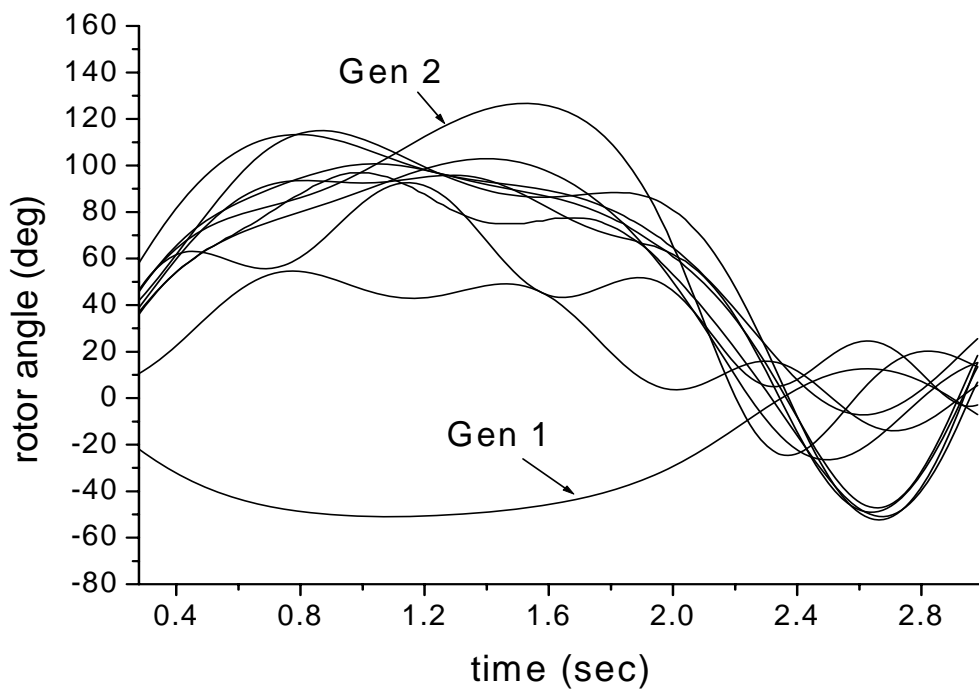


Figure VI.4 Swing curves after rescheduling for Case B

The dynamic performance of the system after dynamic security dispatch is simulated and shown in Figure VI.4. Although in a short interval the swing curve of generator 2 exceeds the threshold 120 degree at around $t = 1.6$ sec, the deviation is within the tolerance η and all generators remain in synchronism with each other in the study period. The total fuel cost is now increased to 36,690 \$/hr, which is 571 \$/hr, i.e. 1.58%, larger than that in the pre-rescheduling conditions and is 352 \$/hr larger than the rescheduled fuel cost in Case A. This indicates that higher cost has to be associated with dynamic security dispatch to prevent more serious instability.

Case C:

In this case the fault is applied at bus 27 and cleared by tripping line 27-28 at $t_{cl} = 0.20$ sec, which is larger than the critical clearing time of 0.17 sec. In pre-rescheduling state, the dynamic behaviour of the system is shown in Figure VI.5. Generator 5 fails to keep synchronism with others in its second swing, which can be regarded as multi-swing instability.

Similarly, the swing curves in Figure VI.6 illustrate the survival of the proposed dynamic security dispatch if the contingency occurs. The total fuel cost is increased to 36,334 \$/hr, about 215 \$/hr, i.e. 0.6% larger than that in the pre-rescheduling conditions.

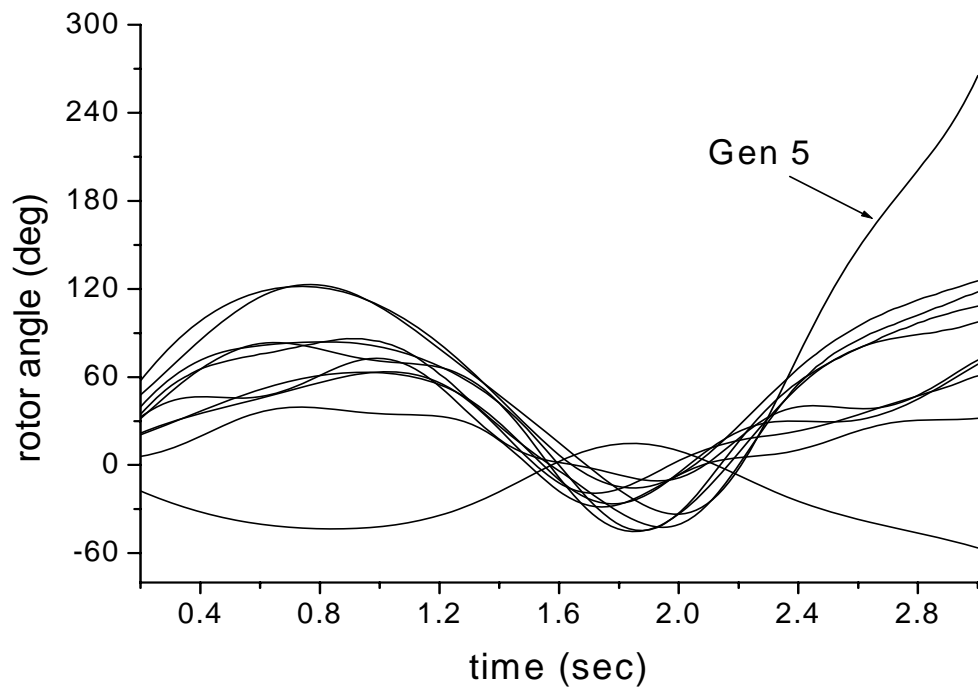


Figure VI.5 Swing curves with pre-rescheduling for Case C

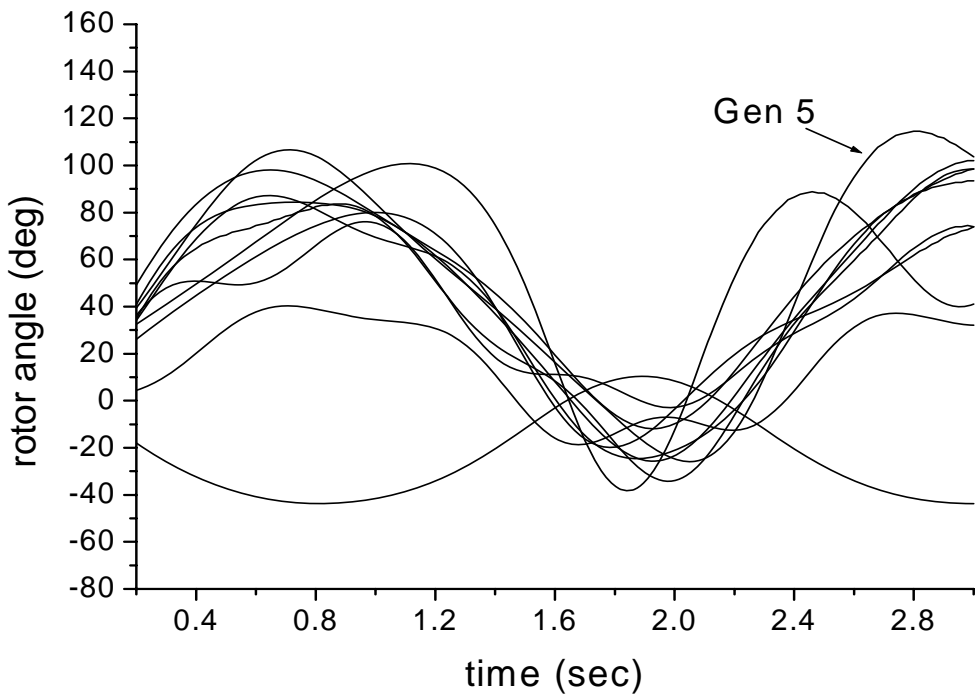


Figure VI.6 Swing curves after rescheduling for Case C

VI.3.2 HEAVY LOADING CONDITIONS

Without the consideration of any transient stability constraints, the total fuel cost is 52,964 \$/hr with the pre-rescheduling in the heavy loading condition. The computation time is 1.94 sec as reported in Table VI.2.

Table VI.2 Comparison between generation pre-rescheduling and rescheduling in heavy loading conditions

Generators	pre-rescheduling (MW)	Case D (MW)
1	1100.0	1100.0
2	911.1	966.1
3	750.0	744.3
4	732.0	701.7
5	608.0	600.1
6	750.0	750.0
7	660.0	654.6
8	640.0	640.0
9	930.0	924.8
10	350.0	350.0
Total cost (\$/hr)	52,964	53,251
Iterate counter	12	44
CPU time (sec)	1.94	359.27

All of the machines except generator 2 have reached their upper limits to satisfy the load demand. Afterwards dynamic simulations are performed to determine whether the system can survive in credible contingencies or not. Case D is taken as

an example for generation rescheduling with dynamic security constraints in the heavy loading condition.

Case D:

In this case the fault is applied at bus 13 and cleared by tripping line 12-13 at $t_{cl} = 0.18$ sec, which is larger than the critical clearing time of 0.17 sec. As shown in Figure VI.7, the system is transient unstable with generator 1 separated from the other machines whilst generator 2 is the first exceeding the threshold.

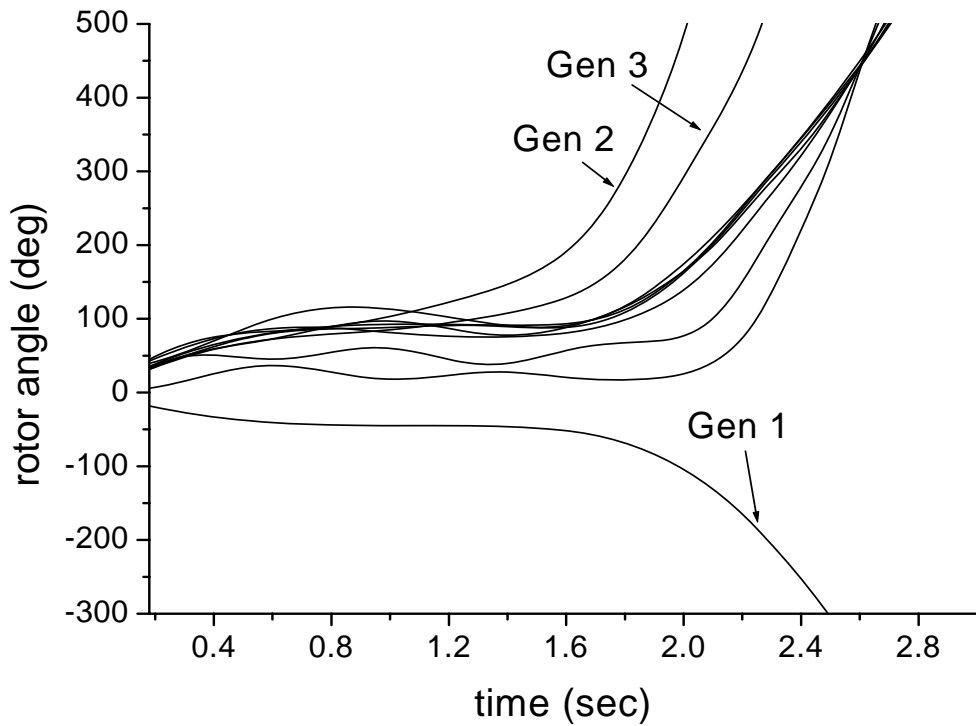


Figure VI.7 Swing curves with pre-rescheduling for Case D

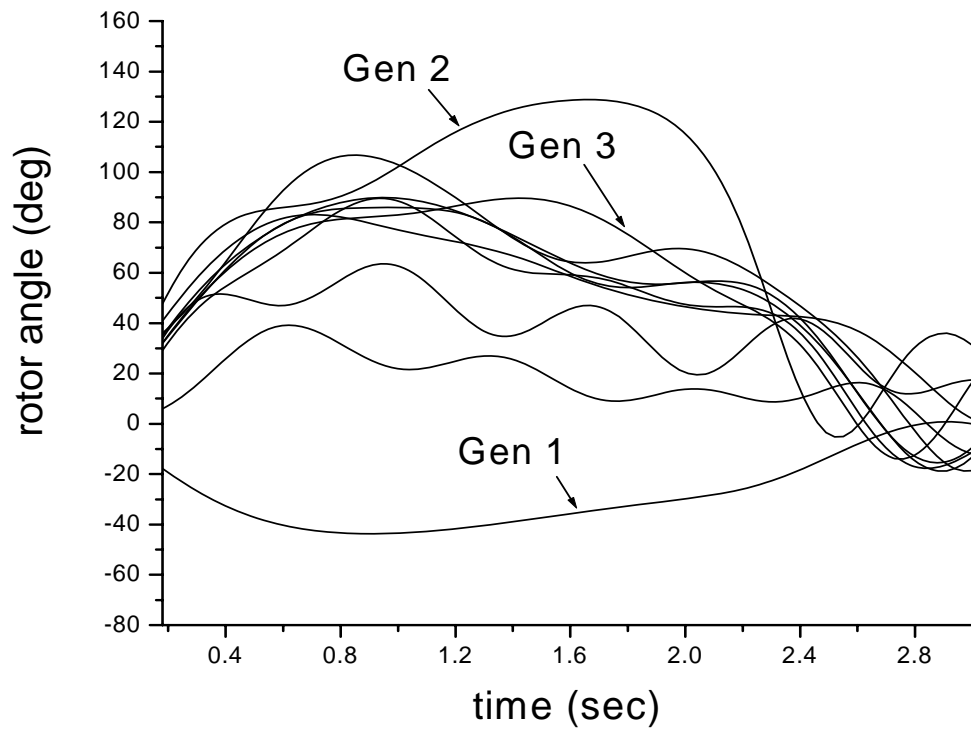


Figure VI.8 Swing curves after rescheduling for Case D

The proposed dynamic security dispatch successfully makes the system survive in the scenarios if the contingency was to occur as illustrated in Figure VI.8. The total fuel cost is increased to 53,251 \$/hr, and is 287 \$/hr, i.e. 0.5%, larger than that in pre-rescheduling conditions.

VI.3.3 GENERATION RESCHEDULING

Generation rescheduling is an effective remedy to alleviate power system insecurity by shifting generation output between machines. In this thesis, the strategy is fulfilled by the proposed dynamic security dispatch. The generation shifts between generators in the above 4 cases are plotted in Figure VI.9-VI.12, respectively. If "spare generation capability" in the figures is zero, it means the corresponding generator output has reached its upper limit and no more generation output available.

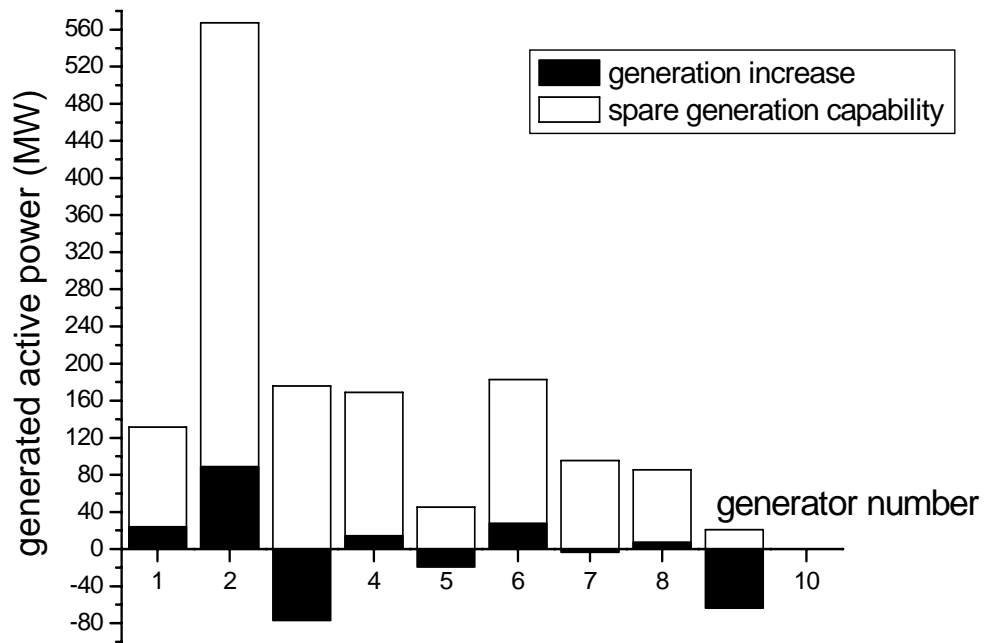


Figure VI.9 Generation rescheduling in Case A

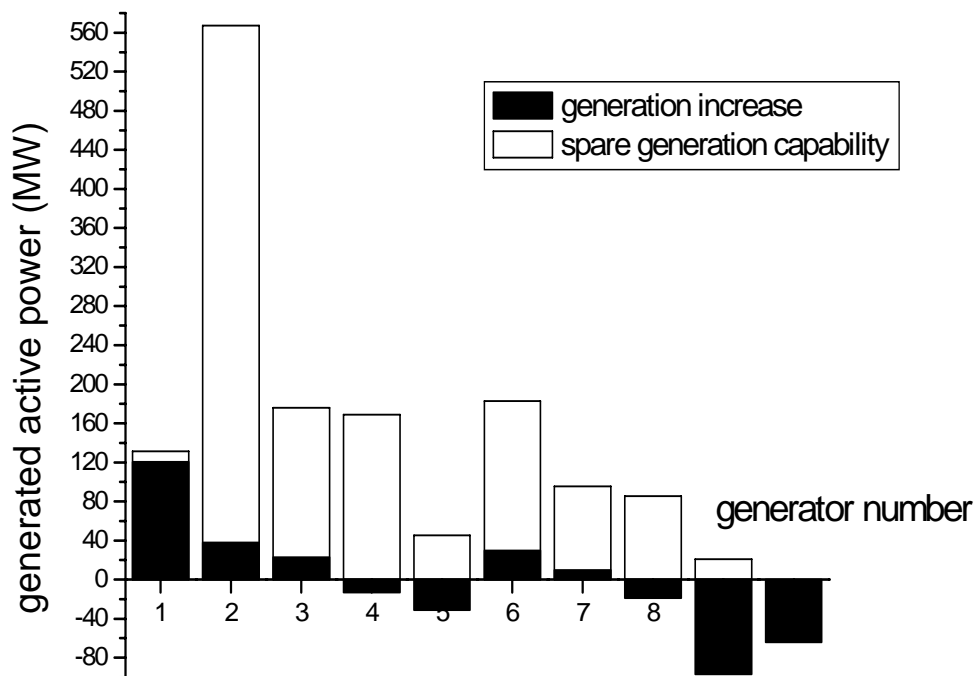


Figure VI.10 Generation rescheduling in Case B

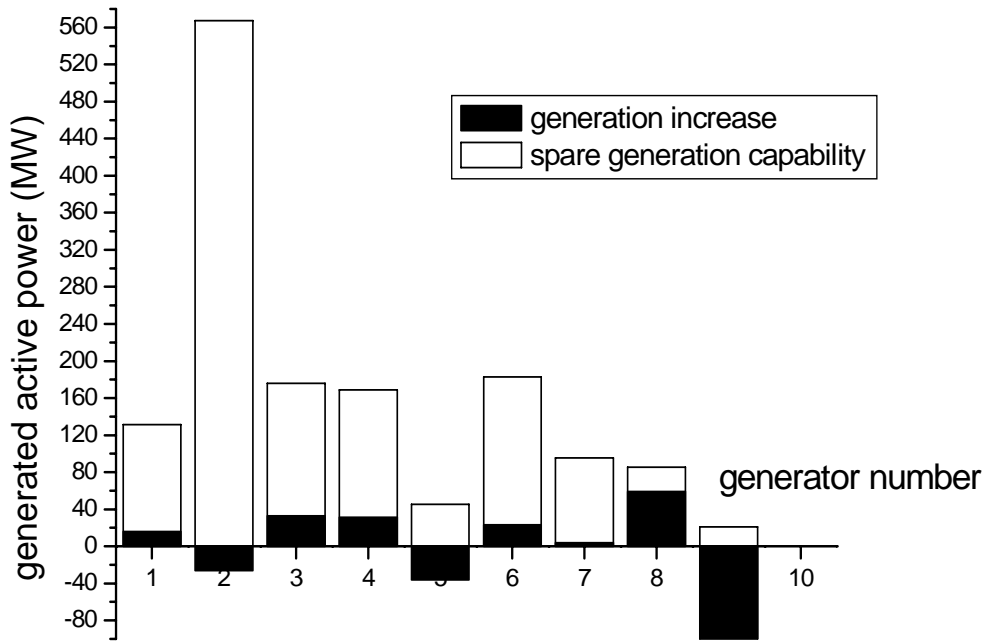


Figure VI.11 Generation rescheduling in Case C

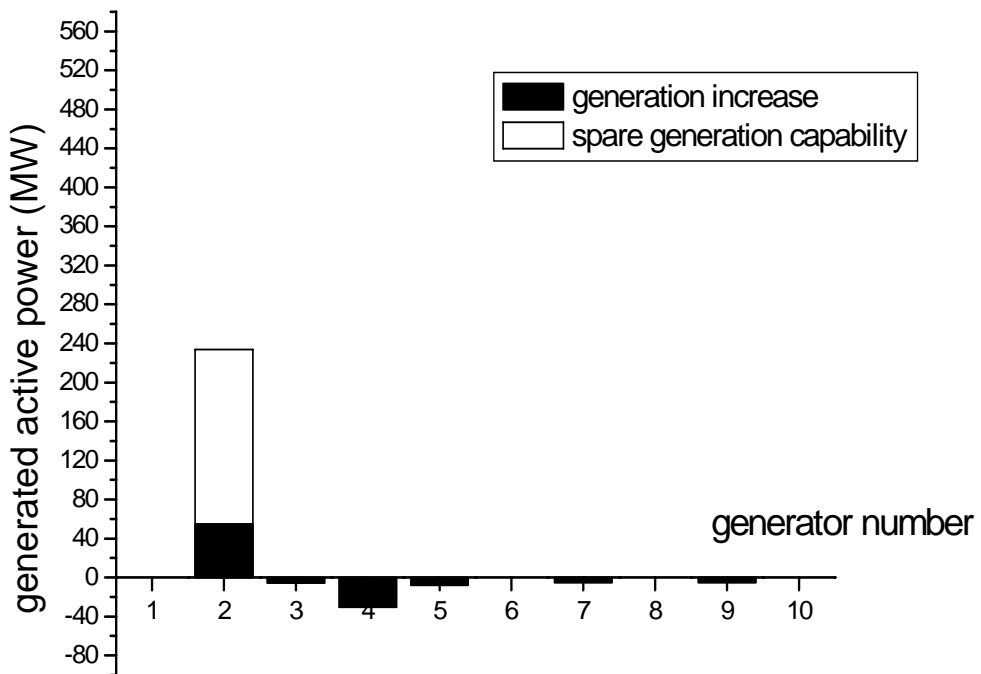


Figure VI.12 Generation rescheduling in Case D

In the pre-rescheduling with base loading conditions, except generator 10, all the other generators still have generator capacity for implementing the rescheduling. Take Case B as an example, which suffered a more serious contingency compared with Case A and C, the system behaves unstable with generator 1, which has the largest inertia, lags behind other machines. After the optimization for dynamic security dispatch, the output of generator 1 is increased almost to its upper limit as shown in Figure VI.10. It can be explained that more loads should be supplied by the lagged machine via rescheduling.

In the pre-rescheduling with heavy loading conditions, all the generation outputs, except generator 2, have reached their upper limit and no more outputs are available. After the generation rescheduling, the active outputs of generator 3, 4, 5, 7 and 9 are pulled back from the upper limits, and the loading demand is shifted to generator 2 without consideration of transmission loss.

VI.3.4 COMPUTATION ANALYSIS

It is recognized that the time to introduce transient stability constraints into the optimization would have a large impact on the convergence. If it is too early, the optimization may fail to converge as the initial point is too far away from the power flow solution; on the contrary, if it is too late, the optimization may have converged closely to one stationary point and may fail to eliminate the dynamic constraint violations. In this thesis, the transient stability constraints are introduced when the maximum power flow mismatch is less than 10 MW, i.e. started from the 6th iteration for Case B, as shown in Figure VI.13, for example. As an illustration of the optimization process for Case B, the changes of the complementary gap, maximum power flow mismatch, and instability instant in the optimization are plotted in Figure VI.13.

Compared with pre-rescheduling conditions, the proposed security dispatch is more computationally intensive with the consideration of dynamic stability

constraints. As show in Table VI.1 and VI.2, the computation time for security dispatch is significantly more when compared with the pre-rescheduling dispatch although the number of the iterations is not changed much in different cases. The increased time is mainly spent on performing numerical integrations to obtain the Jacobian and Hessian matrices of transient stability constraints.

Nevertheless, the proposed algorithm shows good convergence characteristics in the base loading cases, i.e. Case A, B, and C; whilst more iterates are needed for the heavily stressed Case D because of the very limited room for manoeuvre.

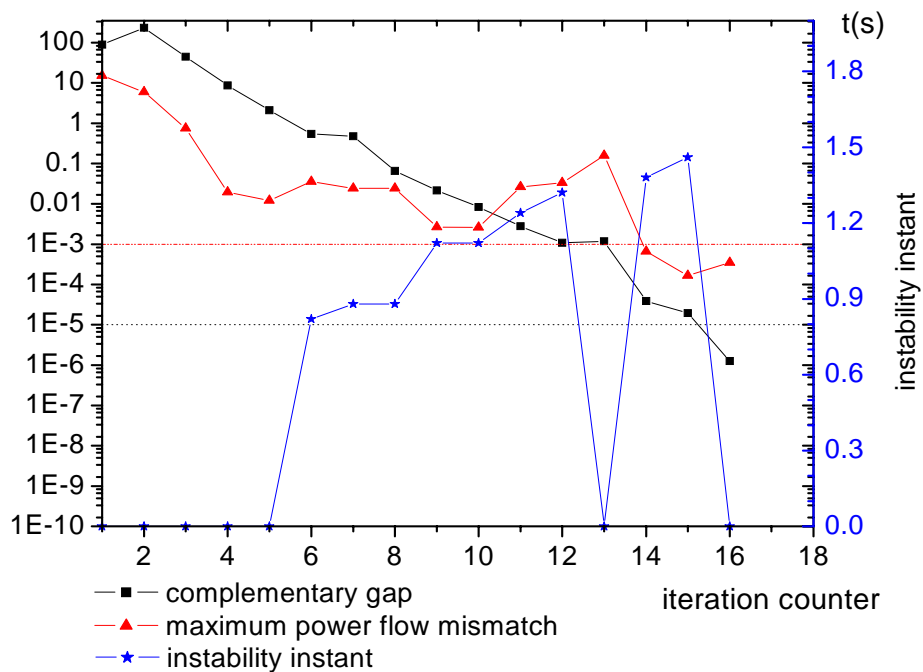


Figure VI.13 Change of maximum power flow mismatch, complementary gap and instability instant in the optimization for Case B

VI.4 MULTI-CONTINGENCY CONSTRAINTS

For large power systems, the number of credible contingencies would be huge. Dynamic security dispatch, as one tool for preventive control, should guarantee the capability of the system to survive in all the credible contingencies. Practically,

preventive control is carried out in the normal or alert state of the operation, which is before the occurrence of contingencies. It is uncertain which contingency should be included for dynamic security dispatch. Thus dynamic security dispatch with respect to single contingency might deteriorate the security level in other contingencies. Multi-contingency cases should be considered in the dispatch [22,35] for the improvement of the overall security level. In this study, the definition of "multi-" or "single-" contingency in preventive control is according to [35]. "Single contingency" is defined as one fault (with or without reclosure) or two faults (simultaneous or cascading), etc. Multi-contingency, such as contingency (A+B), is defined as either contingency A or contingency B will occur at the same operating point. In other word, for preventive control based on transient stability constrained OPF, the system remains stable no matter which contingency A and B occurs.

Practically, a well-engineered power system should be stable in most contingencies if not all although the number of credible contingencies could be huge. Only the most dangerous contingencies are considered for dispatch [8,24]. Contingencies should be first screened to remove the very stable cases and leave the marginal stable or unstable ones for further analysis in order to reduce the computation efforts. Contingency screening by direct methods and intelligent methods could be very effective, and the number of contingencies which needs to be further process could be reduced from a few thousands to a few dozens. After that, multi-contingency constraints should be considered to obtain a secure solution for all credible contingencies.

In the following New England 39-bus system study, the credible contingency set consists of all possible three-phase single-line faults. In total, there are 68 contingencies, and in each contingency, a 200ms three-phase fault is applied at the end of the line and is then cleared with the faulty line tripped simultaneous at the ends of the line. After the contingency screen, 11 severe contingencies were found as listed in Table VI.3, which are transient unstable. The superscript "*" refers to which bus the fault is close to.

Table VI.3 List of severe contingencies

Contingency	1	2	3	4	5	6
Fault location	12*-35	26*-31	26*-34	34*-26	27*-28	34*-33
Contingency	7	8	9	10	11	
Fault location	35*-36	36*-37	37*-36	36*-38	39*-38	

Table VI.4 Results of single contingency involved dispatch

C	Dynamic security dispatch with single-contingency										
	1	2	3	4	5	6	7	8	9	10	11
1	S	U	U	U	U	U	U	U	U	U	U
2	U	S	U	U	U	U	U	U	U	U	U
3	U	S	S	U	U	U	U	U	U	U	U
4	U	S	S	S	U	S	U	U	U	U	S
5	U	S	S	S	S	S	S	U	S	U	U
6	U	S	S	U	U	S	U	U	U	U	U
7	S	U	U	U	U	U	S	S	S	S	S
8	U	U	U	U	U	U	U	S	U	S	S
9	S	U	U	U	S	U	S	S	S	S	S
10	U	U	U	U	U	U	U	U	U	S	S
11	U	U	U	U	U	U	U	U	U	U	S
Cost (\$/hr)	36155	36227	36218	36128	36334	36155	36130	36282	36178	36397	36466
ΔCost (\$/hr)	36	108	99	9	215	36	11	163	59	278	347
CPU Time (sec.)	115.5	228.1	111.9	217.4	91.6	231.3	43.4	58.6	44.5	105.2	80.0

Each single contingency in the severe contingency list (as listed in the second row of Table VI.4) is first considered individually for generation rescheduling, i.e. 11 cases in total. The rescheduling results obtained from each case are tested on all the 11 severe contingencies (as listed in the first column of Table VI.4). The stability results obtained are summarized in Table VI.4. The symbols S (stable) and U (unstable) state the stability of a system with optimal rescheduled generation obtained for a given single contingency and tested against any single contingencies (C). As expected, the optimal dispatches for each single contingency are different. The total fuel cost increased from the pre-rescheduling conditions varies from 9 to 347 \$/hr. The variance is due to the differences in the severity of the contingencies. It is obvious that all the optimal operating point obtained for single contingency cannot ensure the stability of all contingencies. This clearly shows that consideration of a single contingency alone is not sufficient and multi-contingency has to be taken into account in the dynamic security dispatch in order to ensure the system security for all contingencies.

The selection of the multi-contingency can be easily observed from Table VI.4, in which the inclusion of Contingency 1 covers Contingency (1,7,9), Contingency 2 covers Contingency (2-6), and Contingency 11 covers Contingency (4,7-11). Thus the combination of Contingency (1+2+11) is able to cover the whole credible contingency set (1-11). In Table VI.5, multi-dimensional contingency related preventive control is summarized. Four combination of multi-contingency (1+5), (5+10), (1+3+11) and (1+2+11) are studied here. Compared with single contingency, the dispatch cost is higher with multi-contingency considered. For instance, the dispatch cost for multi-contingency (1+5) is 299 \$/hr and 215 \$/hr larger than that with single contingency 1 and 5, respectively. More importantly, with the multi-contingency (1+2+11), the operation point obtained from the proposed dispatch is transient stable for all contingencies (1-11), but with the highest cost increment of 523 \$/hr.

Table VI.5 Results of multi-contingency involved dispatch

C	Dynamic security dispatch with multi-contingency			
	1+5	5+10	1+3+11	1+2+11
1	S	S	S	S
2	U	U	U	S
3	U	U	S	S
4	U	U	S	S
5	S	S	S	S
6	S	U	S	S
7	S	S	S	S
8	U	S	S	S
9	S	S	S	S
10	U	S	S	S
11	U	U	S	S
Cost (\$/hr)	36454	36399	36640	36642
Δ Cost (\$/hr)	335	220	521	523
CPU Time (sec.)	289.0	170.0	875.2	732.4

VI.5 SUMMARY

In this chapter, a novel approach for dynamic security dispatch is proposed. Dynamic security dispatch is implemented as an extended OPF problem to minimize the economic cost while the stability of all credible contingencies can be maintained. This SIP problem is solved based on local reduction of infinity norm. The case study on New England 39-bus system demonstrates that the proposed method for dynamic dispatch is effective in both single and multi-contingency cases.

Chapter VII CONCLUSION AND FUTURE WORK

VII.1 CONCLUSION

With the advent of competitive market environment, economical pressure and intensified transactions have forced electric power systems to operate much closer to their security limits than ever before, while they are often subjected to disturbances such as bus fault, line outage, generation loss and even load shedding. In order to ensure the system security to survive in all possible abnormal conditions, advanced dynamic security assessment and control is in great need, for example, the calculation of dynamic available transfer capability in the interfaces of the interconnected grids, the dynamic security dispatch to improve the security level with less control cost, etc. However, in practical operation, it is an extremely difficult task to reconcile the conflict between economics and security requirements in power systems operation.

So far, in spite of the efforts made by researchers, the study in this area has not developed enough to propose effective preventive strategies to integrate the economics and dynamic security in one framework. This thesis makes contributions to formulate such category of problems mathematically as a family of dynamic security constrained OPF. The effective methodology is developed to deal with the optimization of power flow with transient stability constraints using SIP.

Firstly, transient stability constrained OPF is generalized mathematically as SIP problems with finitely many variables and finitely many constraints. Infinite-dimensional constraints for transient stability, based on the coherence of the rotor angle with the COI and PEBS concept respectively, are converted equivalently by SIP methods to finite-dimensional constraints. In the transformation, L_1 and L_∞ norm local reduction methods are developed with clear practical definitions. The extension of SIP methods in the solution of transient stability constrained OPF makes

it solvable by conventional OPF methods.

Secondly, the direct primal dual interior point method is employed as a suitable nonlinear programming method for solving the equivalent problem. The technical crux in the calculation of the Jacobian and Hessian matrices of the transient stability constraints is overcome with the employment of implicit function relation and chain rule in the derivative derivation. Besides, the multi-local maximizers for L_∞ norm local reduction method are simply detected based on intermediate value theorem.

Thirdly, two significant bottlenecks are broken in the implementation of SIP in transient stability constrained OPF. One is the complicated derivation of the Hessian matrix for transient stability constraints. Improved BFGS method with superlinear convergence characteristic is proposed to avoid the complex derivation of Hessian matrix. Different from traditional BFGS methods, the approximated Hessian is formulated by the summation of the easy and difficult computation parts. Only the difficult part, associated with transient stability constraints, is updated approximately with BFGS techniques; while the rest, as the easy part, is calculated accurately. The other one is the huge computation efforts in the local reduction transformation of the transient stability constraints. With only the most effective section of transient stability constraints included, the computation efforts in the local reduction and derivatives calculation are alleviated remarkably, which is illustrated by numerical tests.

Finally, the calculation of dynamic ATC and dynamic security dispatch are formulated as transient stability constrained OPF problems and solved using SIP methods. The proposed methods are fully validated in WSCC 9-bus system and New England 39-bus system. The validation also shows the adaptability of the proposed methodology in such category of practical issues related with dynamic security and economy in power systems. Multi-contingency cases are able to be handled simultaneously to obtain an optimal solution which is secure for the specific credible contingency set.

VII.2 FUTURE WORK

The integration of economy and security in one framework is a significantly important task in power system study and still in its experimental stage. With the contribution of the study in transient stability constrained OPF in this thesis, several issues is expected to be dealt with in study forward. Future work may be conducted in the following directions.

Firstly, the infeasibility of the optimization needs to be detected accurately and speedily. If infeasibility detected, i.e. the proposed preventive control schemes, such as generation rescheduling, fails to produce a stable operation point for critical contingencies, more effective control strategies in emergency, such as angle control of phase-shifters and load shedding, are then necessary to be implemented via other means. The coordination of preventive and emergency control is important to build a higher level security framework for power systems with economic operation state.

Secondly, more effective contingency screening scheme should be developed to identify representative set of critical contingencies such that only the minimum set of contingencies needs to be dealt with in the transient stability constrained OPF solver.

Thirdly, the computation performance should be improved in the future. Theoretically, transient stability constrained OPF is inherently a SIP problem. Even in programming study, SIP is still an underdeveloped area for further study. More suitable and effective SIP techniques should be applied to solve the problems in power systems. Numerically, the huge computational efforts need to be decreased. Especially, the time-consuming and complicit calculation of the Jacobian and Hessian matrix of transient stability has to be solved for the future on-line application of the proposed method.

REFERENCE

1. B. Stott, O. Alsac, and A.J. Monticelli, "Security analysis and optimization," Proc. of IEEE, Vol.75, No.12, pp. 1623-1644, Dec. 1987.
2. V. Vittal, "Consequence and impact of electric utility industry re-structuring on transient stability and small signal stability analysis," Proc. of IEEE, Vol.88, No.2, pp.196-206, Feb. 2000.
3. Y. Mansour, "Competition and system stability: the reward and the penalty," Proc. of IEEE, Vol.88, No.2, pp.228-234, Feb. 2000.
4. P. Kundur, J. Paserba, V.Ajjarapu, G. Andersson, A. Bose, C. Canizares, N. Hatziargyriou, D. Hill, A. Stankovic, C. Taylor, T. Van Cutsem, and V.Vittal, "Definition and Classification of Power System Stability, IEEE/CIGRE Joint Task Force on Stability Terms and Definitions Report," IEEE Trans. Power Syst., Vol. 19, No. 3, pp.1387-1401, Aug. 2004.
5. U.S.-Canada Power System Outage Task Force, "Final report on the August 14, 2003 blackout in the United States and Canada: causes and recommendations," <http://www.nerc.com/~filez/blackout.html>, 2004.
6. D. Novosel, M.M. Begovic, and V. Madani, "Shedding light on blackouts," IEEE Power and Energy Magazine, Vol. 2, No. 1, pp. 32- 43, Jan./Feb. 2004.
7. G. Anderson, P. Donalek, R. Farmer, N. Hatziargyriou, I. Kamwa, P. Kundur, N. Martins, J. Paserba, P. Pourbeik, J. Sanchez-Gasca, R. Schulz, A. Stankovic, C. Taylor, and V. Vittal, "Causes of the 2003 major grid blackouts in North America and Europe, and recommended means to improve system dynamic performance," IEEE Trans. Power Syst., Vol.20, No.4, pp. 1922- 1928, Nov. 2005.

8. D.K. Kuo and A. Bose, "A generation rescheduling method to increase the dynamic security of power systems," *IEEE Trans. Power Syst.*, Vol. 10, No. 1, pp. 68-76, Feb. 1995.
9. A.A. Fouad, "Dynamic security assessment practices in North America," *IEEE Trans. Power Syst.*, Vol.13, No.3, pp. 1310-1321, Aug. 1988.
10. Y. Xue, V. Cutsem, and M. Pavella, "Real-time analytic sensitivity method for transient security assessment and preventive control," *IEE Proc. C, Gener. Transm. Distrib.*, Vol. 135, No. 2, pp. 107-117, Mar. 1988.
11. V. Miranda, J.N. Fidalgo, J.A.P. Lopes, and L.B. Almeida, "Real time preventive actions for transient stability enhancement with a hybrid neural network-optimization approach," *IEEE Trans. on Power Syst.*, Vol. 10, No. 2, pp. 1029-1035, May 1995.
12. M.L. Scala, M. Trovato, and C. Antonelli, "On-line dynamic preventive control: an algorithm for transient security dispatch," *IEEE Trans. Power Syst.*, Vol. 15, No. 2, pp. 601-610, May 1998.
13. Y. Kato and S. Iwamoto, "Transient stability preventive control for stable operating condition with desired CCT," *IEEE Trans. Power Syst.*, Vol. 17, No. 4, pp. 1154-1161, Nov. 2002.
14. R.V. Daniel and M. Pavella, "A comprehensive approach to transient stability control: part i – near optimal preventive control," *IEEE Trans. Power Syst.*, Vol. 18, No. 4, pp. 1446-1452, Nov. 2003.
15. R.V. Daniel and M. Pavella, "A comprehensive approach to transient stability control: part ii - open loop emergency control," *IEEE Trans. Power Syst.*, Vol. 18, No. 4, pp. 1454-1460, Nov. 2003.
16. D. Gan, R.J. Thomas, and R.D. Zimmerman, "Stability-Constrained optimal power flow," *IEEE Trans. Power Syst.*, Vol. 15, No. 2, pp. 535-540, May 2000.

17. P.W. Sauer, K.D. Demaree, and M.A. Pai, "Stability limited load supply and interchange capability," IEEE Trans. on PAS, Vol. 102, No. 3, pp. 3637-3643, Nov. 1983.
18. C. Hwang, V. Vittal, and A.A. Fouad, "Determination of interface flow stability limits by sensitivity analysis of transient energy margin," Proc. of IFAC Symposium on Power Systems and Power Plant Control, pp. 189-194, Seoul, Aug. 1989.
19. A.L. Bettiol, L. Wehenkel, and M. Pavella, "Transient stability-constrained maximum allowable transfer," IEEE Trans. Power Syst., Vol. 14, No. 2, pp. 654-659, May 1999.
20. E.D. Tuglie, M. Dicorato, M.L. Scala, and P.A. Scarpellini, "Static optimization approach to assess dynamic available transfer capability," IEEE Trans. Power Syst., Vol. 15, No. 3, pp. 1069-1076, Aug. 2000.
21. W. Li and A. Bose, "A coherency based rescheduling method for dynamic security," IEEE Trans. Power Syst., Vol. 13, No. 3, pp. 810-815, Aug. 1998.
22. S. Bruno, E.D. Tuglie, and M.L. Scala, "Transient security dispatch for the concurrent optimization of plural postulated," IEEE Trans. Power Syst., Vol. 17, No. 3, pp. 707-714, Aug. 2002.
23. T.B. Nguyen and M.A. Pai, "Dynamic security-constrained rescheduling of power systems using trajectory sensitivities," IEEE Trans. Power Syst., Vol. 18, No. 2, pp. 848-854, May 2003.
24. A.A. Fouad and J. Tong, "Stability constrained optimal rescheduling of generation," IEEE Trans. Power Syst., Vol. 8, No. 1, pp. 105-112, Feb. 1993.

25. K.N. Shubhanga and A.M. Kulkarni, "Stability-constrained generation rescheduling using energy margin sensitivities," *IEEE Trans. Power Syst.*, Vol. 19, No. 3, pp. 1402-1412, Nov. 2004.
26. A.K. David and X. Lin, "Dynamic security enhancement in power-market systems," *IEEE Trans. Power Syst.*, Vol. 17, No. 2, pp. 431-438, May 2002.
27. S.N. Singh and A.K. David, "Dynamic security constrained congestion management in competitive electricity markets," *IEEE Power Engineering Society Winter Meeting, Singapore, 2000.*
28. O. Alsac, J. Bright, M. Prais, and B. Stott, "Further developments in LP-based optimal power flow," *IEEE Trans. Power Syst.*, Vol.5, No.3, pp. 697-711, Aug. 1990.
29. J. Carpentier and P. Bornard, "Towards an integrated secure optimal operation of power systems," in *International Conference on Advances in Power System Control, Operation and Management*, Vol. 1, pp. 1-16, Nov. 1991.
30. E. Vaahedi, Y. Mansour, and E.K. Tse, "A general purpose method for on-line dynamic security assessment," *IEEE Trans. Power Syst.*, Vol.13, No.1, pp. 243-249, Feb. 1998.
31. L. Chen, Y. Tada, H. Okamoto, R. Tanabe, and A. Ono, "Optimal operation solutions of power systems with transient stability constraints," *IEEE Trans. Circuits Syst.*, Vol. 48, No. 3, pp. 327-339, Mar. 2001.
32. R.J. Thomas and R.D. Zimmerman et al., "An internet-based platform for testing generation scheduling auctions," in *Hawaii International Conference on System Sciences, Hawaii, January 1998.*

33. S.C. Savulescu and L.G. Leffler, "Computation of parallel flows and the total and available transfer capability," 1997 PICA Tutorial.
34. J.A. Momoh, R.J. Koessler, M.S. Bond, B. Stott, D.I. Sun, A. Papalexopoulos, and P. Ristanovic, "Challenges to optimal power flow," IEEE Trans. Power Syst., Vol.12, No.1, pp.444-455, Feb., 1997.
35. Y. Yuan, J. Kubokawa, and H. Sasaki, "A solution of optimal power flow with multicontingency transient stability constraints," IEEE Trans. Power Syst., Vol. 18, No. 3, pp. 1094-1102, Aug. 2003.
36. Y. Sun, X. Yang, and H.F. Wang, "Approach for optimal power flow with transient stability constraints," IEE Proc. -Gener. Transm. Distrib., Vol. 151, No. 1, pp. 8-18, Jan. 2004.
37. P. Kundur, Power system stability and control, McGraw-Hill, 1994.
38. P.W. Sauer and M.A. Pai, Power system dynamics and stability, Prentice-Hall Inc., 1998.
39. E.W. Kimbark, Power system stability Volume III-Synchronous machines, John Wiley & Sons Inc., 1956.
40. J. Fong and C. Pottle, "Parallel processing of power system analysis problems via simple parallel microc omputer structure," IEEE Trans. on PAS, Vol. PAS-97, No. 5, pp 1834-1841, Sept./Oct. 1978.
41. F.L. Alvarado, "Parallel solution of transient problems by trapezoidal integration," IEEE Trans. on PAS, Vol. PAS-98, No. 3, pp. 1080-1090, May/Jun. 1979.

42. M. Lascalea, M. Bruccoli, F. Torelli, and M. Trovato, "A Gauss-Jacobi-block-Newton method for parallel transient stability analysis," IEEE PES Winter Meeting, Atlanta, Feb. 1990.
43. M.A. Pai, S.K. Ghoshal, and A. Kulkarni, "A predictor corrector algorithm in the parallel solution of power system dynamics," Power Symposium 1990, Proc. of Twenty-Second Annual North American, pp 118-125, 15-16 Oct 1990.
44. IEEE Committee Report, "Parallel processing in power system computation," IEEE Trans. Power Syst., Vol. 7, No. 2, pp 629-638, May 1993.
45. J.S. Chai and A. Bose, "Bottlenecks in parallel algorithm for power system stability analysis," IEEE Trans. Power Syst., Vol. 8, No. 1, pp 9-15, Feb. 1993.
46. K.W. Chan, R.W. Dunn, and A.R. Daniels, "Efficient heuristic partitioning algorithm for parallel processing of large power systems network equations," IEE Proc.-Gener. Transm. Distrib., Vol. 142, No. 6, pp 625-630, Nov 1995.
47. D. Xia and G. Heydt, "On line transient stability decomposition-aggregation and high order derivatives," IEEE Trans. on PAS, Vol. 102, No. 7, pp. 2038-2046, 1983.
48. M.H. Haque and A.H.M.A. Rahim, "Determination of first swing stability limit of multimachine power systems through Taylor series expansions," IEE Proc. C, Gener. Transm. Distrib., Vol. 136, No. 6, pp. 373-379, Nov. 1989.
49. Z. Guo and Z. Liu, "Fast Transient Stability Simulation by Higher Order Taylor Series Expansions," Proc. Of the CSEE, Vol. 11, No. 3, pp. 9-15, May 1991.

50. P.C. Magnusson, "Transient energy method of calculating stability," AIEE Trans., Vol. 66, pp. 747-755, 1947.
51. P.D. Aylett, "The energy integral-criterion of transient stability limits of power systems," Proc. IEE, Vol. 105c, No. 8, pp. 527-536, Sept. 1958.
52. G.E. Gless, "Direct method of Lyapunov applied to transient power system stability," IEEE Trans. on PAS, Vol. 85, No. 2, pp. 159-168, 1966.
53. A.H. El-Abiad and K. Nagappan, "Transient stability regions of multimachine power systems," IEEE Trans. on PAS, Vol. 85, No. 2, pp. 169-178, 1966.
54. M.A. Pai, Power system stability, North Holland Publishing Co., New York, 1981.
55. M.A. Pai, Energy function analysis for power system stability, Kluwer Academic Publishers, 1989.
56. S. Fu, Y. Ni, and Y. Xue, Direct methods for stability analysis, China Electric Power Press, Beijing, 1990.
57. A.A. Fouad and V. Vittal, Power system transient stability analysis using the transient energy function method, Prentice-Hall, 1992.
58. S. Liu and J. Wang, Energy function analysis for power system transient stability, Shanghai Jiao Tong University Press, Shanghai, 1996.
59. T. Athay, R. Podmore, and S. Virmani, "A practical method for direct analysis of transient stability," IEEE Trans. on PAS, Vol. 98, No. 2, pp. 573-584, Mar. 1979.

60. A.A. Found and S.E. Stanto, "Transient stability of multi-machine power system parts I and II," IEEE Trans. on PAS, Vol.100, No. 7, pp. 3408-3424, 1981.
61. V. Vittal, S. Rajagopal, and A.A. Fouad, "Transient stability analysis of stressed power systems using the energy function method," IEEE Trans. Power Syst., Vol. 3, No. 1, pp 239-244, Feb. 1988.
62. N. Kakimoto, Y. Ohsawa, and M. Hayashi, "Transient stability analysis of electric power system via Lure' type Lyapunov functions, parts I and II," Trans. IEE of Japan, Vol. 98, No. 516, May 1978.
63. H.D. Chiang, F.F. Wu, and P.P. Varaiya, "Foundations of direct methods for power system transient stability analysis," IEEE Trans. Circuits and Systems, Vol. 34, pp. 160-173, Feb. 1987.
64. H.D. Chiang, F.F. Wu, and P.P. Varaiya, "Foundations of the potential energy boundary surface method for power system stability analysis," IEEE Trans. Circuits and Systems, Vol. 35, No. 6, pp. 712-728, Feb. 1988.
65. H.D. Chiang, F.F. Wu, and P.P. Varaiya, "A BCU method for direct analysis of power system transient stability," IEEE PES Summer Meeting, 1991.
66. Y. Xue and V. Cutsem, "A Simple direct method for the fast transient stability assessment of large power system," IEEE Trans. on Power Syst., Vol. 4, No. 2, pp. 400-412, May 1988.
67. Y. Xue, V. Custem, and M. Pavella, "Extended equal-area criterion: justifications generalizations, applications." IEEE Trans. on Power Syst., Vol. 4, No. 1, pp. 44-52, Feb. 1989.

68. Y. Xue and M. Pavella, "Extended equal-area criterion: an analytical ultra-fast method for transient stability assessment and preventative control of power systems," *Int. J. Electric Power & Energy*, Vol. 11, No. 2, pp. 131-149, 1989.
69. Y. Xue and M. Pavella, "Critical-cluster identification in transient stability studies," *IEE Proc. C, Gener. Transm. Distrib.*, Vol. 140, No. 6, pp. 481-489, Nov. 1993.
70. G.A. Maria, C. Tang, and J. Kim, "Hybrid transient stability analysis," *IEEE Trans. on Power Syst.*, Vol. 5, No. 2, pp. 384-393, May 1990.
71. K.W. Chan, R.W. Dunn, and A.R. Daniels, "On-Line Stability Constraint Assessment for Large Complex Power Systems," *Electric Power Systems Research*, pp.169–176, Vol. 46, No. 3, Sep, 1998.
72. J. Carpentiers, "Contribution a.l'etude du dispatching economique," *Bull.Soc. Francaise Elect.*, ser.8, Vol.3, pp. 431-447, 1962.
73. H.W. Dommel and T.F. Tinney, "Optimal power flow solutions," *IEEE Trans. On PAS*, Vol.87, No.5, pp.1866-1876, 1968.
74. S.M. Chen and F.C. Schweppe, "A generation reallocation and load shedding algorithm," *IEEE Trans. on PAS*, Vol. 98, No. 1, pp. 26-34, Jan/Feb 1979.
75. IEEE Working Group report, "Description and bibliography of major economy-security functions, parts I, II, III," *IEEE Trans. on PAS*, Vol. 100, No. 1, pp. 211-235, Jan. 1981.
76. A. Monticelli, M.V.F. Pereira, and S. Granville, "Security-constrained optimal power flow with post-contingency corrective rescheduling," *IEEE Trans. on Power Syst.*, Vol. 2, No. 1, pp. 175-182, Feb. 1987.

77. L.S. Vargas, V.H. Quintana, and A. Vannelli, "A tutorial description of an interior point method and its applications to security-constrained economic dispatch," *IEEE Transactions on Power Syst.*, Vol. 8, No. 3, pp. 1315-1324, Aug. 1993.
78. Y. Wu, A.S. Debs, and R.E. Marsten, "A nonlinear direct predictor-corrector primal-dual interior point algorithm for optimal power flows," *IEEE Trans. on Power Syst.*, Vol. 9, No. 2, pp. 876-893, May 1994.
79. S. Ghosh and B.H. Chowdhury, "Security-constrained optimal rescheduling of real power using hopfield neural network," *IEEE Trans. on Power Syst.*, Vol. 11, No. 4, pp. 1743-1748, Nov. 1996.
80. M. Aganagic and S. Mokhtari, "Security constrained economic dispatch using nonlinear Dantzig-Wolfe decomposition," *IEEE Trans. on Power Syst.*, Vol. 12, No. 1, pp. 105-112, Feb. 1997.
81. M.A. El-Kady, C.K. Tang, V.F. Carvalho, A.A. Fouad, and V. Vittal, "Dynamic security assessment utilizing the transient energy function method," *Proc. of 1985 PICA Conference, San Francisco*, pp.132-139, May 1985.
82. V. Vittal, E.Z. Zhou, C. Hwang and A.A. Fouad, "Derivation of stability limits using analytical sensitivity of the transient energy margin," *IEEE Trans. Power Syst.*, Vol. 4, No. 4, pp. 1363-1372, Nov. 1989.
83. A. Berizzi, G. Demartini, M. Delfanti, P. Marannino, and G. Rizzi, "Security constrained OPF for optimal transaction scheduling in an open access environment," in *Proc. 13th Power Systems Computational Conf.*, pp. 1214–1219.

84. X. Zhang, Y.H. Song, Q. Lu, and S. Mei, "Dynamic available transfer capability (ATC) evaluation by dynamic constrained optimization," *IEEE Trans. Power Syst.*, vol. 19, no. 2, pp. 1240-1242, May 2004.
85. F. Allella and D. Lauria, "Fast optimal dispatch with global transient stability constraint," *IEE Proc. C, Gener. Transm. Distrib.*, Vol. 148, No. 5, pp. 471-476, Sept. 2001.
86. G.B. Dantzig (1963). *Linear programming and extensions*, Princeton University Press, Princeton, New Jersey, 1963.
87. E. Polak, "Semi-infinite optimization in engineering design," in: A.V. Fiacco and K.O. Kortanek, ed., *Semi-infinite programming and applications*, Springer-Verlag, New York, pp.236-248, 1983.
88. E. Polak, D.Q. Mayne, and D.M. Stimler, "Control-system design via semi-infinite optimization - a review," *Proc. of IEEE*, Vol. 72, No. 12, pp. 1777-1794, Dec. 1984.
89. E. Polak, "On the mathematical foundations of nondifferentiable optimizations in engineering design," *SIAM Rev.*, Vol. 29, pp. 21-89, Mar. 1987.
90. R. Hettich and K.O. Kortanek, "Semi-infinite programming: theory, methods, and applications," *SIAM Rev.*, Vol. 35, No. 3, pp. 380-429, Sept. 1993.
91. R. Hettich, "An implementation of a discretization method for semi-infinite programming," *Mathematical Programming*, Vol. 34, pp. 354-361, 1986.
92. R. Reemtsen, "Some outer approximation methods for semi-infinite optimization problems," *Journal of Computational and Applied Mathematics*, Vol. 53, pp. 87-108, 1994.

93. R. Reemtsen and J.J. Ruckmann, *Semi-Infinite Programming*. Kluwer Academic Publisher, 1998.
94. K.L. Teo, X.Q. Yang, and L.S. Jennings, "Computational discretization algorithms for functional inequality constrained optimization," *Annals of Operations Research*, Vol. 98, pp. 215-234, 2000.
95. G.A. Watson, "Globally convergent methods for semi-infinite programming," *BIT*, Vol. 21, pp. 362-373, 1981.
96. C.J. Goh and K.L. Teo, "Alternative algorithms for solving nonlinear function and functional inequalities," *Applied Mathematics and Computation*, Vol. 41, pp. 159-177, 1991.
97. S. Ito, Y. Liu, and K. L. Teo, "A dual parameterization method for convex semi-infinite programming," *Annals of Operations Research*, Vol. 98, pp. 189-213, 2000.
98. Y. Liu, K.L. Teo, and S. Ito, "Global optimization in quadratic semi-infinite programming, topics in numerical analysis," *Computing Supplement*, Vol. 15, pp. 119-132, 2001.
99. S.Y. Wu, S.C. Fang, and C.J. Lin, "Solving quadratic semi-infinite programming problems by using relaxed cutting plane scheme," *Journal Computational and Applied Mathematics*, Vol. 129, pp. 89-104, 2001.
100. O. Stein, *Bi-level strategies in semi-infinite programming*, Kluwer Academic Publishers, 2003.
101. E. Polak, *Optimization: Algorithms and Consistent Approximations*, Springer-Verlag, New York, 1997.

102. C.J. Price and I.D. Coope, "An exact penalty function algorithm for semi-infinite programs," BIT, Vol. 30, pp. 723-734, 1990.
103. A.R. Conn and N.I.M Gould, "An exact penalty function algorithm for semi-infinite programs," Mathematical Programming, Vol. 37, pp. 19-40, 1987.
104. Y. Tanaka, M. Fukushima, and T. Ibaraki, "A globally convergent SQP method for semi-infinite non-linear optimization," Journal of Computational and Applied Mathematics, Vol. 23, pp. 141-153, 1988.
105. M.L. Scala, G. Lorusso, R. Sbrizzai, and M. Trovato, "A qualitative approach to the transient stability," IEEE Trans Power Syst., Vol.11, No.4, pp.1996-2002, Nov., 1996.
106. D.G. Luenberger, Linear and non linear programming, second edition, Kluwer Academic Publishers, 2003.
107. G. Still, "Generalized semi-infinite programming: Theory and methods," European Journal of Operational Research, vol. 119, no. 2, pp. 301-313, 1999.
108. M.S. Bazaraa, H.D. Sherali and C.M. Shetty, Nonlinear programming: theory and algorithms, third edition, A John Wiley & Sons, Inc., Publication, Hoboken, New Jersey, 2003.
109. R.A. Tapia, M.W. Trosset et. al. "An Extension of the Karush-Kuhn-Tucker Necessity Conditions to Infinite Programming," SIAM Review, vol. 36, no. 1, pp. 1-17, 1994.
110. D.I. Sun, B. Ashley, B. Brewer, A. Hughes, and W.F. Tinney, "Optimal power flow by Newton approach," IEEE Trans on Power Apparatus and Systems, Vol. 103, No.10, pp.2864-2880, Oct. 1984.

111. A. Santos and G.R.M. Costa, "Optimal-power-flow solution by Newton's method applied to an augmented Lagrangian function," IEE Proceedings-Gen., Trans. and Distr., Vol. 142, No. 1, pp. 33-36, Jan. 1995.
112. K. Iba, H. Suzuki, K.I. Suzuki, and K. Suzuki, "Practical reactive power allocation/operation planning using successive linear programming," IEEE Trans on Power Syst., Vol. 3, No. 2, pp. 558-566, May 1988.
113. R.C. Burchett, H.H. Happ, and K.A. Wirgau, "Quadratically convergent optimal power flow," IEEE Trans on PAS, Vol. 103, No. 11, pp. 3267-3276, 1984.
114. N. Grudimin, "Reactive power optimization using successive quadratic programming method," IEEE Trans on Power Syst., Vol. 13, No. 4, pp. 1219-1225, Nov. 1998.
115. N.K. Karmarkar, "A new polynomial time algorithm for linear programming," Combinatorica, Vol. 4, pp. 273-395, 1984.
116. I.J. Lustig, R.E. Marsten, and D.F. Shanno, "Interior point methods for linear programming: computational state of the art," ORSA Journal on Computing, Vol. 6, No. 1, pp.1-14, 1994.
117. J.A. Momoh, S.X. Guo, E.C. Ogbuobiri, and R. Adapa, "The quadratic interior point method solving power system optimization problems," IEEE Trans on Power Syst., Vol. 9, No. 3, pp. 1327-1336, Aug. 1994.
118. L.S. Vargas, V.H. Quintana, and A. Vannelli, "A tutorial description of an interior point method and its applications to security-constrained economic

- dispatch," IEEE Trans on Power Systems, Vol. 8, No. 3, pp. 1315-1324, Aug. 1993.
119. S. Granville, "Optimal reactive dispatch through interior point methods," IEEE Trans on Power Systems, Vol. 9, No. 1, pp. 136-146, Feb. 1994.
120. Y.C. Wu, A.S. Debs, and R.E. Marsten, "A direct nonlinear predictor-corrector primal-dual interior point algorithm for optimal power flows," IEEE Trans on Power Systems, Vol. 9, No. 2, pp. 876-883, May 1994.
121. H. Wei, H. Sasaki, and R. Yokoyama, "An application of interior point quadratic programming algorithm to power system optimization problems," IEEE Trans. Power Syst., Vol. 13, No. 3, pp. 260-266, Sept. 1996.
122. X. Yan and V.H. Quintana, "An efficient predictor-corrector point algorithm for security-constrained economic dispatch," IEEE Trans on Power Syst., Vol. 12, No. 2, pp. 803-810, May 1997.
123. H. Wei, H. Sasaki, J. Kubokawa, and R. Yokoyama, "An interior point nonlinear programming for optimal power flow problems with a novel data structure," IEEE Trans. Power Syst., Vol. 13, No. 3, pp. 870-877, Sept. 1998.
124. G.L. Torres and V.H. Quintana, "An interior-point method for nonlinear optimal power flow using voltage rectangular coordinates," IEEE Transactions on Power Systems, Vol. 13, No. 4, pp. 1211-1218, Nov. 1998.
125. X. Yan and V.H. Quintana, "Improving an interior-point-based OPF by dynamic adjustments of step sizes and tolerances," IEEE Trans on Power Systems, Vol. 14, No. 2, pp. 709-717, May 1999.

126. M. Liu, S.K. Tso, and Y. Cheng, "An extended nonlinear primal-dual interior-point algorithm for reactive-power optimization of large-scale power systems with discrete control variables," *IEEE Trans on Power Syst.*, Vol. 17, No. 4, pp. 982-991, Nov 2002.
127. A.V. Fiacco and G.P. McCormick, *Nonlinear Programming: Sequential Unconstrained Minimization Techniques*, John Wiley & Sons, New York, 1968
128. C. Floudas and P.M. Pardalos, *State of the art in global optimization: computational methods and applications*, Boston, Kluwer Academic Publishers, 1996.
129. C.T. Kelley, *Iterative methods for optimization*, number 18 in *Frontiers in Applied Mathematics*, SIAM, Philadelphia, 1999.
130. J.E. Dennis and H.F. Walker, "Convergence theorems for least-change secant update methods," *SIAM J. Numer. Anal.*, Vol. 18, pp. 949-987, 1981.
131. *Transmission Transfer Capability*, A reference document for calculating and reporting the electric power transfer capability of interconnected systems. North American Electric Reliability Council, May 1995.
132. *Available Transfer Capability Definitions and Determination*, A framework for determining available transfer capabilities of the interconnected transmission networks for a commercially viable electricity market. North American Electric Reliability Council, June 1996.
133. R.D. Christle and B.F. Woollenberg, "Transmission management in the deregulate environment," *Proc. of The IEEE*, Vol. 88, No. 2, pp. 170-195, Feb. 2000.

134. F. Wang and X. Bai, "OPF based transfer capability calculation," Proc. Of the CSEE, Vol. 22, No. 11, pp. 35-40, Nov. 2002.
135. P.M. Anderson and A.A. Fouad, Power System Control and Stability, Revised Printing, IEEE Press Power System Engineering Series, IEEE Press Inc., 1993.
136. K.S. Chandrashekar and D.J. Hill, "Dynamic security dispatch: basic formulation," IEEE Trans. Power Appar. Syst., Vol. 102, No. 7, pp. 2145-2154, Jul. 1983.
137. N. Narasimhamurthi, "On-line real power scheduling in marginally secure power systems," IEEE Trans. Power Appar. Syst., Vol. 103, No. 4, pp. 869-873, Apr. 1984.
138. R. Zimmerman and D. Gan, MATPOWER: A MATLAB power system simulation package rule.

APPENDIX A WSCC 9-BUS SYSTEM [135]

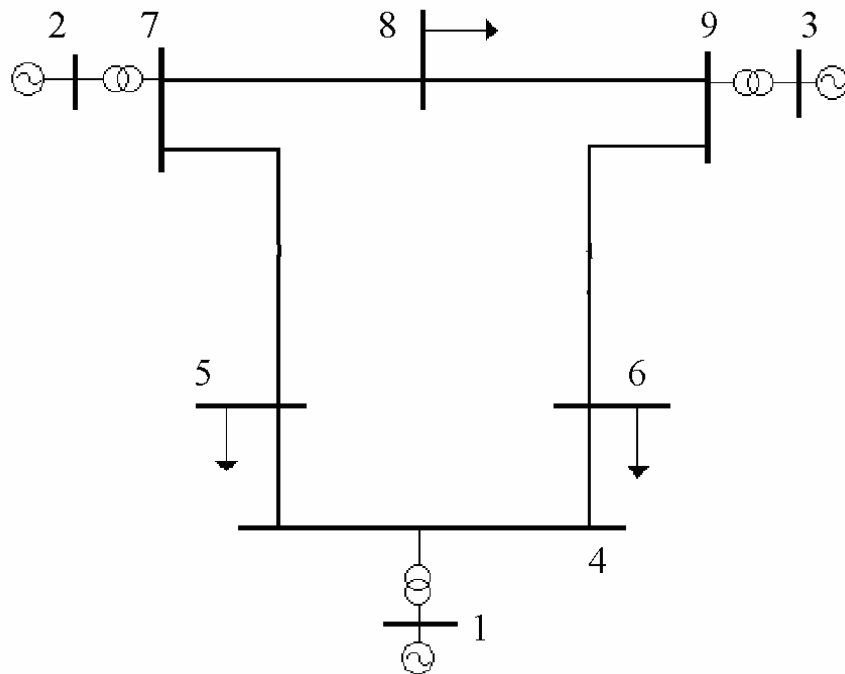


Figure A.0.1 9-Bus System One-Line Diagram

Table A.1 9-Bus System Load

Bus	Real power (MW)	Reactive power (MVar)
5	125.0	50.0
6	90.0	30.0
8	100.0	35.0

Table A.2 Line and transformer data

Bus	Bus	Resistance	Reactance	Susceptance
1	4	0	0.0576	-
2	7	0	0.0625	-
3	9	0	0.0586	-
4	6	0.017	0.092	0.079
4	5	0.01	0.085	0.088
5	7	0.032	0.161	0.153
6	9	0.039	0.17	0.179
7	8	0.0085	0.072	0.0745
8	9	0.0119	0.1008	0.1045

Table A.3 Generator data

Generator	H (Sec)	x_d'	P_{\max}	P_{\min}
1	23.64	0.0608	2.475	0.3
2	6.4	0.1198	1.92	0.3
3	3.01	0.1813	1.28	0.3

Note:

1. Reactance values in Table A.2 are on a 100-MVA base and 230kv voltage base.
2. All values in Table A.3 are on 100-MVA base and machines' rated terminal voltage.

APPENDIX B NEW ENGLAND 39-BUS SYSTEM [55]

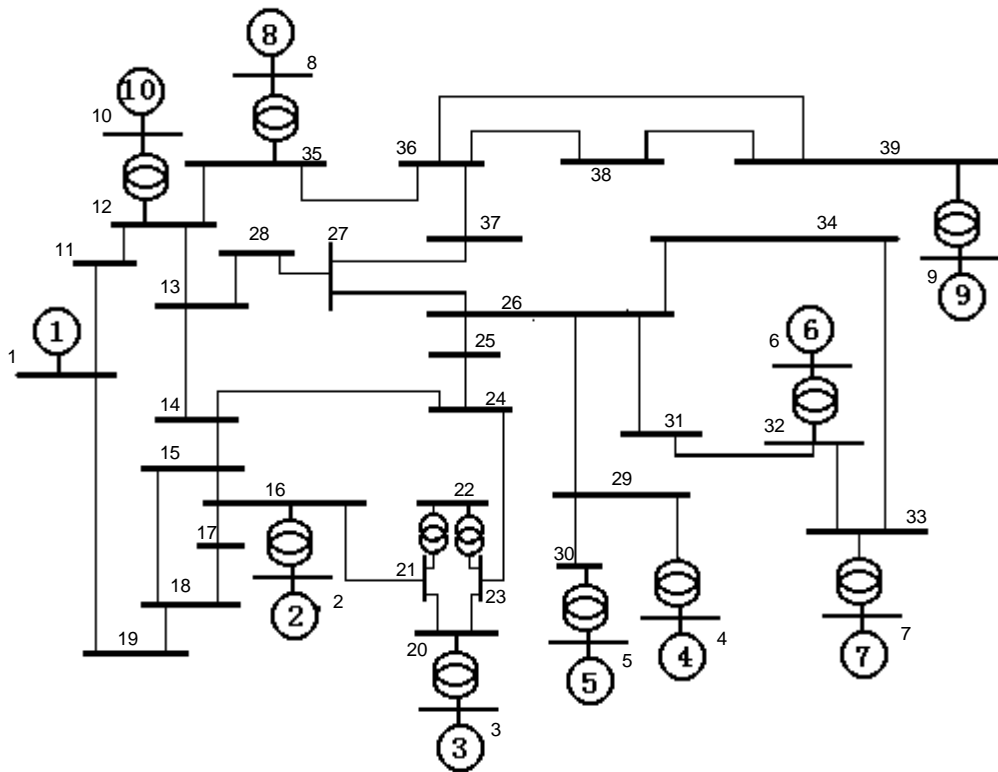


Figure B.0.1 39-Bus System One-Line Diagram

Table B.1 39-Bus System Load

Bus	Real power (MW)	Reactive power (Mvar)
1	1104	250
2	9.2	4.6
13	322	2.4
14	500	184
17	233.8	84
18	522	176
22	7.5	88

25	320	153
26	329.4	32.3
28	158	30
30	680	103
31	274	115
33	247.5	84.6
34	308.6	-92.2
35	224	47.2
36	139	17
37	281	75
38	206	27.6
39	283.5	26.9

Table B.2 Line and transformer data

Bus	Bus	Resistance	Reactance	Susceptance	Transformer Tap
1	11	0.001	0.025	0.375	-
1	19	0.001	0.025	0.6	-
11	12	0.0035	0.0411	0.3494	-
12	13	0.0013	0.0151	0.1286	-
12	35	0.007	0.0086	0.073	-
13	14	0.0013	0.0213	0.1107	-
13	28	0.0011	0.0133	0.1069	-
14	15	0.0008	0.0128	0.0671	-
14	24	0.0008	0.0129	0.0691	-
15	16	0.0002	0.0026	0.0217	-
15	18	0.0008	0.0112	0.0738	-

THE HONG KONG POLYTECHNIC UNIVERSITY

16	17	0.0006	0.0092	0.0565	-
16	21	0.0007	0.0082	0.0694	-
17	18	0.0004	0.0046	0.039	-
18	19	0.0023	0.0363	0.1902	-
20	21	0.0004	0.0043	0.0364	-
20	23	0.0004	0.0043	0.0364	-
23	24	0.0009	0.0101	0.0862	-
24	25	0.0018	0.0217	0.183	-
25	26	0.0009	0.0094	0.0855	-
26	27	0.0007	0.0089	0.0671	-
26	29	0.0016	0.0195	0.152	-
26	31	0.0008	0.0135	0.1274	-
26	34	0.0003	0.0059	0.034	-
27	28	0.0007	0.0082	0.066	-
27	37	0.0013	0.0173	0.1608	-
31	32	0.0008	0.014	0.1282	-
32	33	0.0006	0.0096	0.0923	-
33	34	0.0022	0.035	0.1805	-
35	36	0.0032	0.0323	0.2565	-
36	37	0.0014	0.0147	0.1198	-
36	38	0.0043	0.0474	0.3901	-
36	39	0.0057	0.0625	0.5145	-
38	39	0.0014	0.0151	0.1245	-
2	16	0	0.025	0	1.07
3	20	0	0.02	0	1.07
4	29	0.0007	0.0142	0	1.07

5	30	0.0009	0.018	0	1.009
6	32	0	0.0143	0	1.025
7	33	0.0005	0.0272	0	1
8	35	0.0006	0.0232	0	1.025
9	39	0.0008	0.0156	0	1.025
10	12	0	0.0181	0	1.025
21	22	0.0016	0.0435	0	1.006
23	22	0.0016	0.0435	0	1.006
30	29	0.0007	0.0138	0	1.06

Table B.3 Generator data

Generator	H (Sec)	x_d'	P_{\max}	P_{\min}	Cost coefficient		
					a	b	c
1	500	0.006	11	0	0.006	0.3	0.2
2	30.3	0.0697	11.45	0	0.01	0.3	0.2
3	35.8	0.0531	7.5	0	0.01	0.3	0.2
4	28.6	0.0436	7.32	0	0.01	0.3	0.2
5	26	0.132	6.08	0	0.01	0.3	0.2
6	34.8	0.05	7.5	0	0.01	0.3	0.2
7	26.4	0.049	6.6	0	0.01	0.3	0.2
8	24.3	0.057	6.4	0	0.01	0.3	0.2
9	34.5	0.057	9.3	0	0.006	0.3	0.2
10	42	0.031	3.5	0	0.01	0.3	0.2

Note:

1. All per unit values in Table B.2 are on a 100-MVA base and 345kv voltage base.
2. All values in Table B.3 are in 100-MVA power base and machines' rated terminal voltage.

APPENDIX C NUMERICAL SOLUTION TO ORDINARY DIFFERENTIAL EQUATION

In power system stability analysis, the differential equations to be solved can be expressed by nonlinear ordinary differential equations with known initial values:

$$\frac{dx}{dt} = f(x, t) \quad (C.1)$$

where x is the state vector of n dependent variables and t is the independent variable for time. Thus, the issue of solving x as a function of t , with the initial values x_0 and t_0 respectively, is essential for simulation.

In this section, forth-order Runge-Kutta method and implicit method are presented to the solution of equations of the above form. For simple description and without loss of generality, equation (C.1) is treated as a first-order differential equation as

$$\frac{dx}{dt} = f(x, t) \quad (C.2)$$

C1 FORTH-ORDER RUNGE-KUTTA METHOD

Forth-order R-K method is equivalent to considering up to forth derivative term in the Taylor series expansion. The general formula giving the value of x for the (n+1) step is:

$$x_{n+1} = x_n + \frac{1}{6}(K_1 + 2K_2 + 2K_3 + K_4) \quad (C.3)$$

where

$$K_1 = f(x_n, t_n) \Delta t$$

$$K_2 = f\left(x_n + \frac{K_1}{2}, t_n + \frac{\Delta t}{2}\right) \Delta t$$

$$K_3 = f\left(x_n + \frac{K_2}{2}, t_n + \frac{\Delta t}{2}\right) \Delta t$$

$$K_4 = f(x_n + K_3, t_n + \Delta t) \Delta t \quad (\text{C.4})$$

The physical interpretation of the above solution is as follows:

K_1 = (slope at the beginning of the time step) Δt

K_2 = (first approximation to slope at midstep) Δt

K_3 = (second approximation to slope at midstep) Δt

K_4 = (slope at the end of step) Δt

$$\Delta x = \frac{1}{6}(K_1 + 2K_2 + 2K_3 + K_4)$$

Thus Δx , the incremental value of x , is given by the weighted average of estimates based on slopes at the beginning, midpoint, and the end of the time step.

C2 IMPLICIT INTEGRATION METHODS

Let the solution for x at $t = t_0 + \Delta t$ with respect to equation (C.2) be written in integral form as

$$x = x_0 + \int_{t_0}^t f(x, \tau) d\tau \quad (\text{C.5})$$

Implicit integration methods use interpolation functions for the expression under the integral. Interpolation implies that the functions must pass through the yet unknown points, for equation (C.5) at time t .

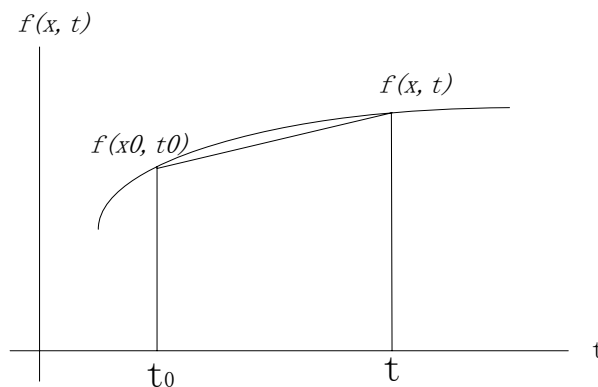


Figure C.0.1 Illustration of trapezoidal rule

The simplest implicit integration method is the trapezoidal rule. It uses linear interpolation. As shown in Figure C.1, the area under the integral of equation (C.5) is

approximated by trapezoids.

The trapezoidal rule for equation (C.5) is given by

$$x = x_0 + \frac{\Delta t}{2} [f(x_0, t_0) + f(x, t)] \quad (\text{C.6})$$

A general formula giving the value of x at $t = t_{n+1}$ is

$$x_{n+1} = x_n + \frac{\Delta t}{2} [f(x_n, t_n) + f(x_{n+1}, t_{n+1})] \quad (\text{C.7})$$

where x_{n+1} appears on both sides of equation (C.7). It implies that the variable x is computed as a function of its value at the previous time step as well as the current value, which is unknown. Therefore, an implicit equation should be solved.